

Astrofisica Nucleare e Subnucleare

Gamma ray Bursts

Bethe Bloch Formula

$$\frac{1}{\rho} \frac{dE}{dx} = -4\pi r_e^2 m_e c^2 \frac{Z_1^2}{\beta^2} N_A \frac{Z}{A} \left[\ln \frac{2m_e c^2 \beta^2 \gamma^2 F}{I} - \beta^2 - \frac{\delta(\beta\gamma)}{2} \right]$$

Für $Z > 1$, $I \approx 16Z^{0.9} \text{ eV}$

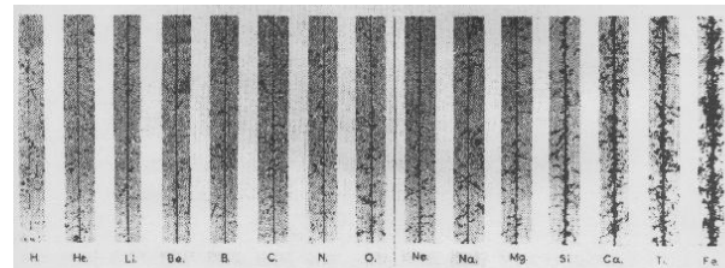
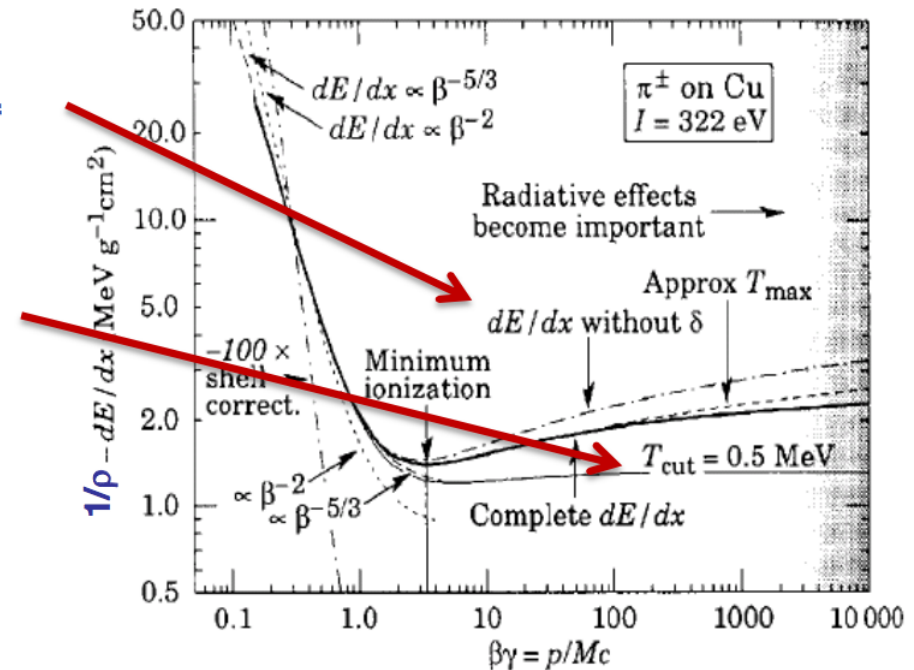
For Large $\beta\gamma$ the medium is being polarized by the strong transverse fields, which reduces the rise of the energy loss \rightarrow density effect

At large Energy Transfers (delta electrons) the liberated electrons can leave the material. In reality, E_{max} must be replaced by E_{cut} and the energy loss reaches a plateau (Fermi plateau).

Characteristics of the energy loss as a function of the particle velocity ($\beta\gamma$)

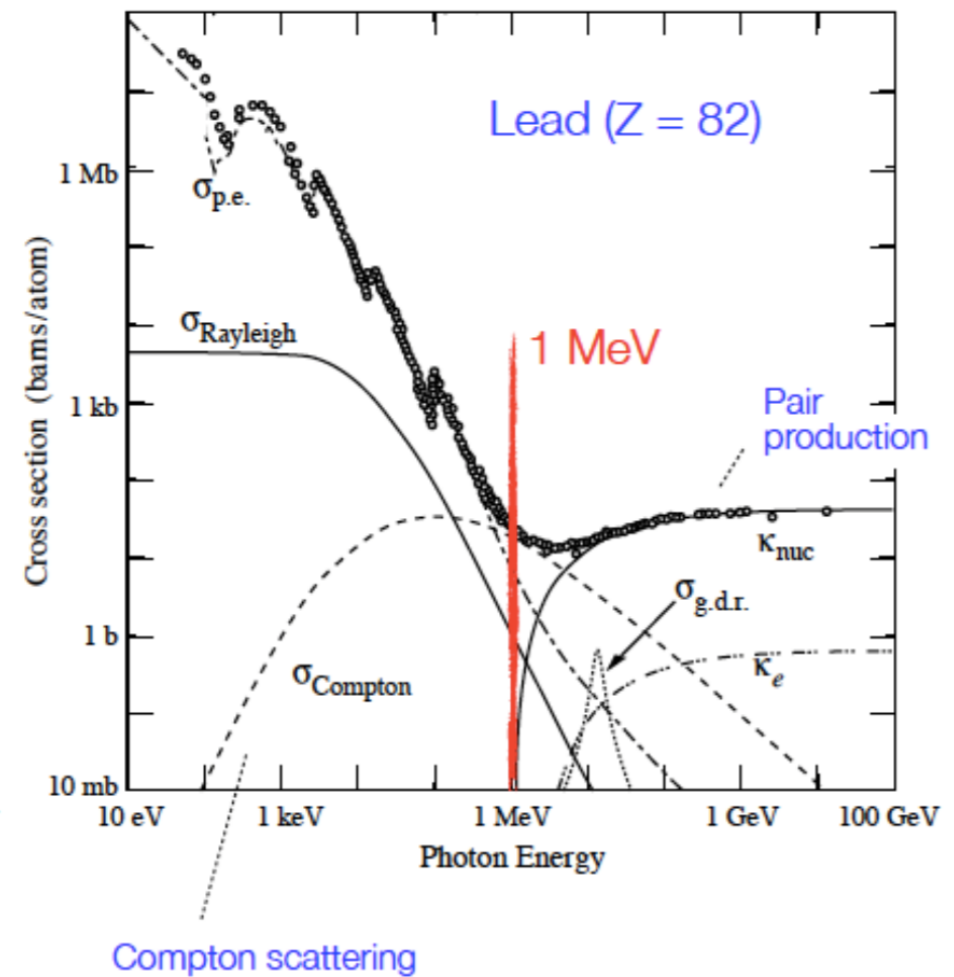
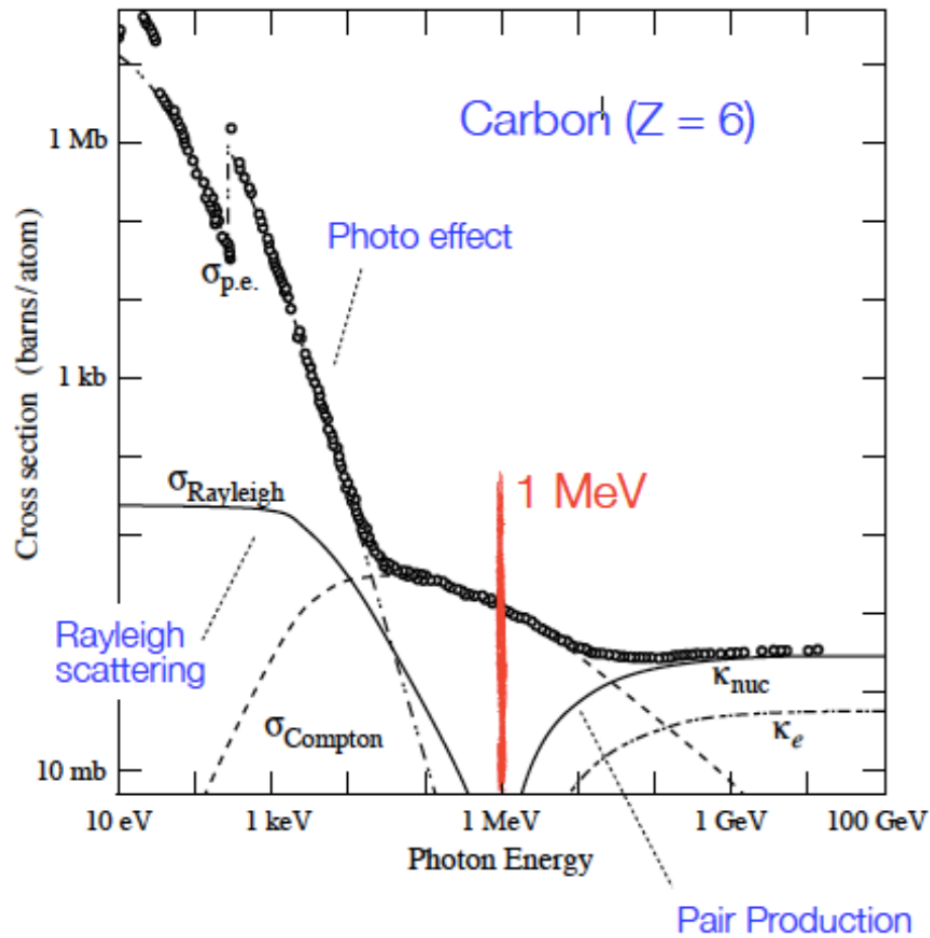
The specific Energy Loss $1/\rho \, dE/dx$

- first decreases as $1/\beta^2$
- increases with $\ln \gamma$ for $\beta = 1$
- is \approx independent of M ($M \gg m_e$)
- is proportional to Z_1^2 of the incoming particle.
- is \approx independent of the material ($Z/A \approx \text{const}$)
- shows a plateau at large $\beta\gamma$ ($\gg 100$)
- $dE/dx \approx 1-2 \times \rho \text{ [g/cm}^3\text{]} \text{ MeV/cm}$

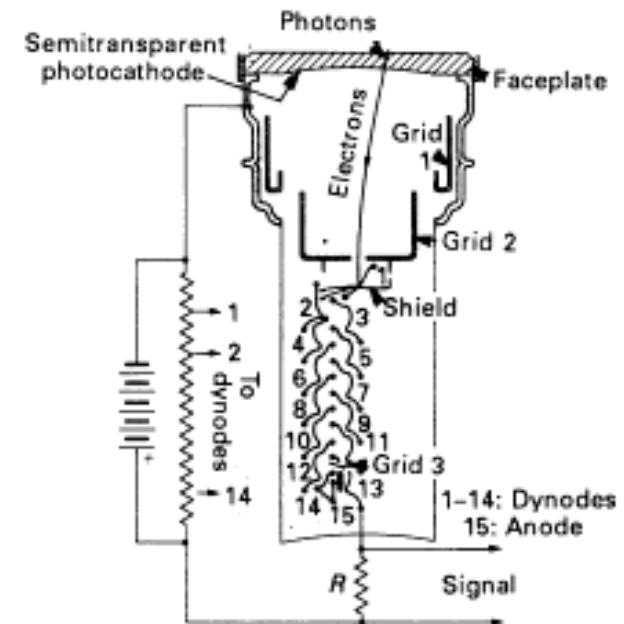
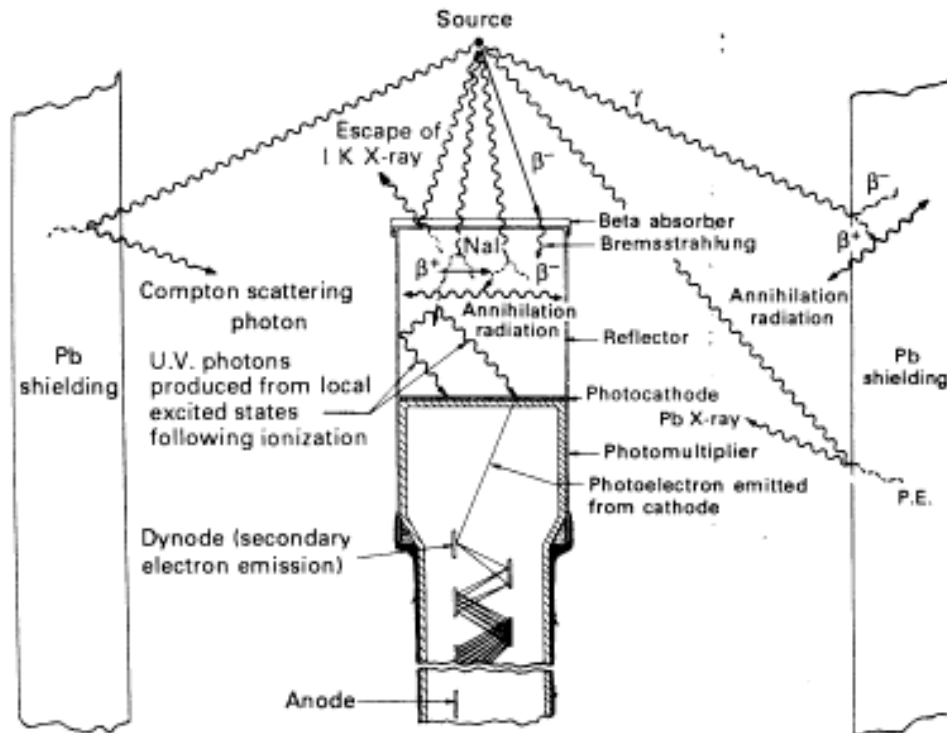


Interactions of photons with matter

Photon Total Cross Sections



Scintillation Detectors



Risposta del rivelatore - 1

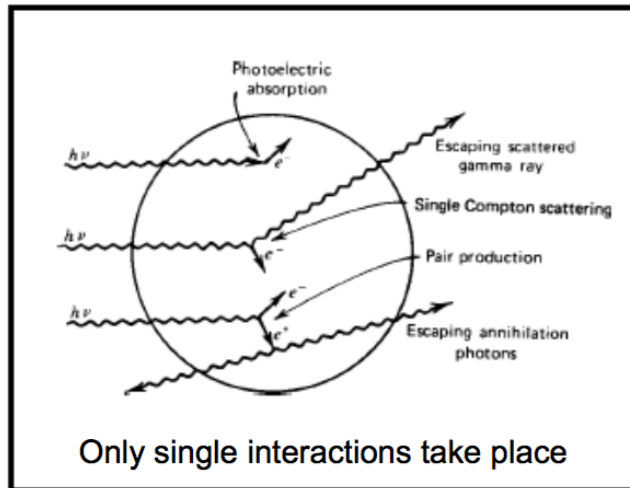


Figure 9: "Small" detector

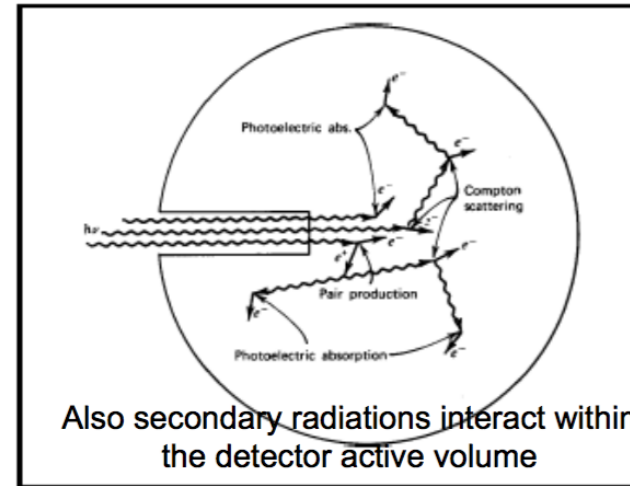


Figure 10: "Large" detector

most of the "secondary products" remain in the detector

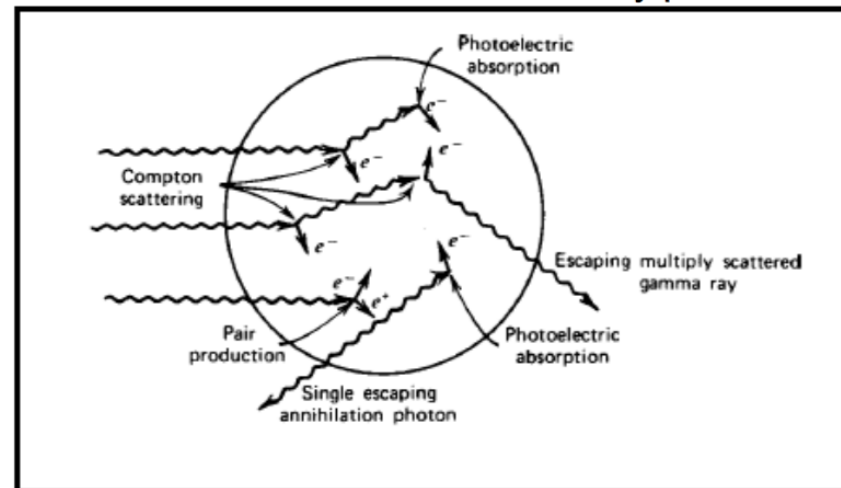


Figure 11: Intermediately sized detector

Risposta del rivelatore - 2

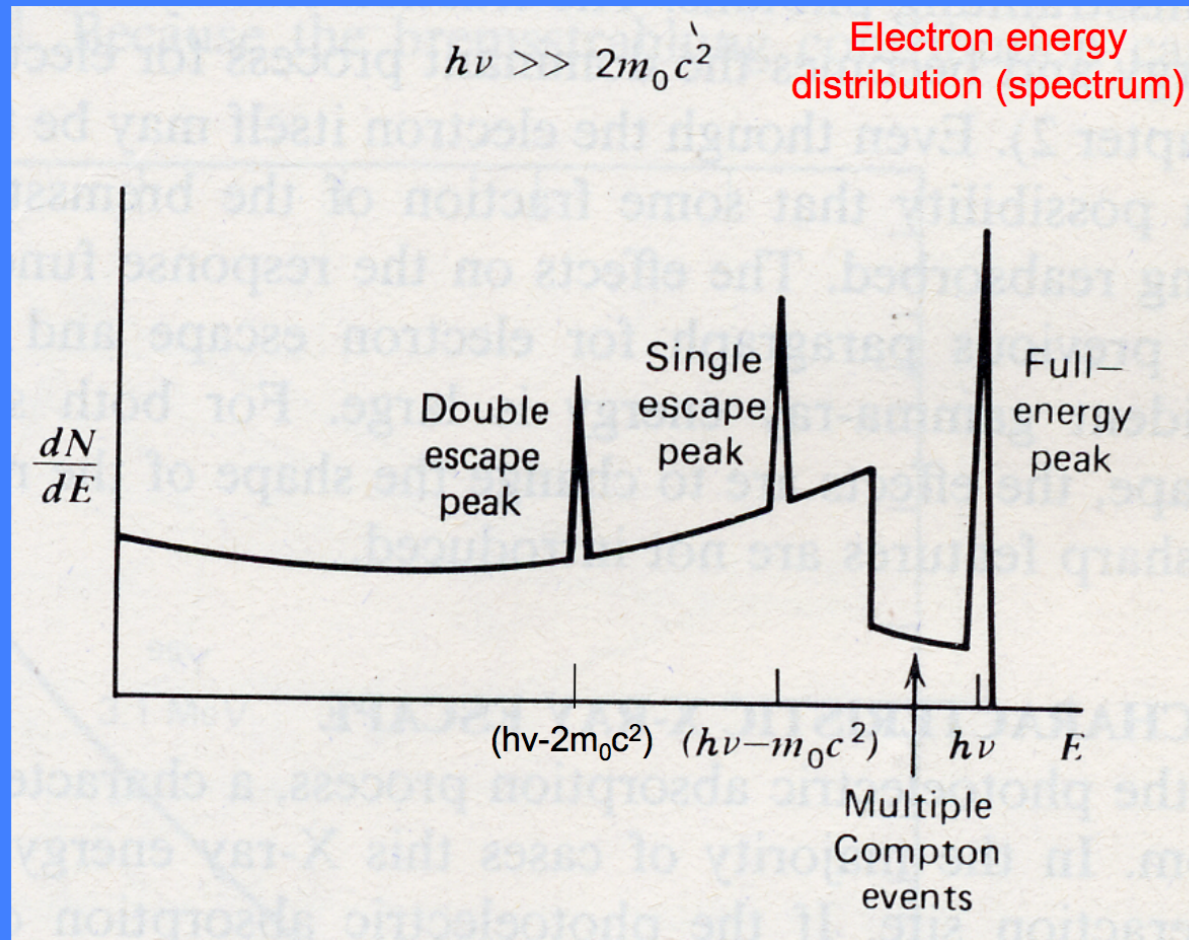


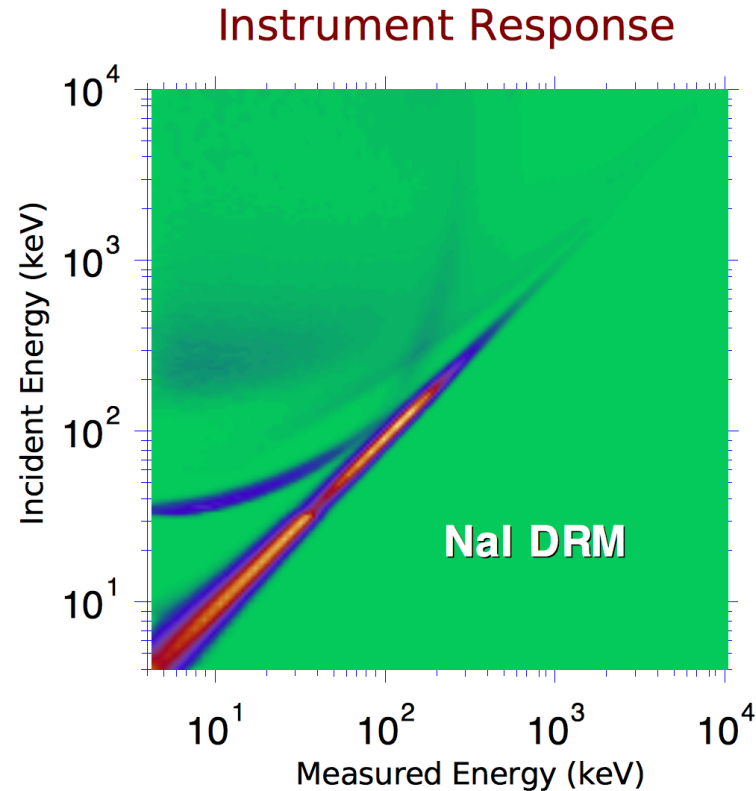
Photo-peak (full-energy peak): all photoelectric events remain in the detector and produce an energy deposit at the energy of the incoming photon

Single-escape peak: one annihilation photon leaves the detector without further interaction

Double-escape peak: both annihilation photons leave the detector (escape)

Case of intermediate-size detector (Knoll)

Detector Response Matrix



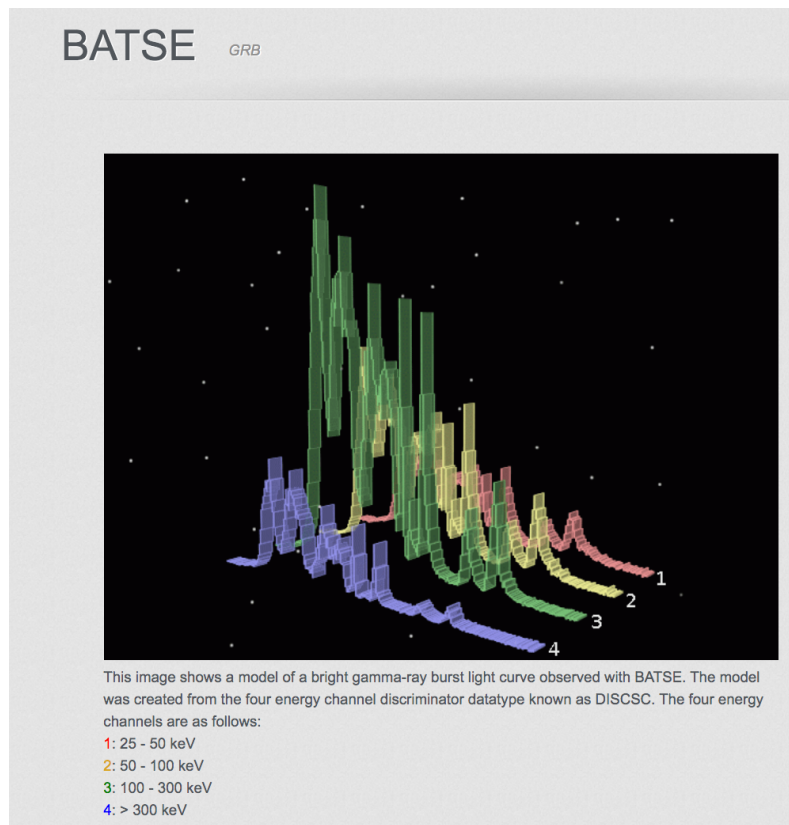
The response of a detector, which signal depends of the energy of an incoming photon, distributes the photon of a certain energy over many pulse height channels according to the gain and energy resolution of the detector. Usually this resolution function is relative complicated and depends on the photon energy. Since the energy acceptance and resolution of a given detector is determined by its design it is convenient to table this function while the photon energy serves as a parameter. This procedure leads directly to a form of a matrix and gives the whole data set the name *detector response matrix*.

Exercise #1

- Find the web sites of BATSE
- Find the web site (if any) of BeppoSAX
- Find the web site of Fermi/GBM
- Find the web site of AGILE/MCAL GRB catalog
- Find the web site of CALET GRBM
- Find the web site of AstroSAT CZTI GRB
- Find the web site of GECAM

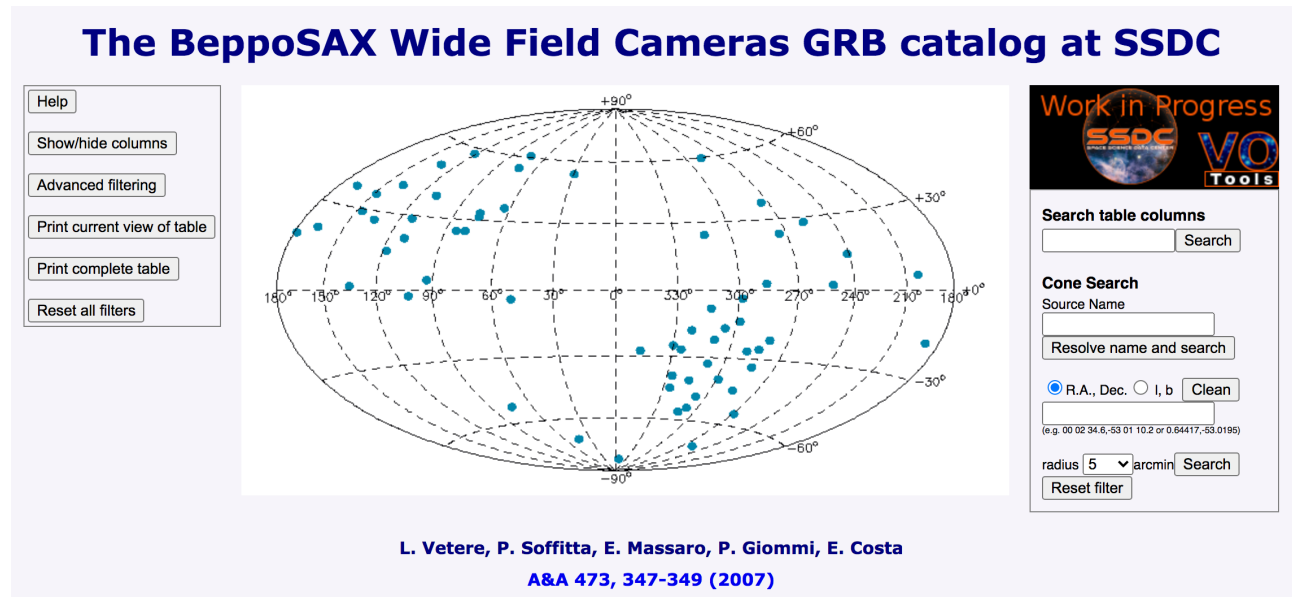
Exercise #1

- Find the web sites of BATSE
- <https://gammaray.nsstc.nasa.gov/batse/>



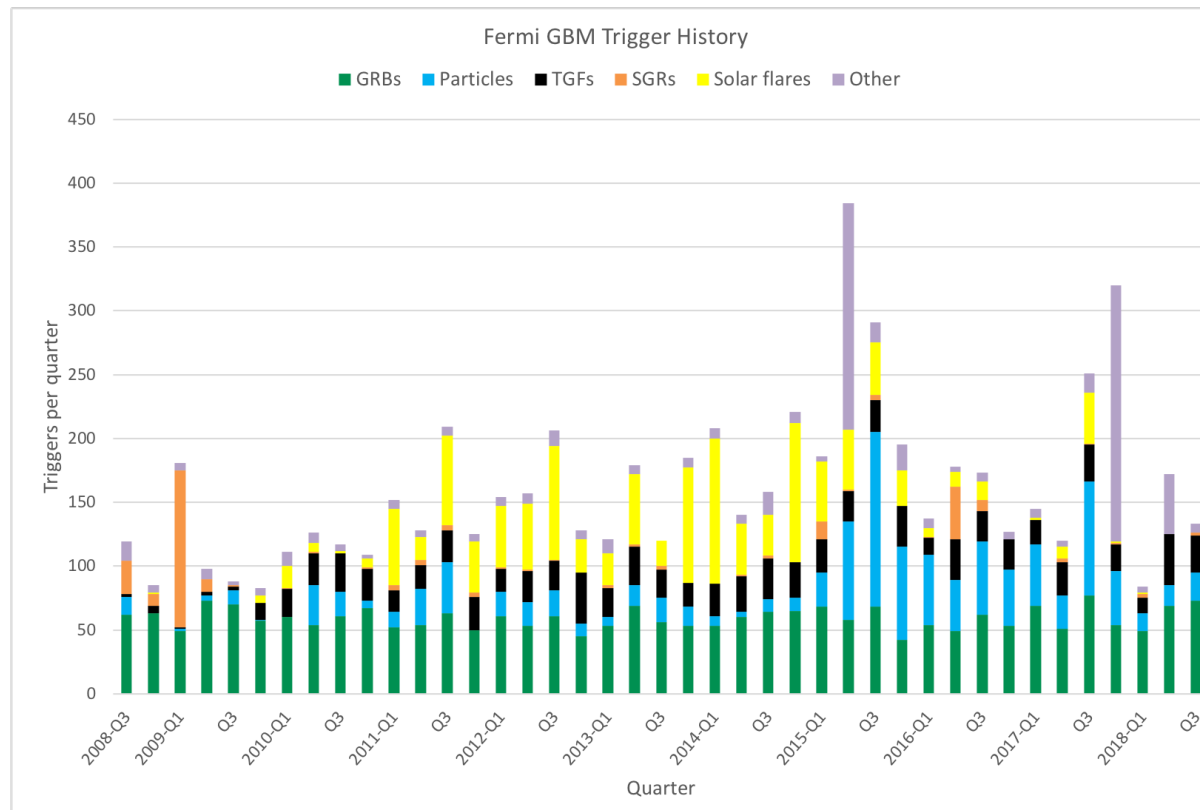
Exercise #1

- Find the web site(s) of BeppoSAX
 - <https://heasarc.gsfc.nasa.gov/W3Browse/all/saxgrbmgrb.html>
 - <https://www.ssdsc.asi.it/bepposax/>
 - https://www.ssdsc.asi.it/grb_wfc/



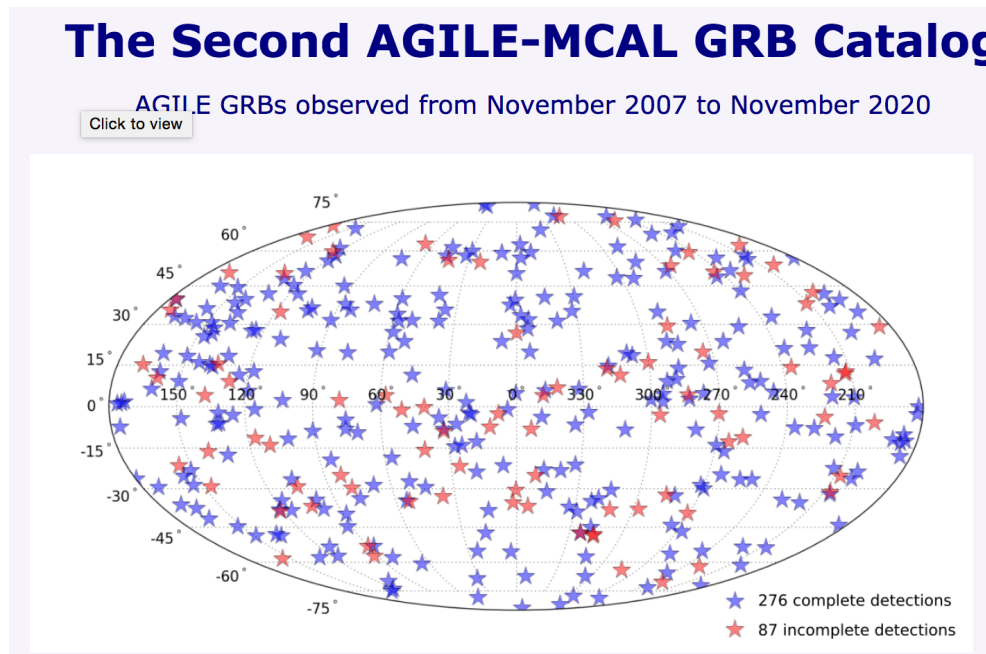
Exercise #1

- Find the web site of Fermi/GBM
- <https://gammarray.nsstc.nasa.gov/gbm/>



Exercise #1

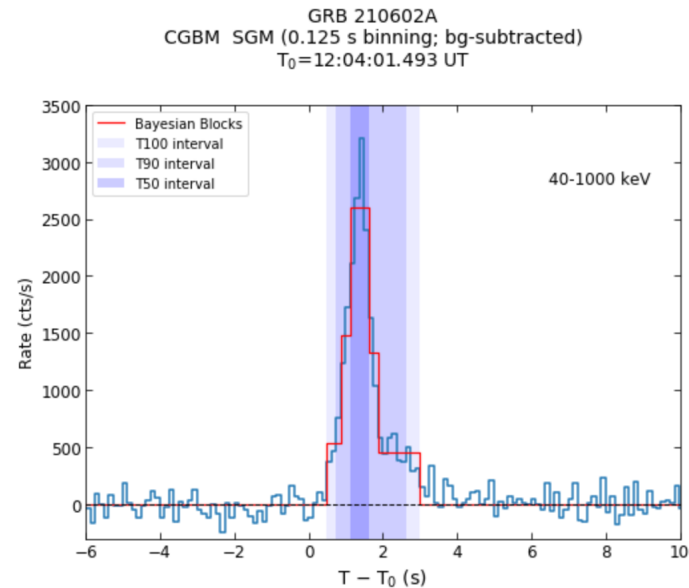
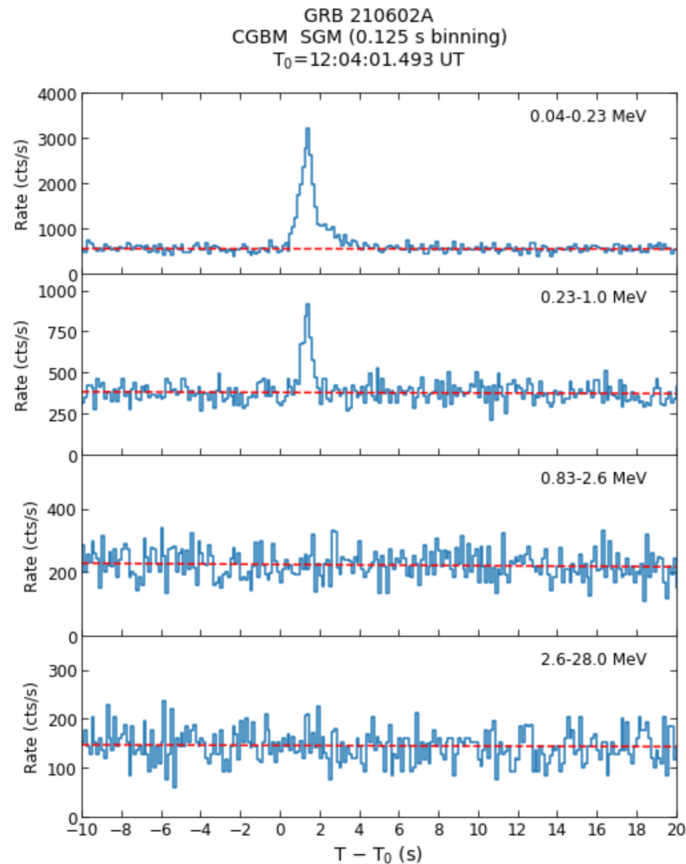
- Find the web sites of AGILE/MCAL GRB catalog
- <https://www.ssdsc.asi.it/mcalgrbcatalog/>
- <https://www.ssdsc.asi.it/mcal2grbcatalog/>



Exercise #1

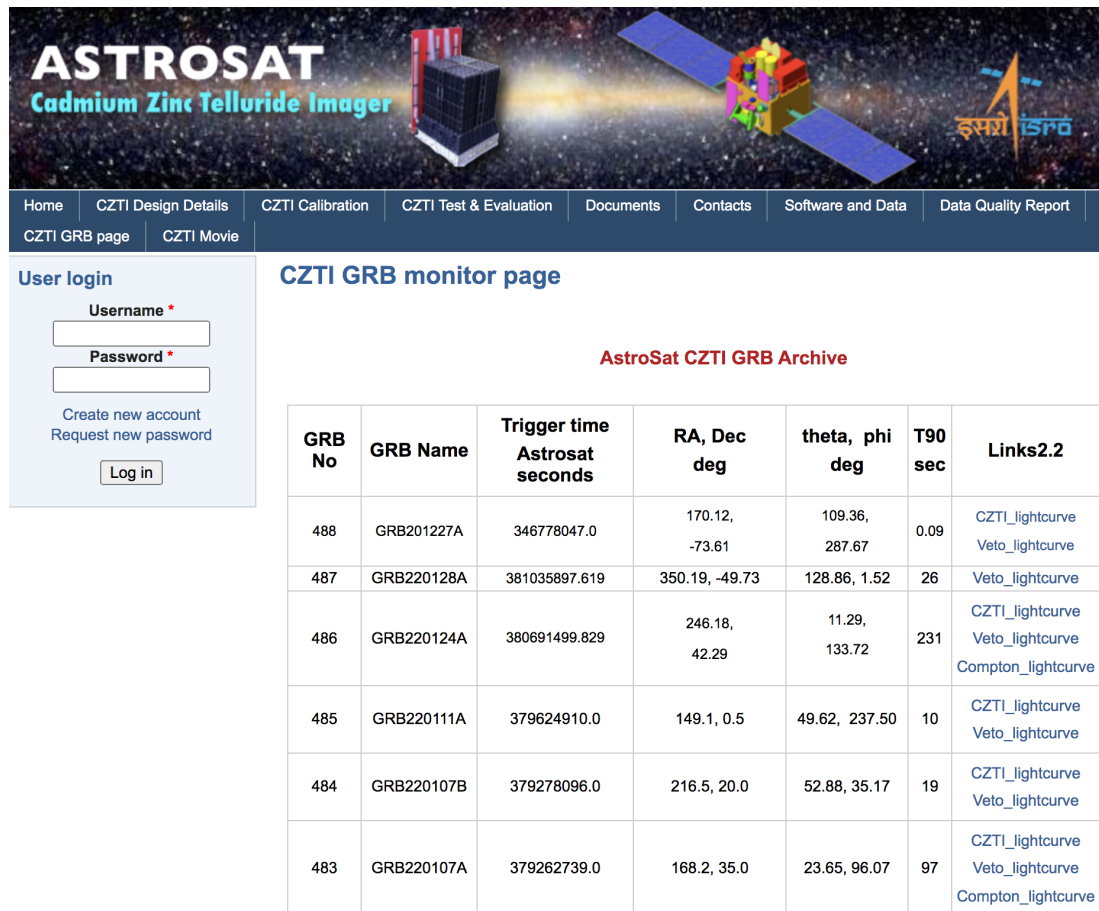
- Find the web site of CALET GRBM
- e.g.

https://cgbm.calet.jp/cgbm_trigger/ground/1306670489/



Exercise #1

- Find the web site of AstroSAT CZTI GRB
- <http://astrosat.iucaa.in/czti/?q=grb>



ASTROSAT
Cadmium Zinc Telluride Imager

Home | CZTI Design Details | CZTI Calibration | CZTI Test & Evaluation | Documents | Contacts | Software and Data | Data Quality Report
CZTI GRB page | CZTI Movie

User login

Username *

Password *

[Create new account](#)
[Request new password](#)

CZTI GRB monitor page

AstroSat CZTI GRB Archive

GRB No	GRB Name	Trigger time Astrosat seconds	RA, Dec deg	theta, phi deg	T90 sec	Links2.2
488	GRB201227A	346778047.0	170.12, -73.61	109.36, 287.67	0.09	CZTI_lightcurve Veto_lightcurve
487	GRB220128A	381035897.619	350.19, -49.73	128.86, 1.52	26	Veto_lightcurve
486	GRB220124A	380691499.829	246.18, 42.29	11.29, 133.72	231	CZTI_lightcurve Veto_lightcurve Compton_lightcurve
485	GRB220111A	379624910.0	149.1, 0.5	49.62, 237.50	10	CZTI_lightcurve Veto_lightcurve
484	GRB220107B	379278096.0	216.5, 20.0	52.88, 35.17	19	CZTI_lightcurve Veto_lightcurve
483	GRB220107A	379262739.0	168.2, 35.0	23.65, 96.07	97	CZTI_lightcurve Veto_lightcurve Compton_lightcurve

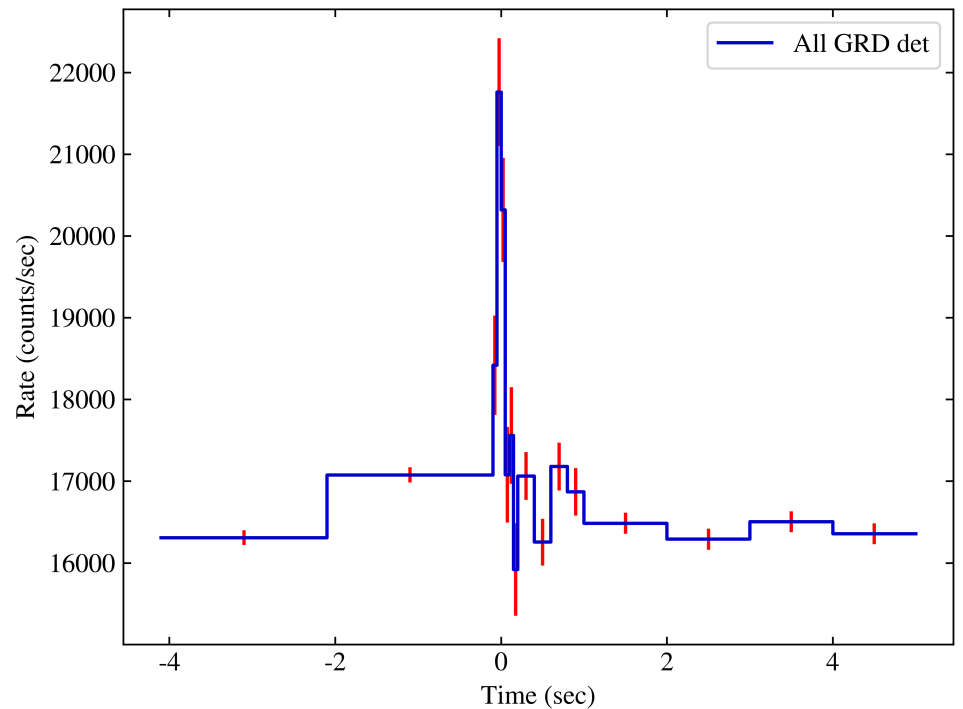
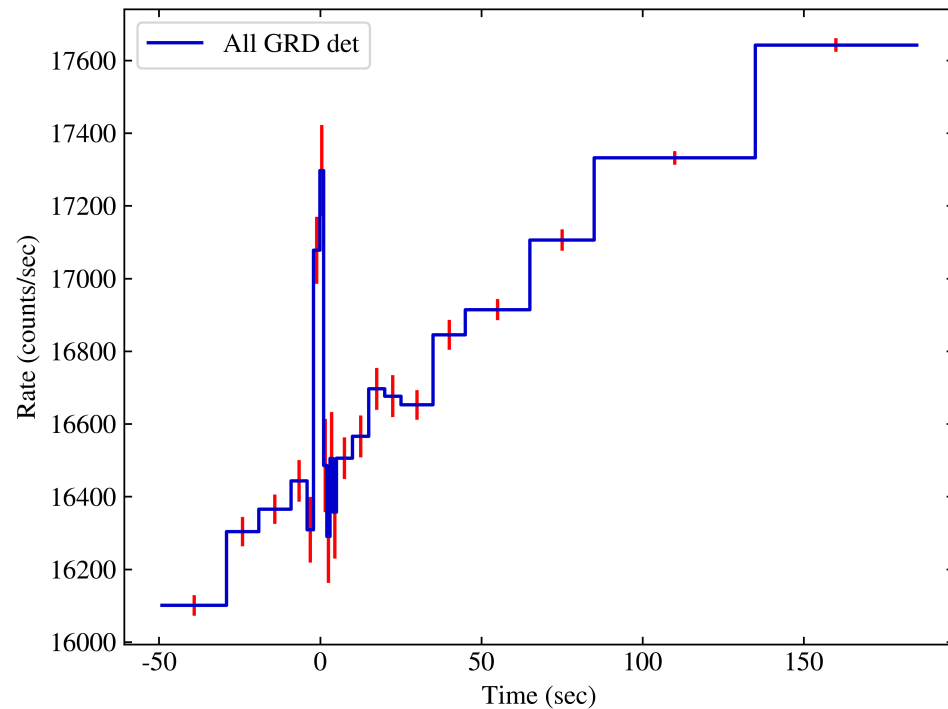
Exercise #1

- Find the web site of GECAM

- e.g.

http://twiki.ihep.ac.cn/pub/GECAM/GRBList/gecamb_lc_grd_all_combine_68795799.png

GECAM-B - Trigger 68795799 - 2021-03-07 05:56:39.100 UT



GRB history

THE ASTROPHYSICAL JOURNAL, 182:L85-L88, 1973 JUNE 1
© 1973. The American Astronomical Society. All rights reserved. Printed in U.S.A.

OBSERVATIONS OF GAMMA-RAY BURSTS OF COSMIC ORIGIN

RAY W. KLEBESADEL, IAN B. STRONG, AND ROY A. OLSON

University of California, Los Alamos Scientific Laboratory, Los Alamos, New Mexico
Received 1973 March 16; revised 1973 April 2

ABSTRACT

Sixteen short bursts of photons in the energy range 0.2–1.5 MeV have been observed between 1969 July and 1972 July using widely separated spacecraft. Burst durations ranged from less than 0.1 s to ~30 s, and time-integrated flux densities from $\sim 10^{-6}$ ergs cm^{-2} to $\sim 2 \times 10^{-4}$ ergs cm^{-2} in the energy range given. Significant time structure within bursts was observed. Directional information eliminates the Earth and Sun as sources.

Subject headings: gamma rays—X-rays—variable stars

I. INTRODUCTION

On several occasions in the past we have searched the records of data from early *Vela* spacecraft for indications of gamma-ray fluxes near the times of appearance of supernovae. These searches proved uniformly fruitless. Specific predictions of gamma-ray emission during the initial stages of the development of supernovae have since been made by Colgate (1968). Also, more recent *Vela* spacecraft are equipped with much improved instrumentation. This encouraged a more general search, not restricted to specific time periods. The search covered data acquired with almost continuous coverage between 1969 July and 1972 July, yielding records of 16 gamma-ray bursts distributed throughout that period. Search criteria and some characteristics of the bursts are given below.

II. INSTRUMENTATION

The observations were made by detectors on the four *Vela* spacecraft, *Vela 5A*, *5B*, *6A*, and *6B*, which are arranged almost equally spaced in a circular orbit with a geocentric radius of $\sim 1.2 \times 10^6$ km.

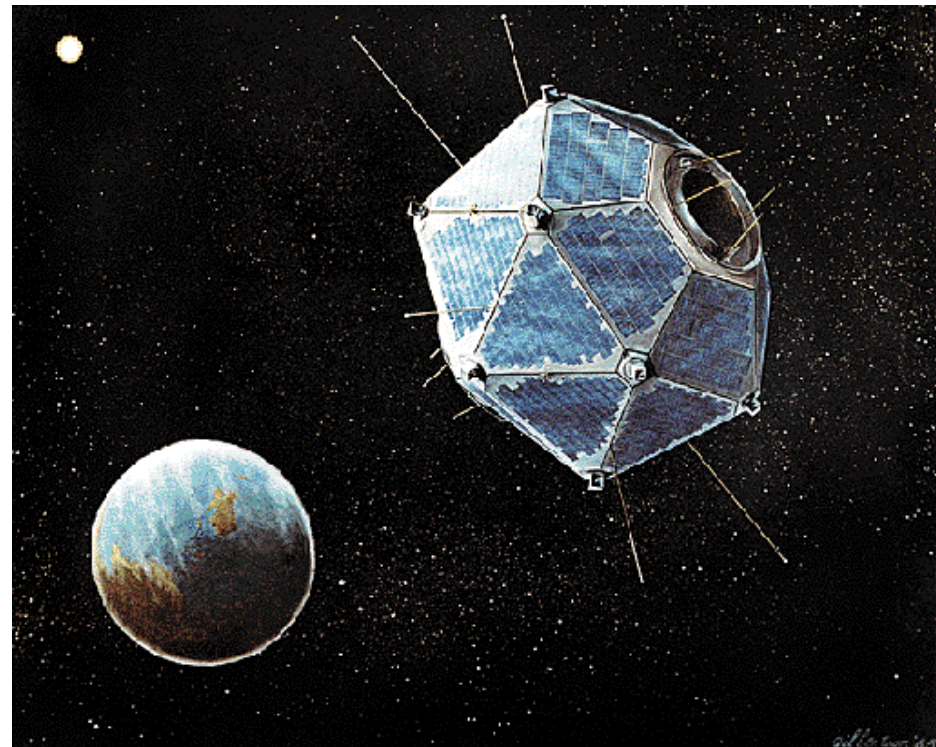
On each spacecraft six 10 cm^3 CsI scintillation counters are so distributed as to achieve a nearly isotropic sensitivity. Individual detectors respond to energy depositions of 0.2–1.0 MeV for *Vela 5* spacecraft and 0.3–1.5 MeV for *Vela 6* spacecraft, with a detection efficiency ranging between 17 and 50 percent. The scintillators are shielded against direct penetration by electrons below ~ 0.75 MeV and protons below ~ 20 MeV. A high-Z shield attenuates photons with energy below that of the counting threshold. No active anticoincidence shielding is provided.

Normalized output pulses from the six detectors are summed into the counting and logics circuitry. Logical sensing of a rapid, statistically significant rise in count rate initiates the recording of discrete counts in a series of quasi-logarithmically increasing time intervals. This capability provides continuous coverage in time which, coupled with isotropic response, is unique in observational astronomy. A time measurement is also associated with each record.

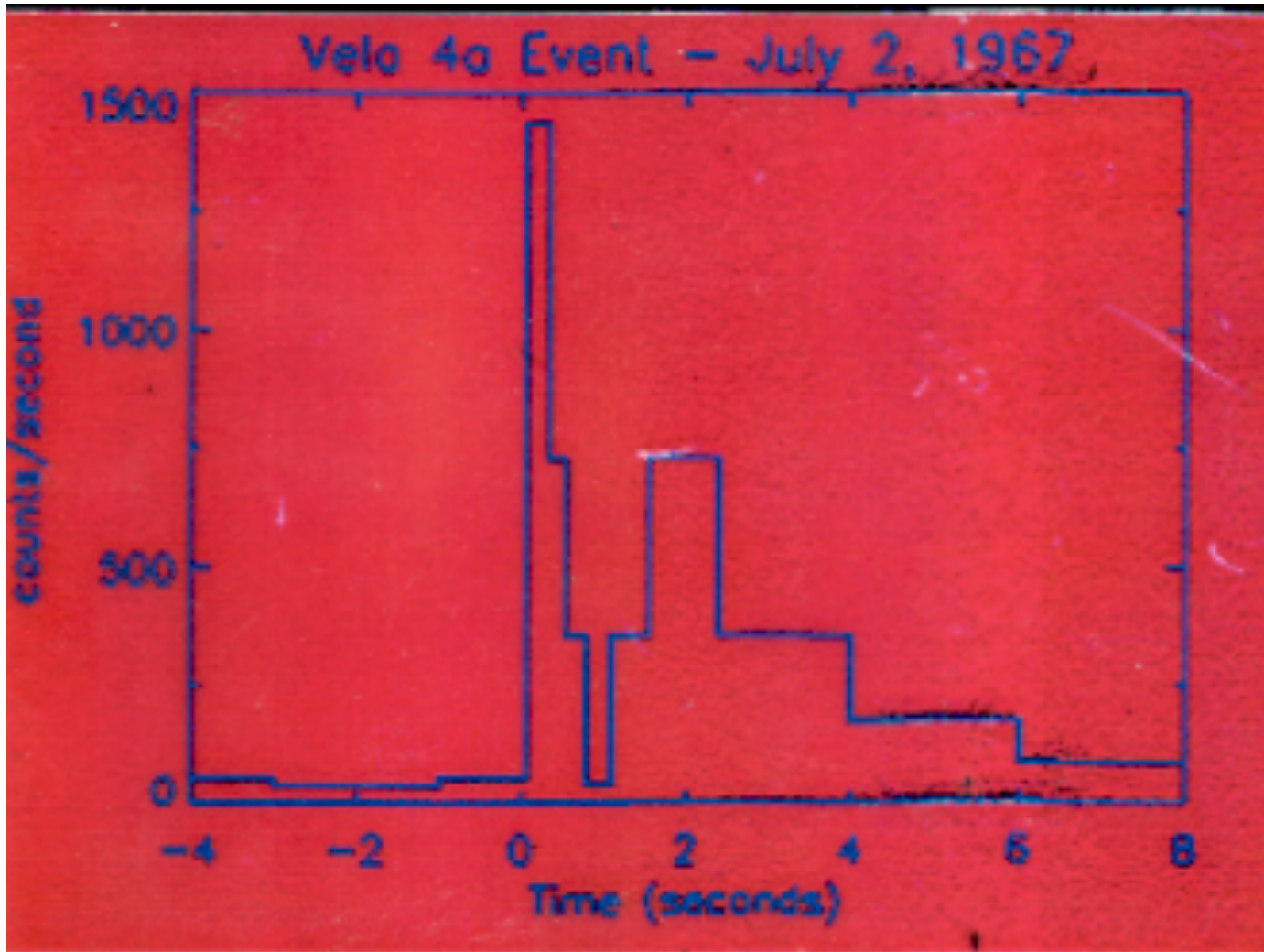
The data accumulations include a background component due to cosmic particles and their secondary effects. The observed background rate, which is a function of the energy threshold, is ~ 150 counts per second for the *Vela 5* spacecraft and ~ 20 counts per second for the *Vela 6* spacecraft.

L85

- Vela satellites discovery (1967 - 1973)



First Detected Gamma-Ray Burst

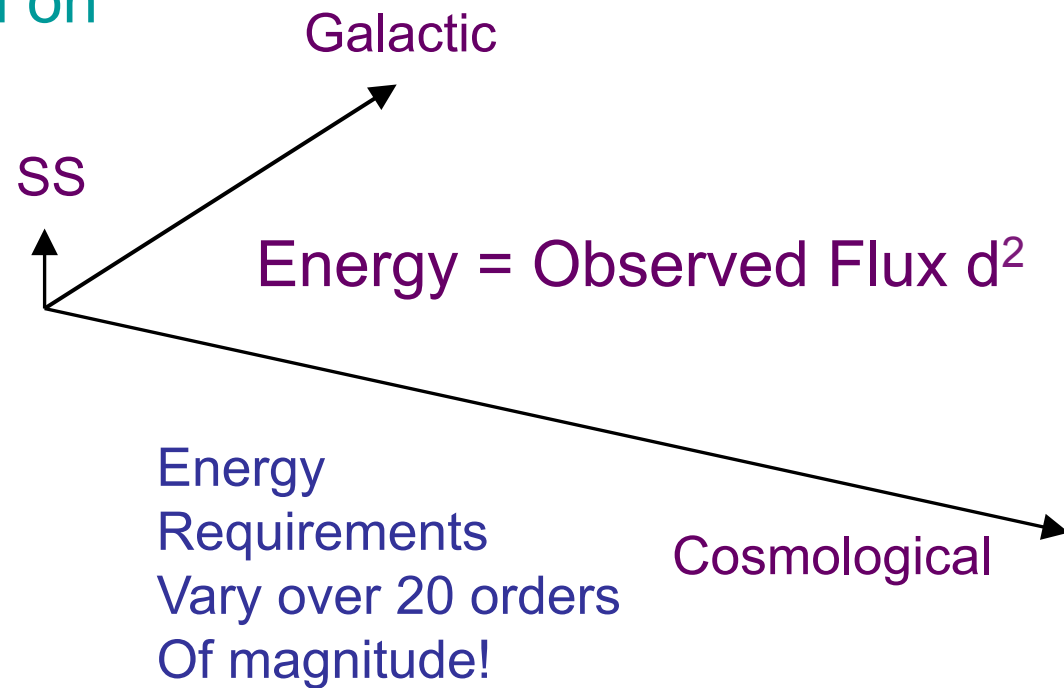


Creativity of Theorists

With so few constraints, theorists came up with all sorts of models relying on a range of physics.

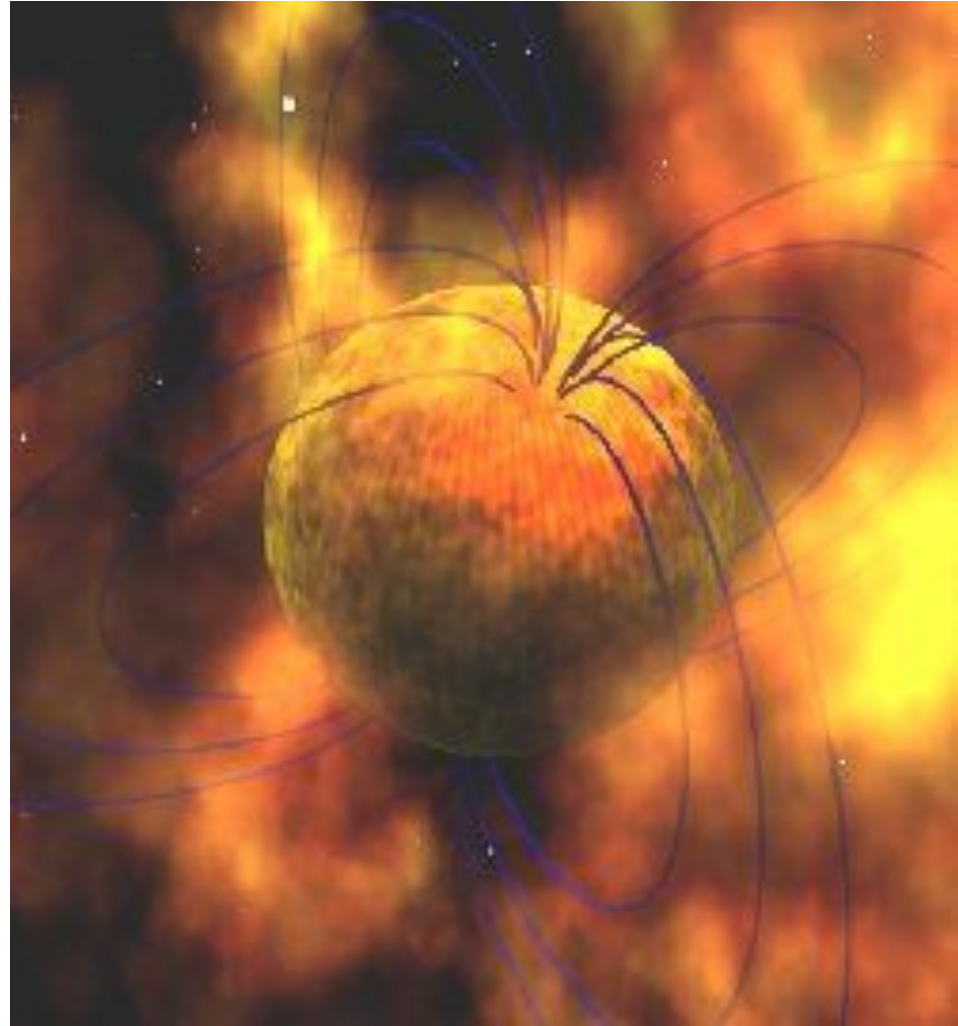
Three Classes based on location:

- Solar System
- Galactic
- Cosmological (outside of the Milky Way)



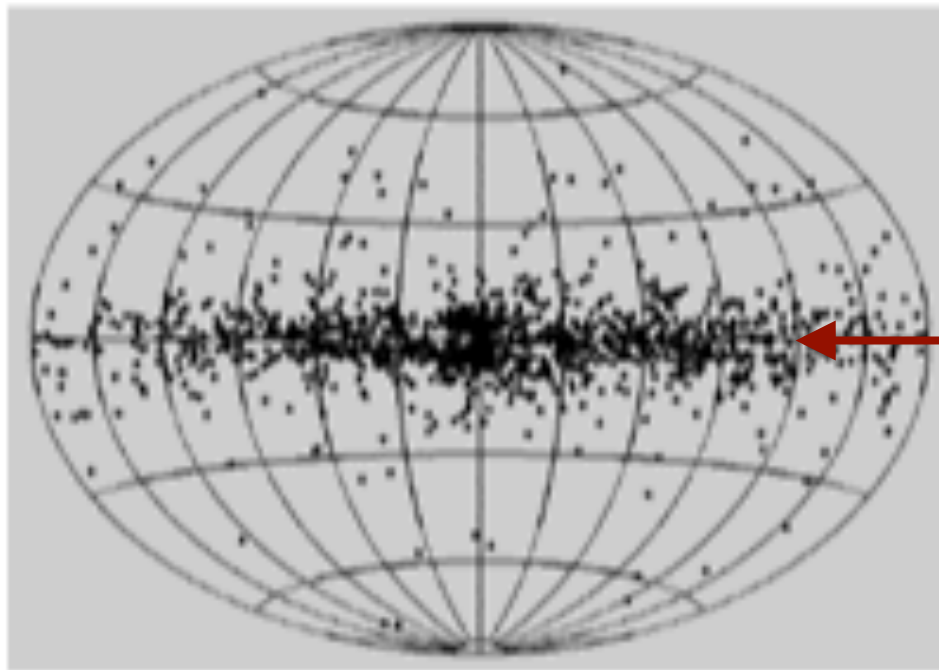
Models for Galactic GRBs

- Accretion
 - I) Binary Companion
 - no companion seen
 - II) SN Fallback – Too long after explosion
- Magnetic Fields
 - ~ 10^{15} G Fields
 - “Magnetars”



If normal GRBs are also neutron stars, GRBs should
Also center around the Galactic Equator.

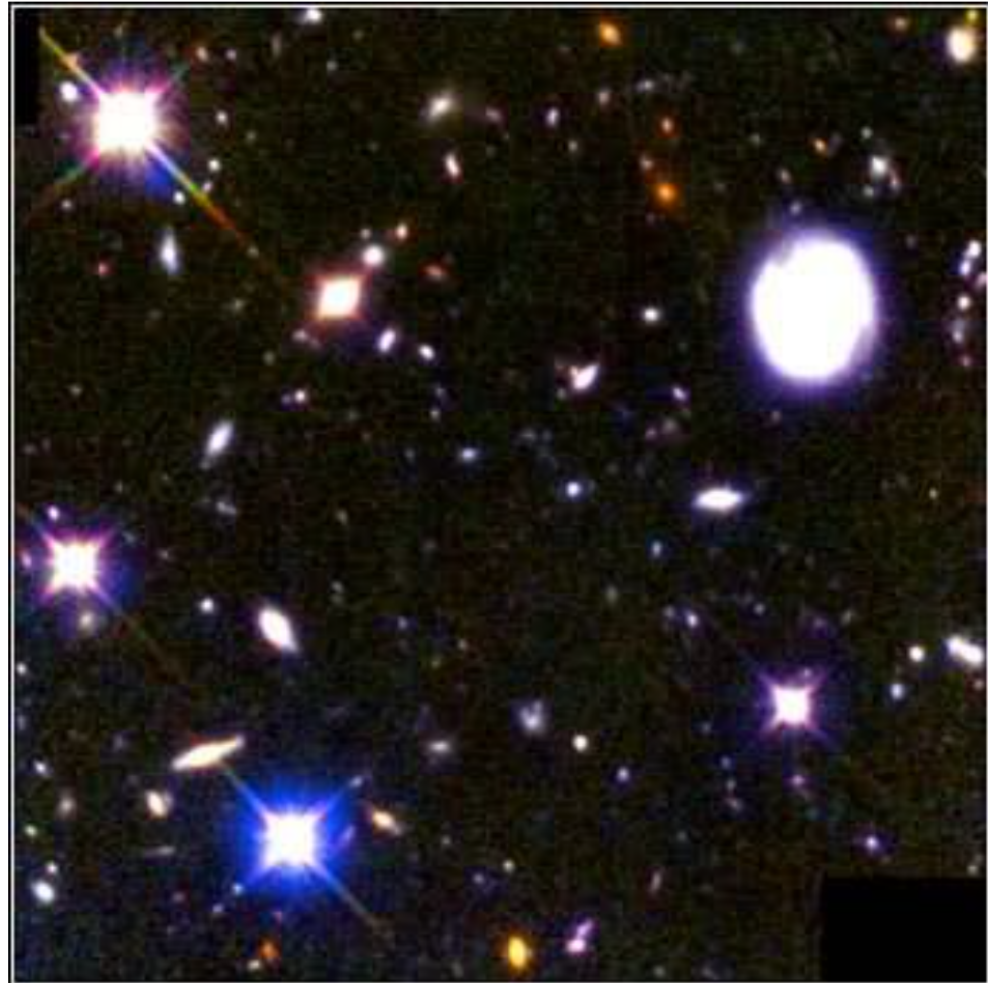
This is a Prediction of the Galactic Models!



Plane of the
Milky Way
Galaxy

Extragalactic Models

- Large distances means large energy requirement (10^{51} erg)
- Event rate rare (10^{-6} - 10^{-5} per year in an L_* galaxy) – Object can be exotic

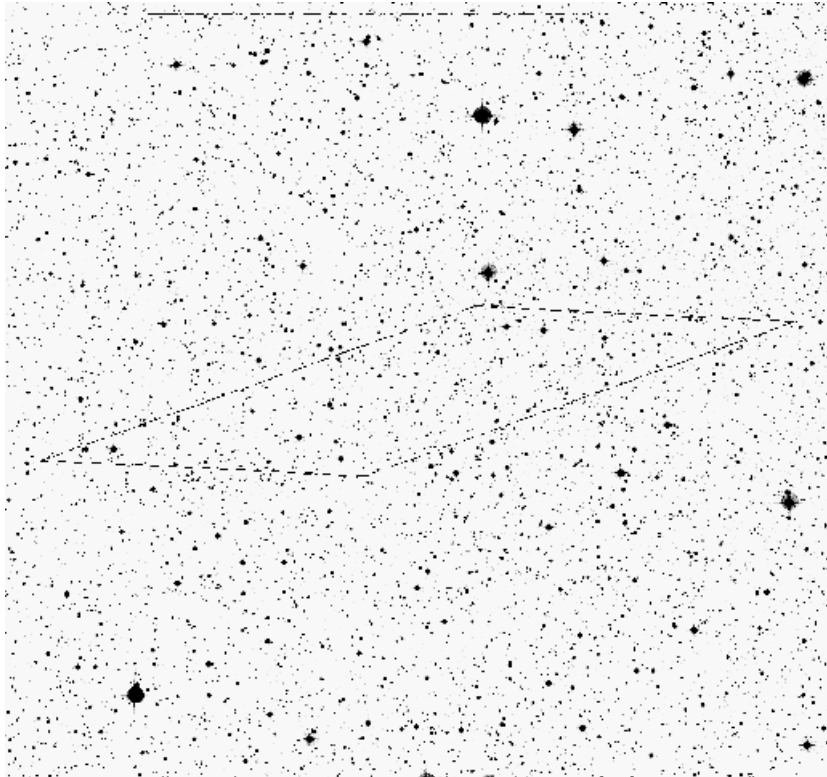


Models for Cosmological GRB

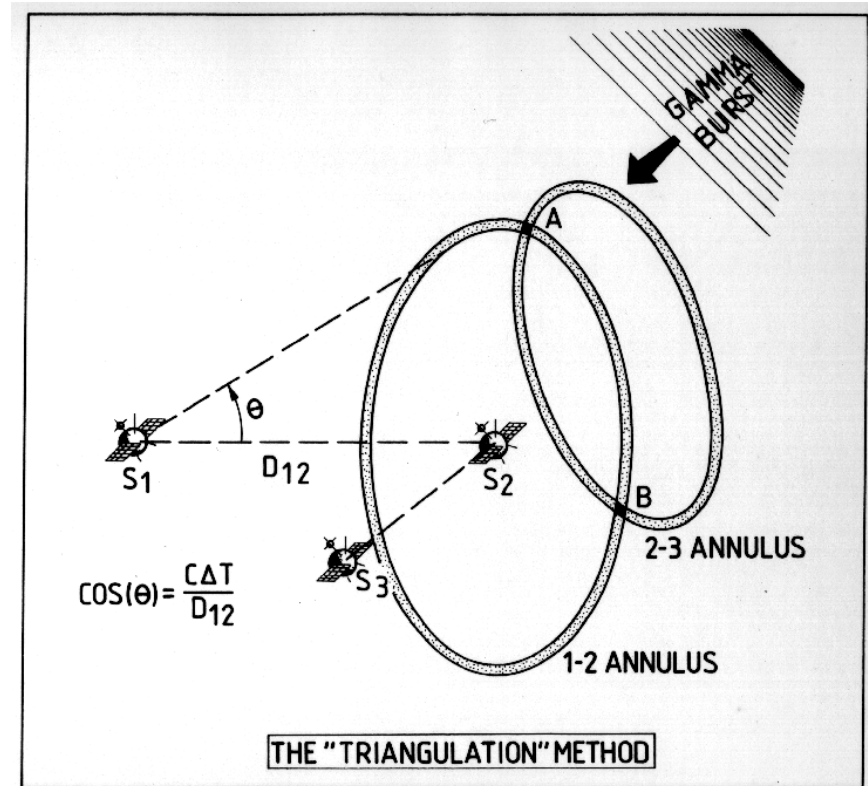


- Collapsing WDs
- Stars Accreting on AGN
- Black Hole Accretion Disks
 - I) Binary Mergers
 - II) Collapsing Stars

GRB History



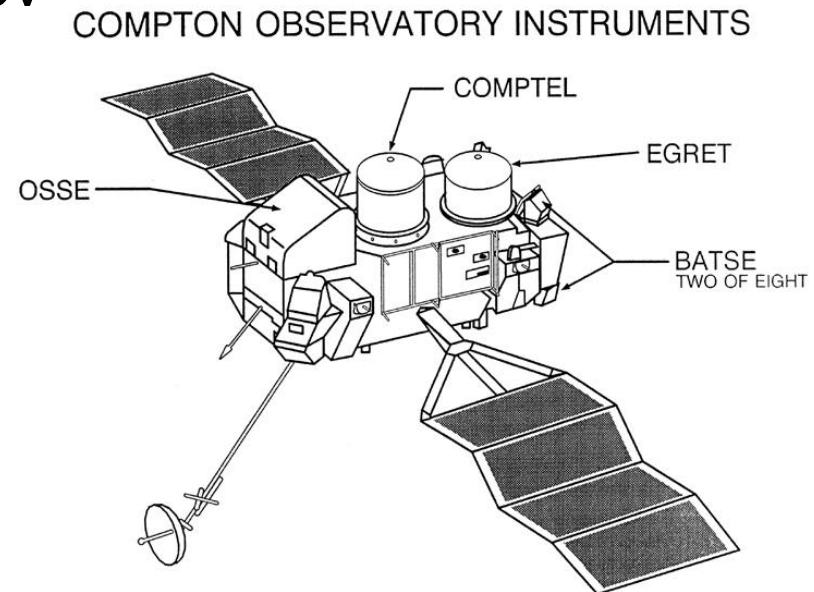
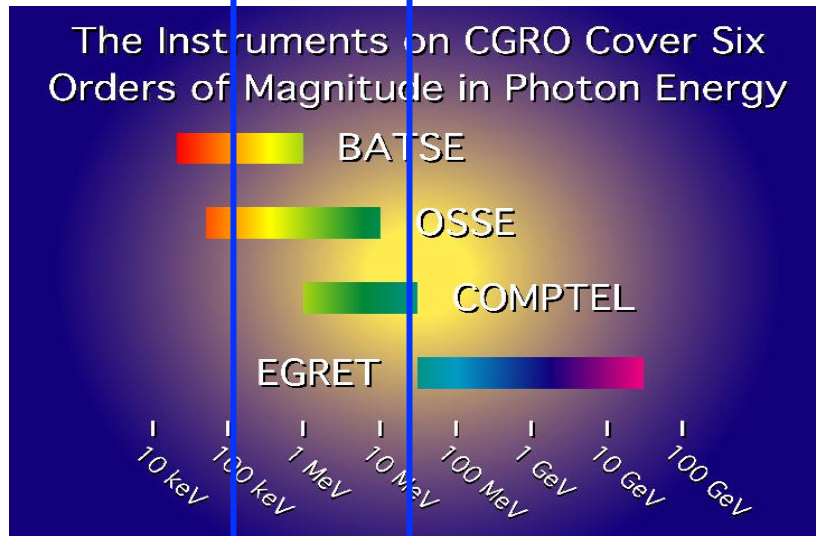
Interplanetary Network (IPN)



<http://www.ssl.berkeley.edu/ipn3/>

The Compton Gamma Ray Observatory

<http://cossc.gsfc.nasa.gov>



The Compton Gamma Ray Observatory (**CGRO**) is a sophisticated satellite observatory dedicated to observing the high-energy Universe. It is the second in NASA's program of orbiting "Great Observatories", following the Hubble Space Telescope. While Hubble's instruments operate at visible and ultraviolet wavelengths, Compton carries a collection of four instruments which together can detect an unprecedented broad range of high-energy radiation called gamma rays. These instruments are the Burst And Transient Source Experiment (**BATSE**), the Oriented Scintillation Spectrometer Experiment (**OSSE**), the Imaging Compton Telescope (**COMPTEL**), and the Energetic Gamma Ray Experiment Telescope (**EGRET**).

The Compton Gamma Ray Observatory

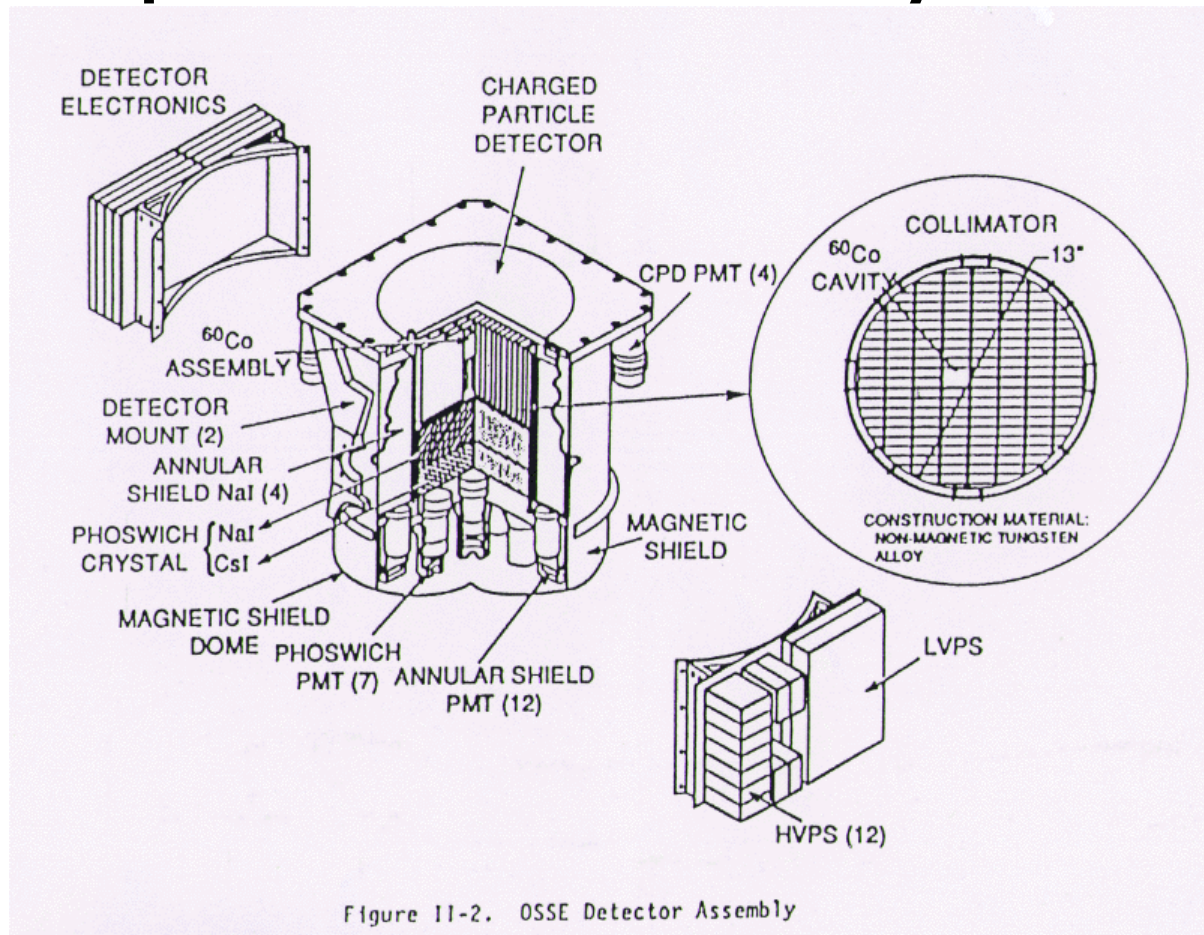
Table 1: SUMMARY OF COMPTON GRO DETECTOR CHARACTERISTICS

	OSSE	COMPTEL	EGRET	BATSE	
				LARGE AREA	SPECTROSCOPY
ENERGY RANGE (MeV)	0.05 to 10.0	0.8 to 30.0	20 to 3 x 10 ⁴	0.03 to 1.3	0.015 to 110
ENERGY RESOLUTION (FWHM)	12.5% at 0.2 MeV 6.0% at 1.0 MeV 4.0% at 5.0 MeV	8.0% at 1.27 MeV 6.5% at 2.75 MeV 6.3% at 4.43 MeV	~20% 100 to 2000 MeV	32% at 0.06 MeV 27% at 0.09 MeV 20% at 0.66 MeV	0.2% at 0.09 MeV 7.2% at 0.66 MeV 5.8% at 1.17 MeV
EFFECTIVE AREA (cm ²)	2013 at 0.2 MeV 1480 at 1.0 MeV 568 at 5.0 MeV	25.8 at 1.27 MeV 29.3 at 2.75 MeV 28.4 at 4.43 MeV	1200 at 100 MeV 1000 at 500 MeV 1400 at 3000 MeV	1000 ea. at 0.03 MeV 1800 ea. at 0.1 MeV 350 ea. at 0.66 MeV	109 ea. at 0.3 MeV 127 ea. at 0.2 MeV 52 ea. at 3 MeV
POSITION LOCALIZATION (STRONG SOURCE)	10 arc min square error box (special mode; 0.1 x Crab spectrum)	0.5 - 1.0 deg (90% confidence; 0.2 x Crab spectrum)	5 to 10 arc min (1 σ radius; 0.2 x Crab spectrum)	3" (strong bursts)	-----
FIELD OF VIEW	3.0° x 11.4°	~ 64°	~ 0.6 sr	4 sr	4 sr
MAXIMUM EFFECTIVE GEOMETRIC FACTOR (cm ² sr)	13	30	1050 (~ 500 MeV)	15000	5000
ESTIMATED SOURCE SENSITIVITY	LINE (3-8) x 10 ⁻³ cm ⁻² s ⁻¹	1.5 x 10 ⁻³ to 6 x 10 ⁻³ cm ⁻² s ⁻¹			0.4% equivalent width (5 sec integration)
(5 x 10 ⁴ sec. on CONTINUUM source, off Galactic Plane)	3 x 10 ⁻⁷ cm ⁻² s ⁻¹ keV ⁻¹ (@1 MeV)	1.6 x 10 ⁻⁴ cm ⁻² s ⁻¹ (3 σ detection, 1-30 MeV)	7 x 10 ⁻⁶ cm ⁻² s ⁻¹ (> 100 MeV) 2 x 10 ⁻⁸ cm ⁻² s ⁻¹ (> 1000 MeV)	3 x 10 ⁻⁸ erg cm ⁻² (1 sec-burst)	

CGRO performance

	BATSE	OSSE	COMPTEL	EGRET
Developer	NASA/Marshall	Naval Research Lab	Univ. N.H. & MPE	NASA/Goddard
Energy Range (MeV)	0.03 to 1.9	0.05 to 10.0	0.08 to 30.0	30.0 to 30000.0
Field of View	entire sky	3.0 x 11.4 degrees	64 degrees	0.6 steradians
Spectral Resolution (FWHM)	32 % at 0.06 MeV 27 % at 0.09 MeV 20 % at 0.66 MeV	12.5 % at 0.2 MeV 5. % at 1.0 MeV 4.0 % at 5.0 MeV	8.8 % at 1.27 MeV 6.5 % at 2.75 MeV 6.3 % at 4.43 MeV	20 %
Effective Area (cm²)	1000 ea. at 0.03 MeV 1800 ea. at 0.1 MeV 550 ea. at 0.55 MeV	2013 at 0.2 MeV 1400 at 1.0 MeV 55 at 5.0 MeV	25.0 at 1.27 MeV 29.3 at 2.75 MeV 29.4 at 4.43 MeV	1200 at 100 MeV 1600 at 500 MeV 1400 at 3000 MeV
Spatial Resolution (for strong sources)	3 degrees	10 x 10 arcminutes	0.5 - 1.0 degrees	5 - 10 arcminutes

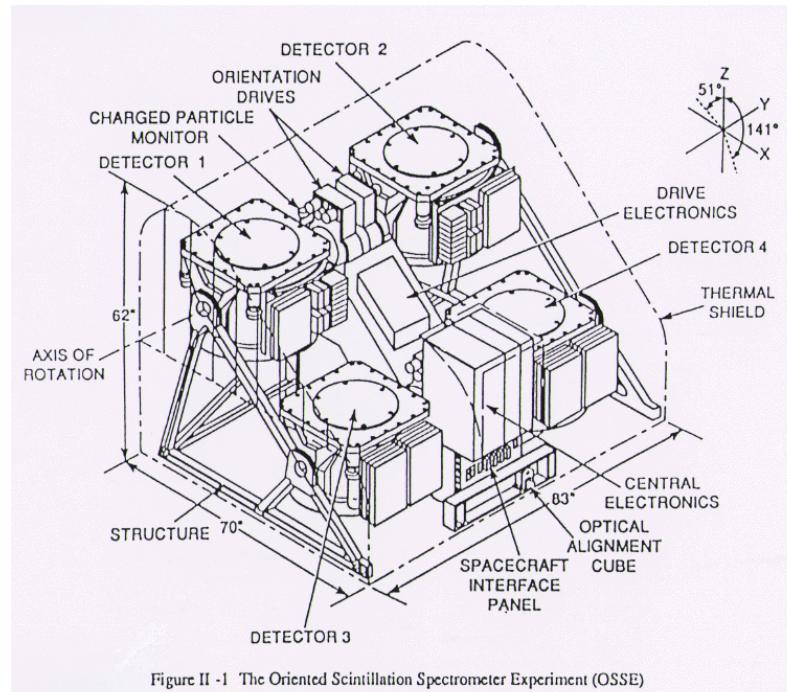
The Compton Gamma Ray Observatory



OSSE

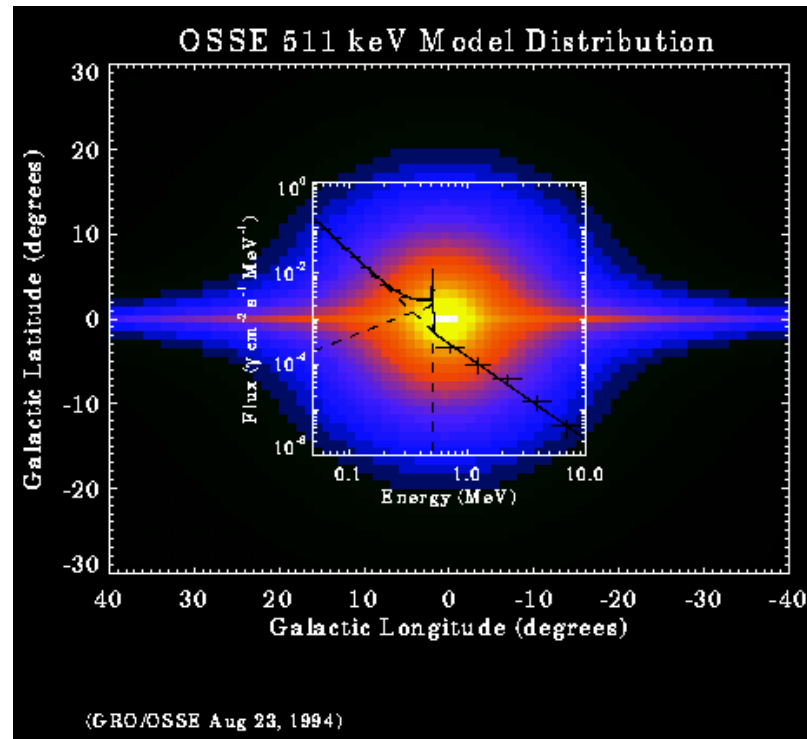
- 0.05-10 MeV
- e^+e^- annihilation, solar flares

OSSE detector



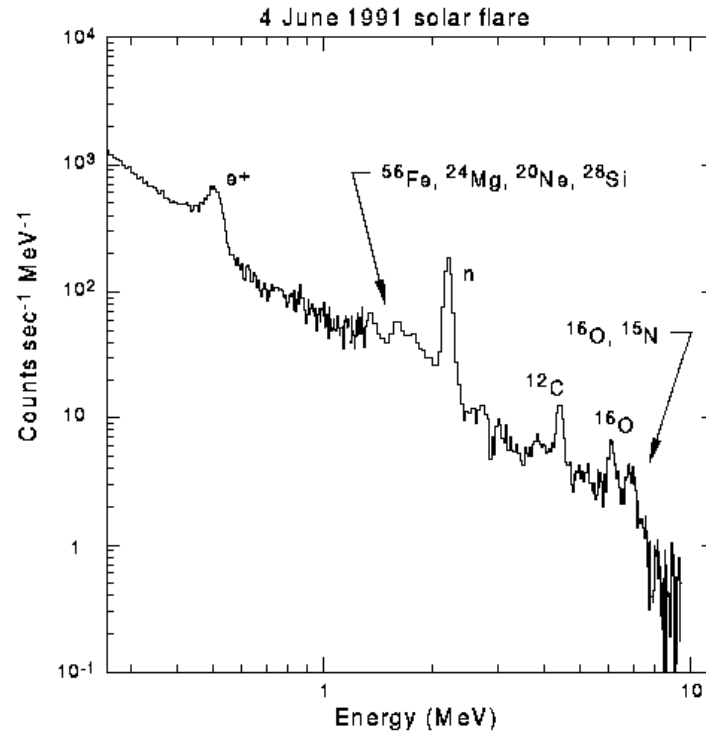
The Oriented Scintillation [Spectrometer](#) Experiment (OSSE) measured the distribution of the energy emitted from a number of gamma-ray sources, and as such studied nuclear lines in solar flares, radioactive decay of nuclei in [supernova](#) remnants, and [matter](#)-antimatter annihilation taking place near the center of our [galaxy](#). OSSE consisted of four NaI scintillation crystals, and was [sensitive](#) to gamma rays with energies ranging from 50 keV to 10 MeV. Each of the detectors could be pointed individually. For most instances, observations of a gamma ray source were alternated with observations of nearby blank sky so as to be able to determine the background gamma ray emission.

The Compton Gamma Ray Observatory



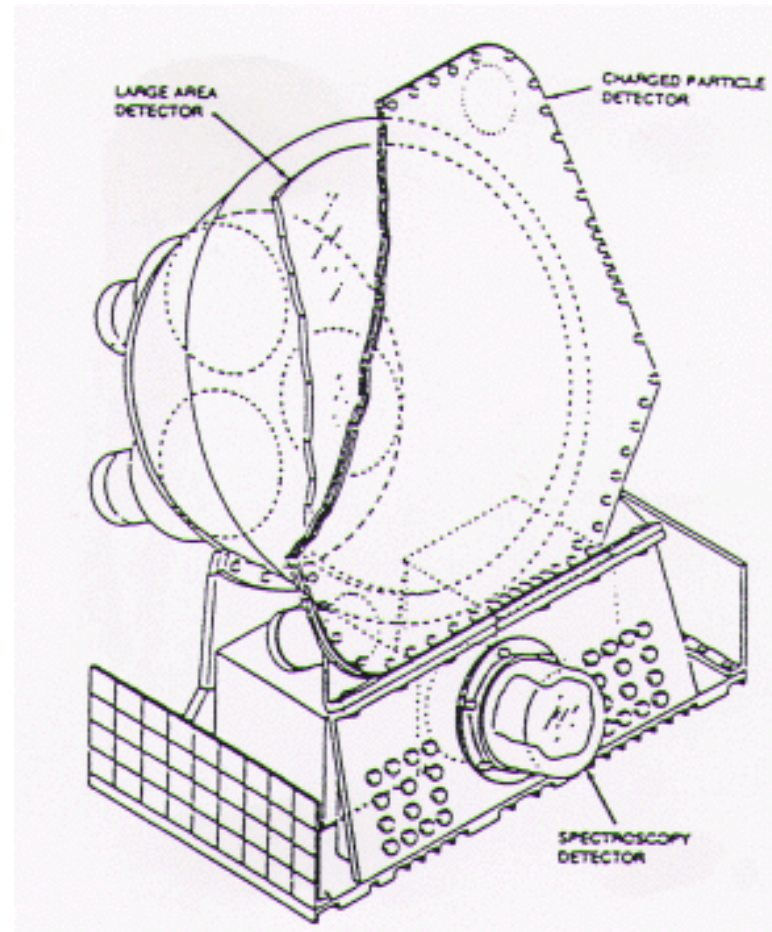
Intensity of gamma-ray emission from [positron-electron annihilation](#) in the plane of our Galaxy near the Galactic center. The emission is at 511 keV, which is the rest-mass energy of the electron and positron. The map is of a model that fits the OSSE 511 keV observations. OSSE has discovered that the radiation is mostly contained in a region of about 10 degrees diameter centered on the center of the Galaxy. The line plot superimposed on the map represents an OSSE observation of the 511 keV emission line.

The Compton Gamma Ray Observatory



On June 4, 1991, the OSSE instrument observed a bright [high-energy flare](#) from an intensely active region of the sun. The energy spectrum of the flare shown in this slide indicates that solar flares accelerate particles to extremely high energies causing interactions which produce nuclear emission lines from excited atomic nuclei of Fe, Mg, Ne, Si, C, O, and N, along with emission lines from the formation of deuterium by neutron capture (labeled "n" in the slide) and electron-positron annihilation (labeled "e+").

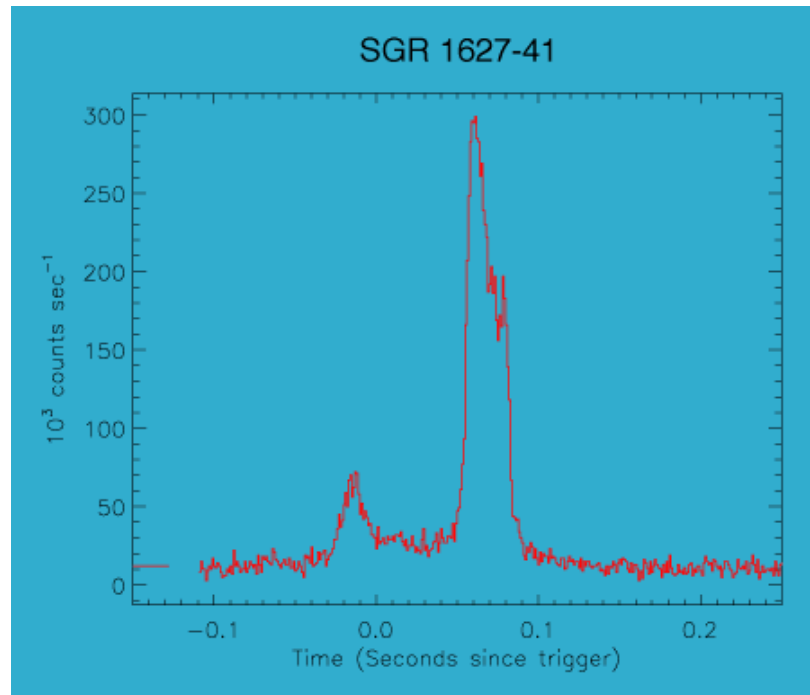
The Compton Gamma Ray Observatory



BATSE

- 20 keV - 10 MeV
- GRB, SGR, X-ray sources

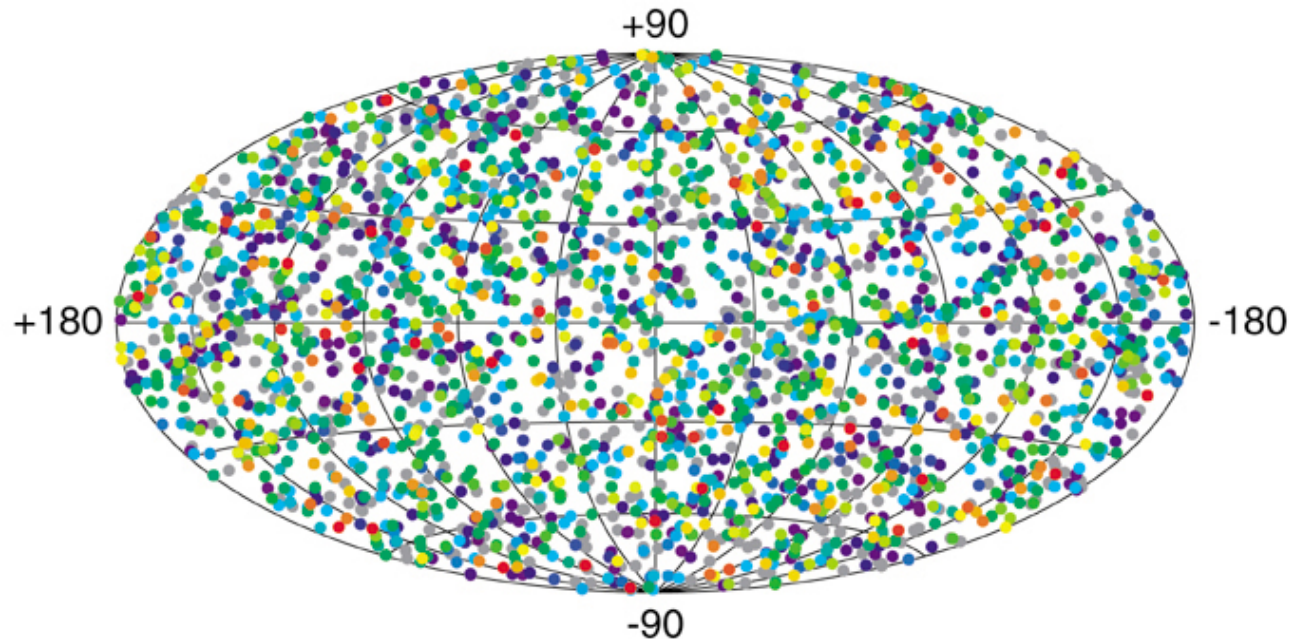
The Compton Gamma Ray Observatory



Soft Gamma Repeaters are one of the biggest success stories of BATSE on CGRO. These recurrent soft X-ray transients were discovered in the early '80s and identified as a separate population of young neutron stars that emitted frequent, but randomly spaced in time, outbursts of low-energy gamma rays, of very short duration, usually tenths of seconds. Until 1998 only three such sources were known; SGR 1627-41 is the first new SGR discovered with BATSE in June 1998. The figure displays a tremendous outburst from the source that reached a peak count rate of ~ 300000 counts s^{-1} , and lasted less than 150 ms. In 1998, SGRs were shown to possess extremely strong magnetic fields, of the order of 10^{14} Gauss, i.e., roughly 1000 times stronger than the average magnetic fields of radio pulsars and binary X-ray pulsars. They now form a well defined new class of objects, together with the Anomalous X-ray Pulsars (AXPs), called "**magnetars**".

The Compton Gamma Ray Observatory

2704 BATSE Gamma-Ray Bursts

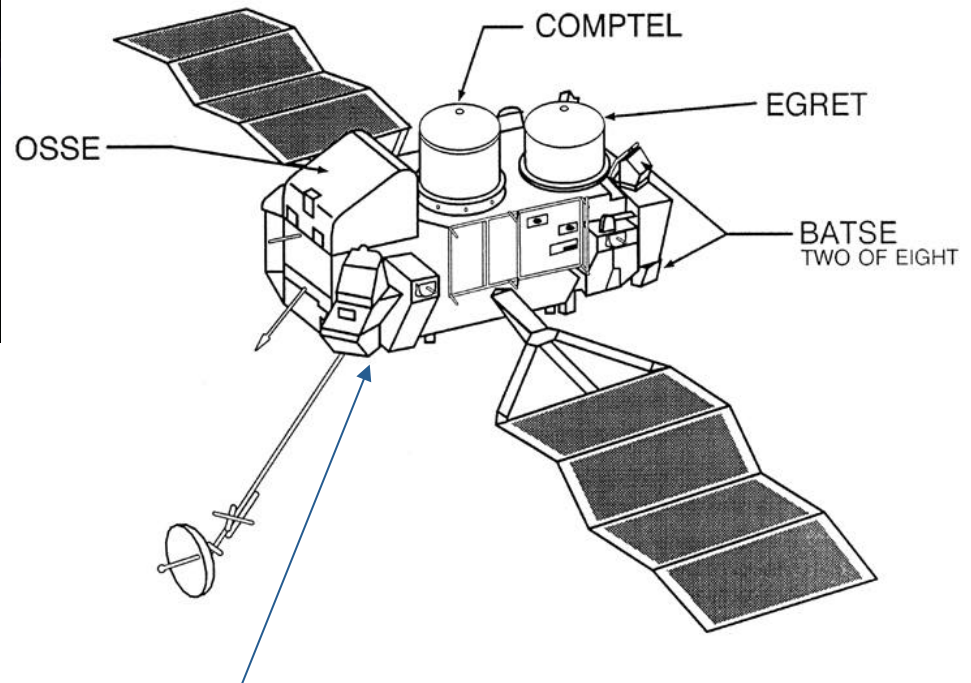


BATSE can determine directions to [gamma-ray bursts](#) with an accuracy of a few degrees. This diagram shows the positions of 2704 bursts detected with BATSE over 9 years of operation. The map is an Aitoff equal-area projection in Galactic coordinates. The only anisotropy detectable in the distribution is due to a small anisotropy in BATSE's sky exposure. The isotropic source distribution, combined with information from the burst intensity distribution, showed conclusively that the burst sources do not reside in the Galactic disk, as previously thought. This discovery initiated a paradigm shift to the view that the sources lie at [cosmological distances](#). Direct redshift measurements have now confirmed this interpretation, making gamma-ray bursts the most powerful explosions in the Universe.

CGRO-BATSE (1991-2000)



COMPTON OBSERVATORY INSTRUMENTS



The Instruments on CGRO Cover Six Orders of Magnitude in Photon Energy

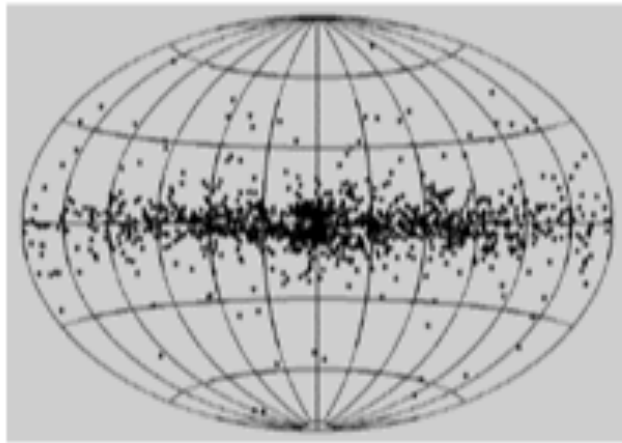


10 keV 100 keV 1 MeV 10 MeV 100 MeV 1 GeV 10 GeV 100 GeV

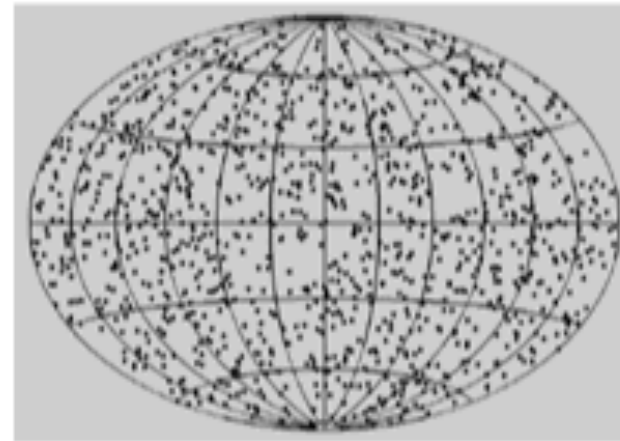
CGRO/BATSE (20 keV ÷ 10 MeV)

GRB history

Distribution of Gamma-Ray Bursts on the Sky



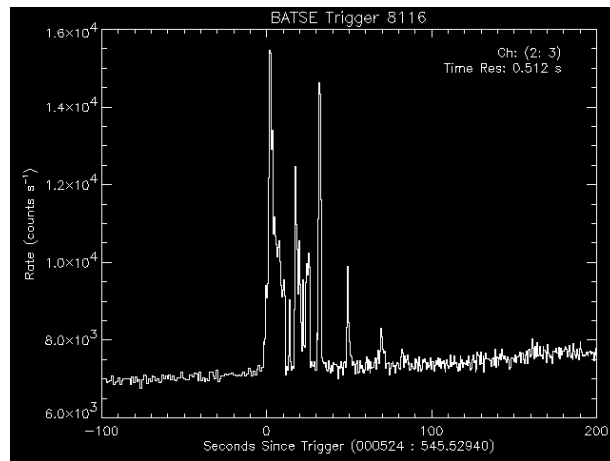
Expected



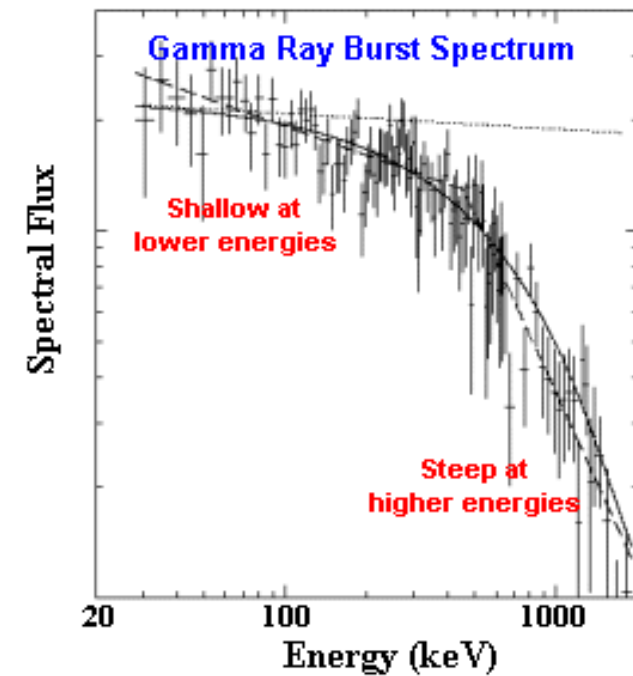
Observed

Gamma-Ray Bursts

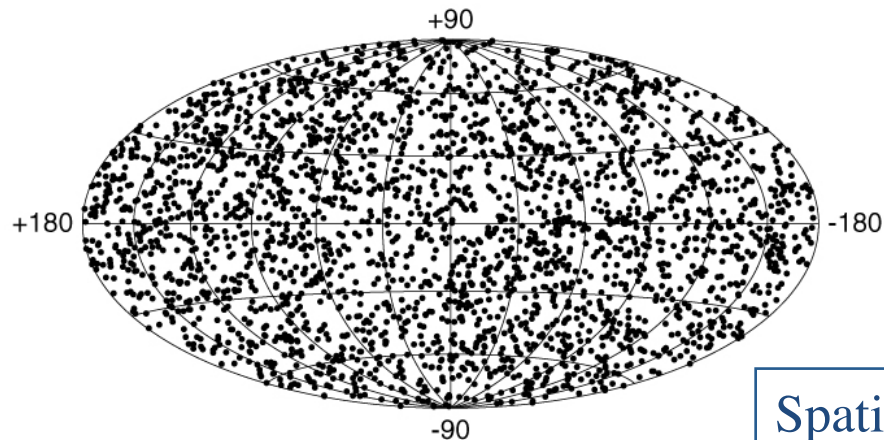
Temporal behaviour



Spectral shape



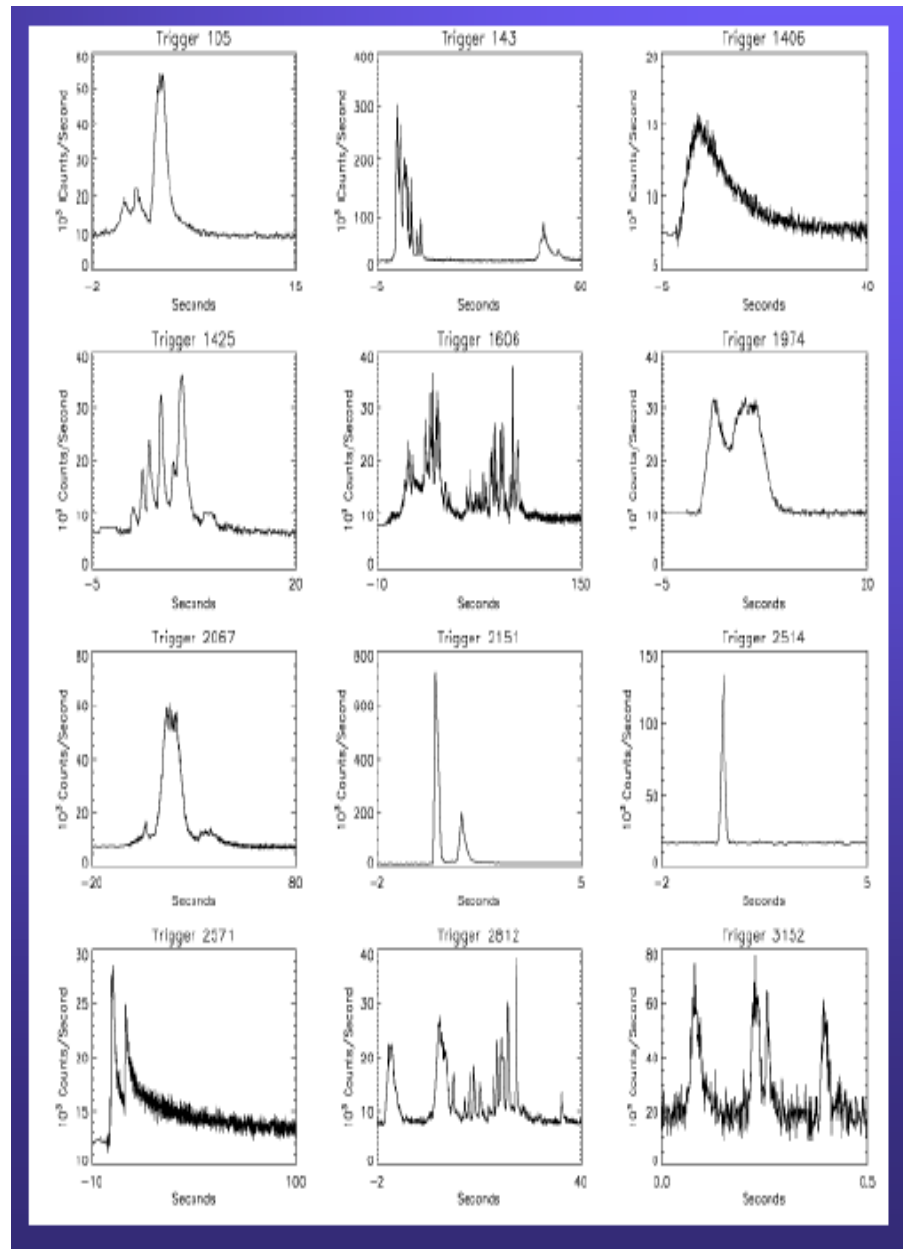
2704 BATSE Gamma-Ray Bursts



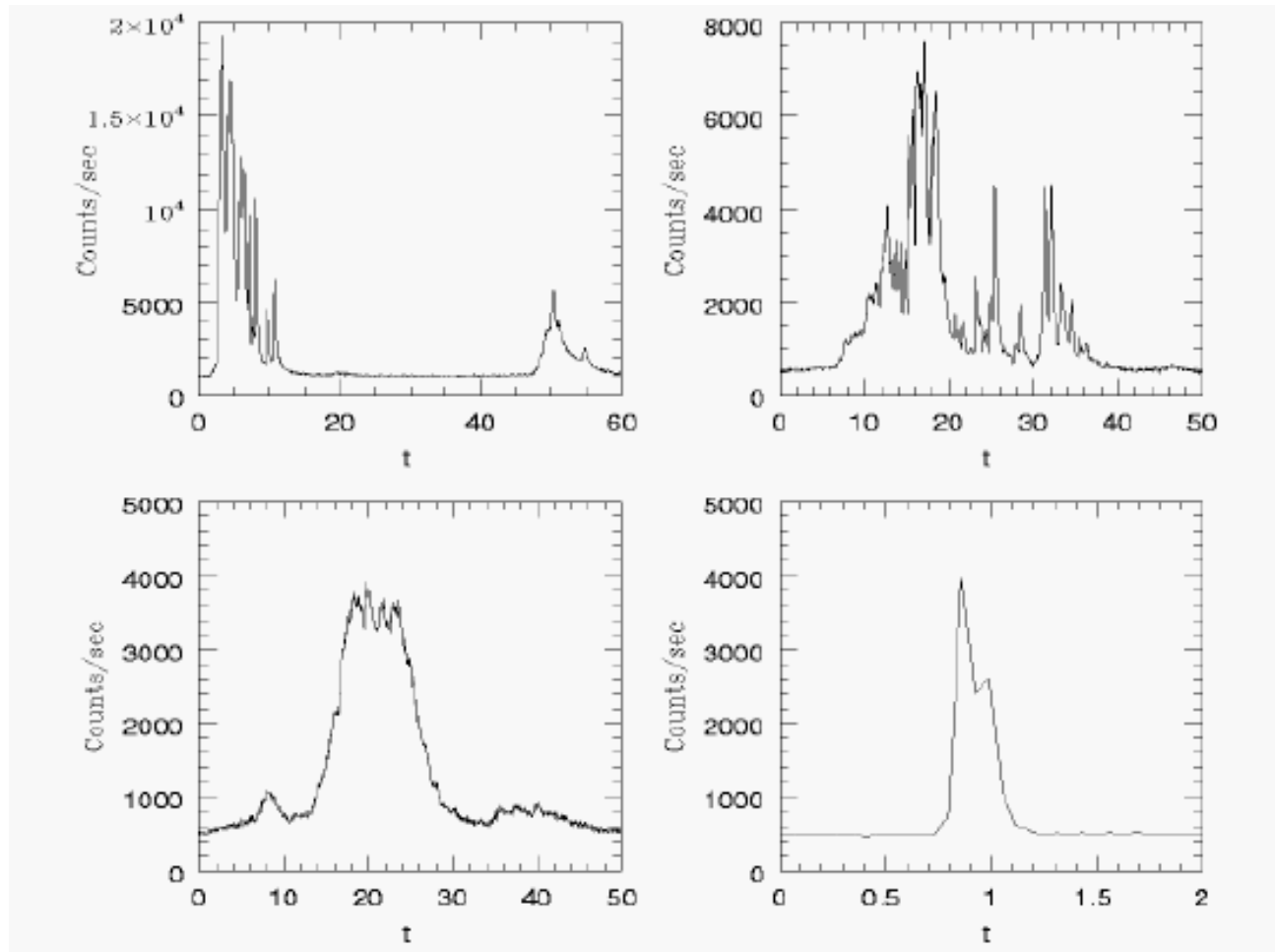
Spatial distribution

The GRB phenomenon

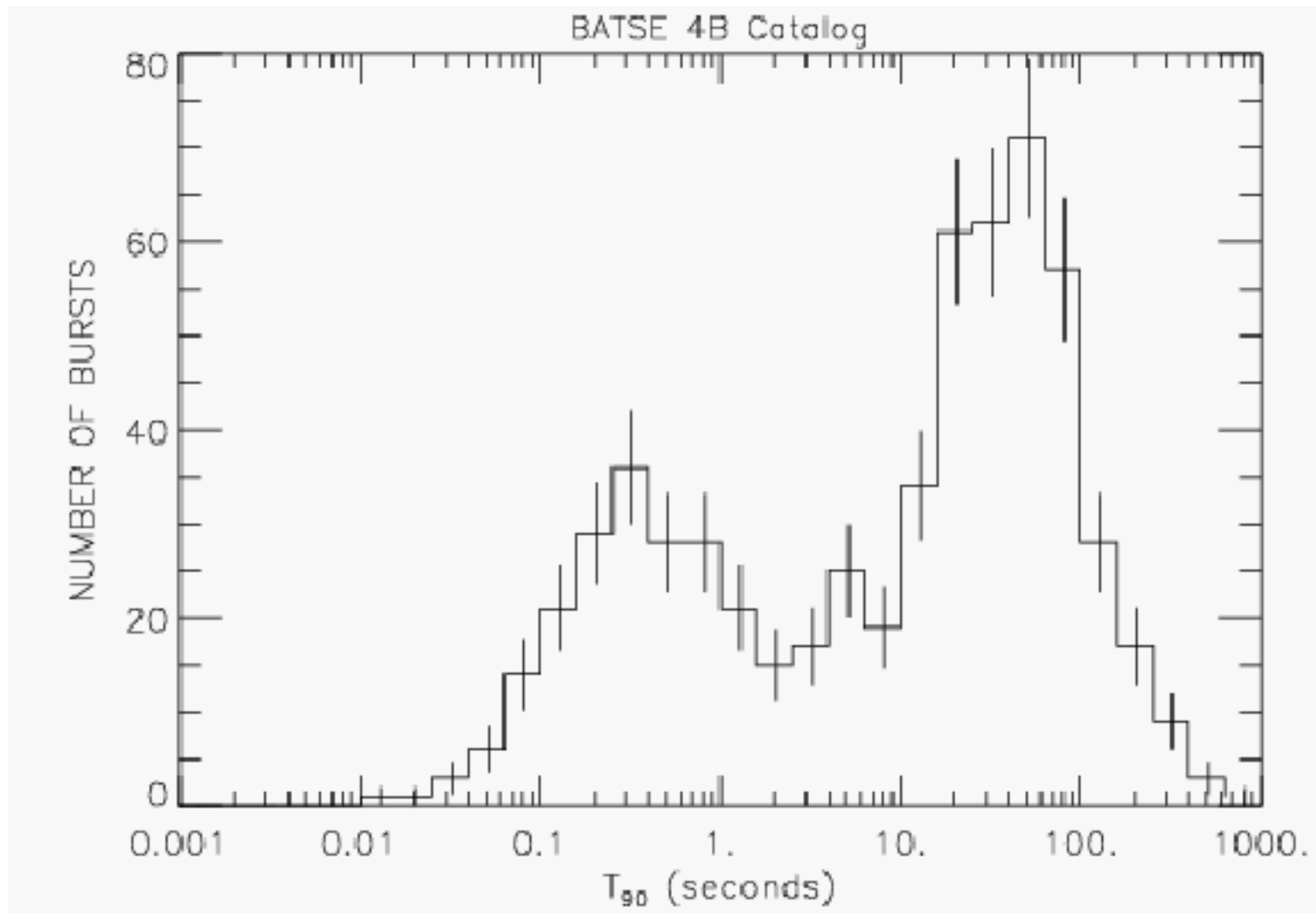
- most of the flux detected from 10-20 keV up to 1-2 MeV
- measured rate (by an all-sky experiment on a LEO satellite): ~ 0.8 / day; estimated true rate ~ 2 / day
- fluences (= av.flux * duration) typically of $\sim 10^{-7}$ – 10^{-4} erg/cm²
- diverse and unclassifiable light curves



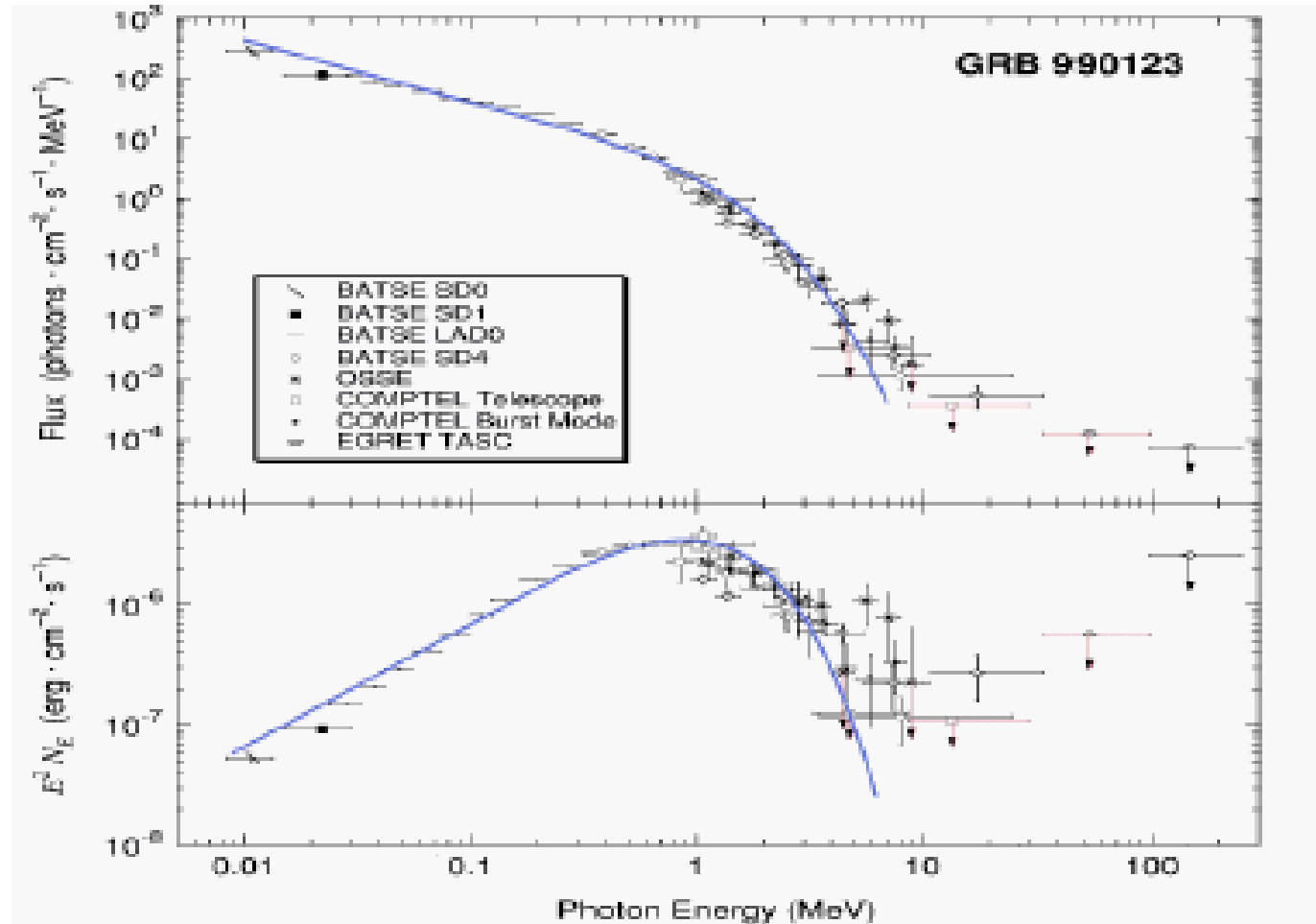
BATSE (1991-2000)



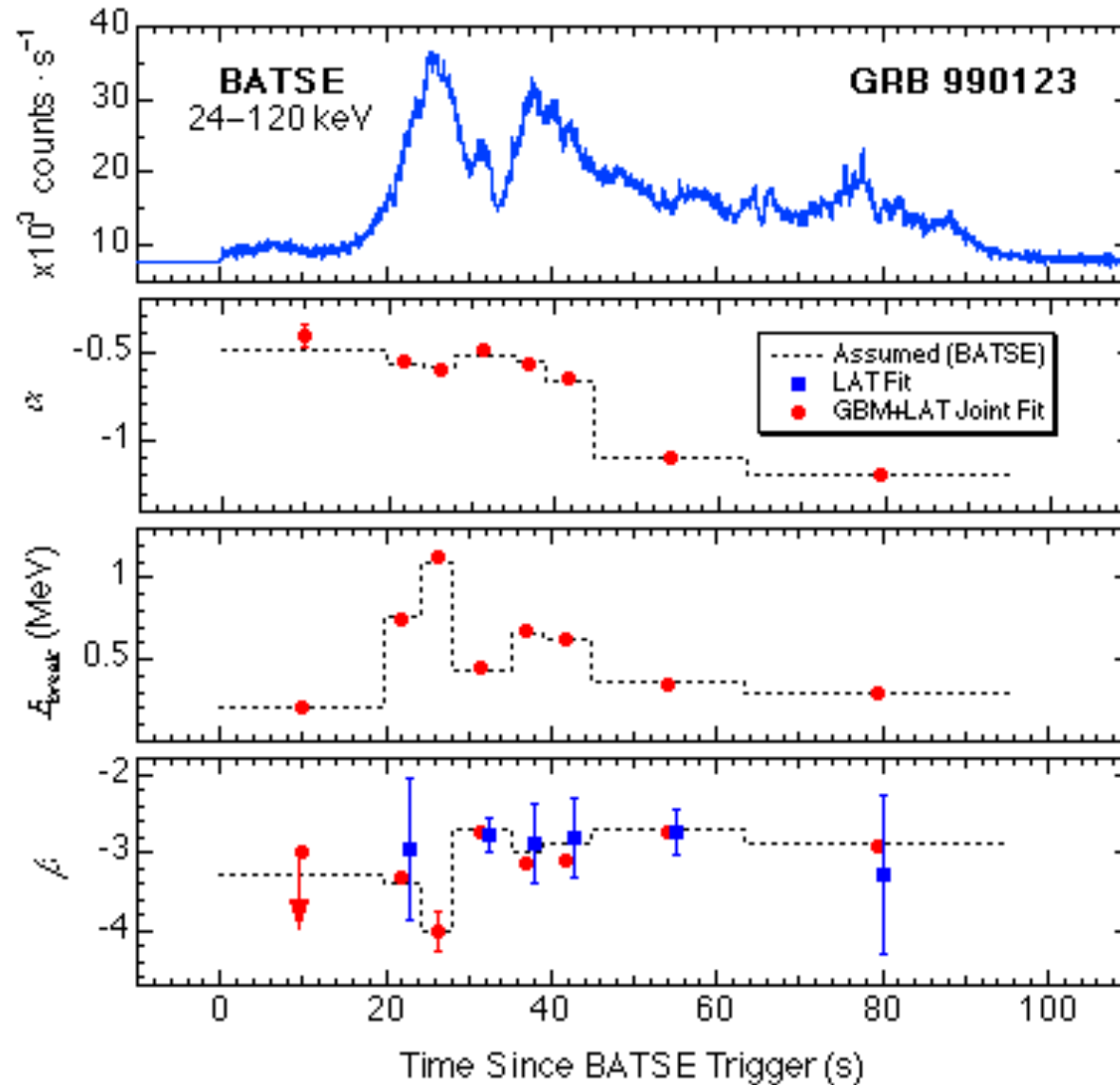
BATSE (1991-2000)



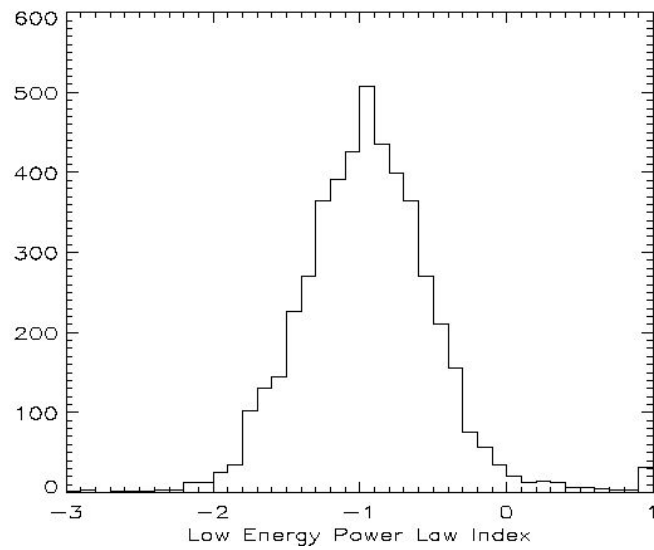
BATSE (1991-2000)



Spectral Evolution

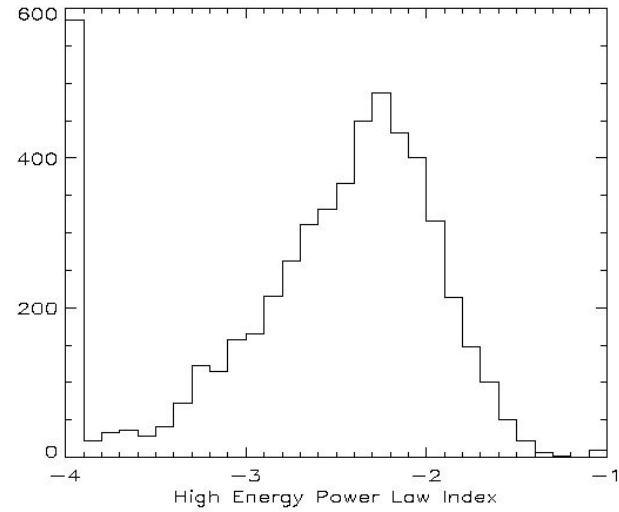


Spectral variability

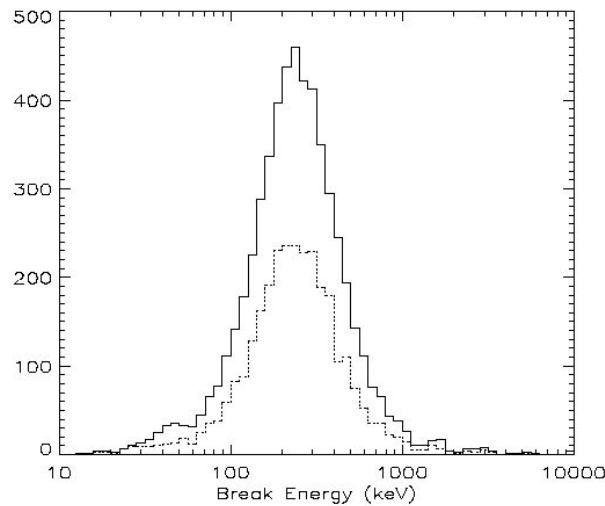


alpha

Epeak



beta



Preece et al. (2000)

The $E_{p,i}$ – Eiso correlation

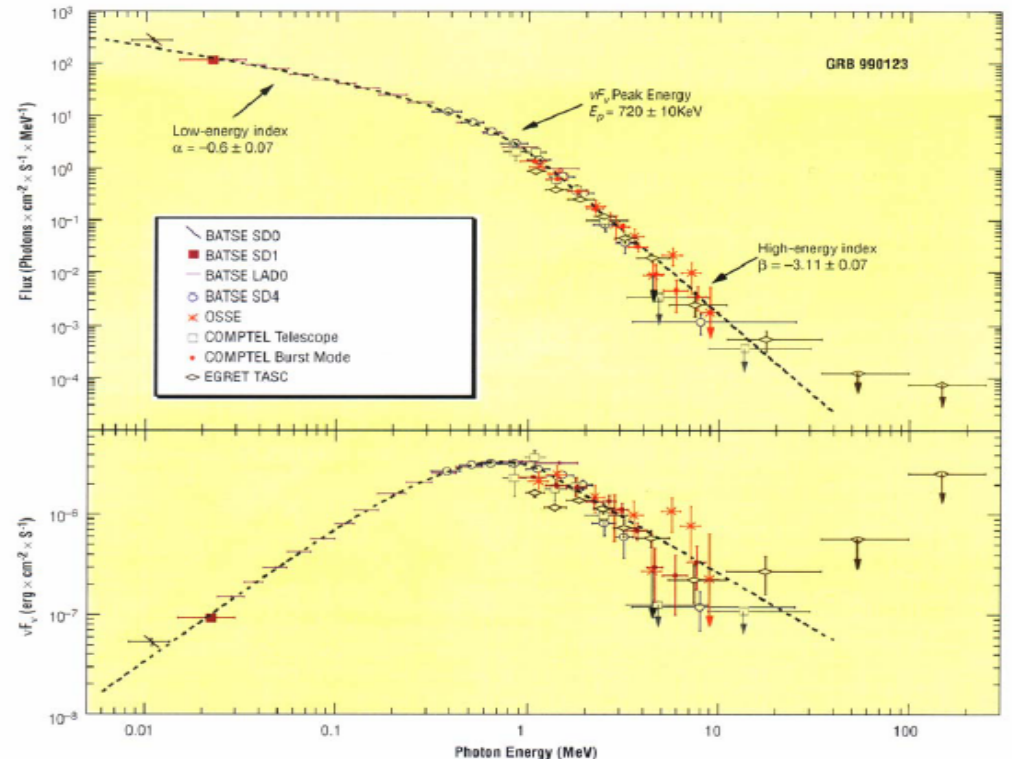
- spectra typically described by the empirical Band function with parameters α = low-energy index, β = high-energy index, E_0 =break energy
- $E_p = E_0 \times (2 + \alpha) =$ peak energy of the νF_ν spectrum

$$N_E(E) = A \left(\frac{E}{100 \text{ keV}} \right)^\alpha \exp \left(- \frac{E}{E_0} \right),$$

$(\alpha - \beta)E_0 \geq E$

$$= A \left[\frac{(\alpha - \beta)E_0}{100 \text{ keV}} \right]^{\alpha - \beta} \exp(\beta - \alpha) \left(\frac{E}{100 \text{ keV}} \right)^\beta,$$

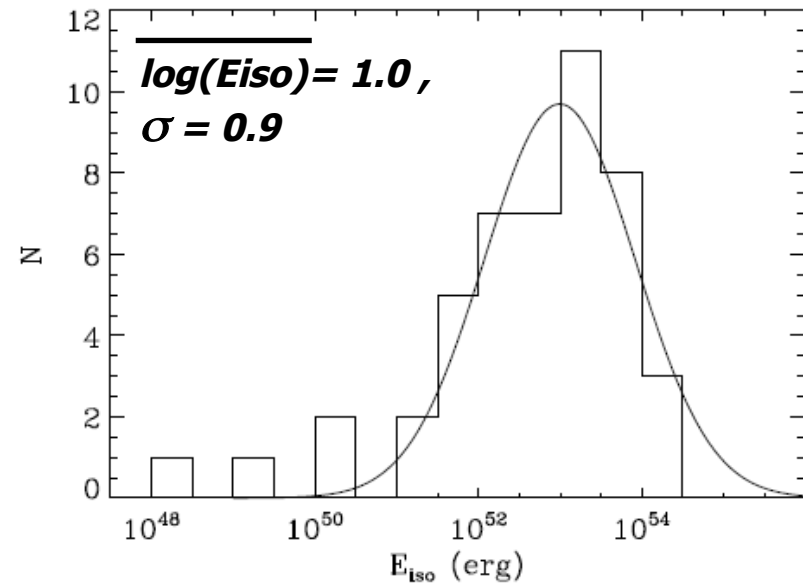
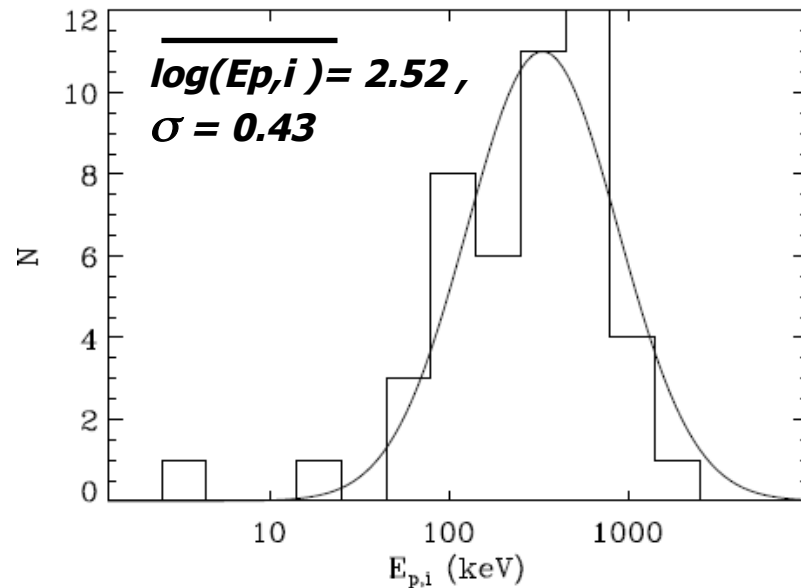
$(\alpha - \beta)E_0 \leq E$



- all GRBs with measured redshift lie at cosmological distances ($z = 0.033 - 6.3$) (except for the peculiar GRB980425, $z=0.0085$)
- from distance, fluence and spectrum, it is possible to estimate the cosmologica-rest farme peak energy $E_{p,i}$ and the radiated energy assuming isotropic emission, E_{iso}

$$E_{p,i} = E_p \times (1 + z)$$

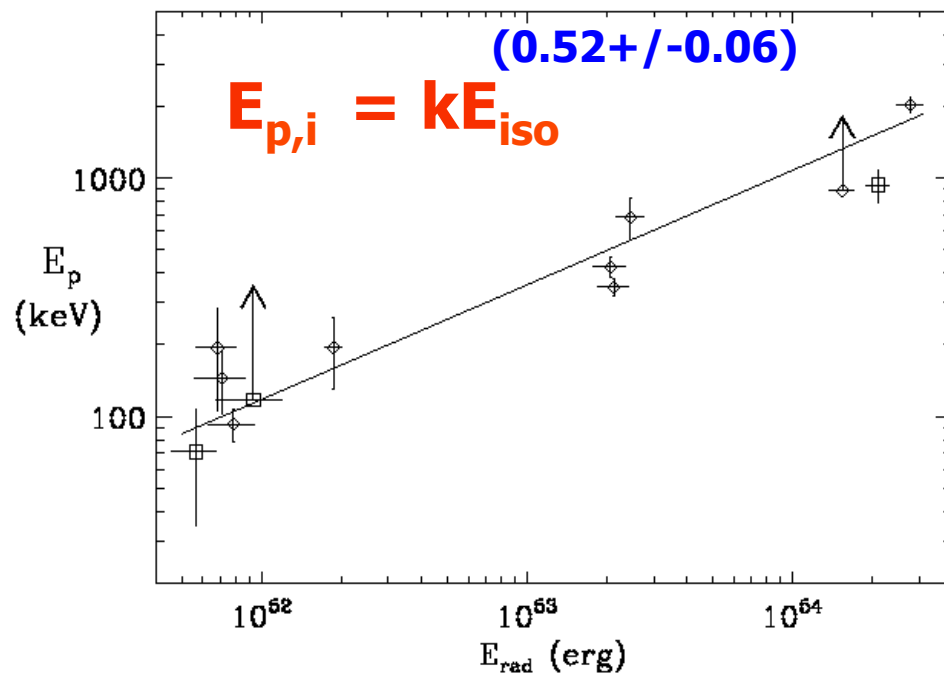
$$E_{\gamma,iso} = \frac{4\pi D_l^2}{(1+z)} \int_{1/1+z}^{10^4/1+z} E N(E) dE \text{ erg}$$



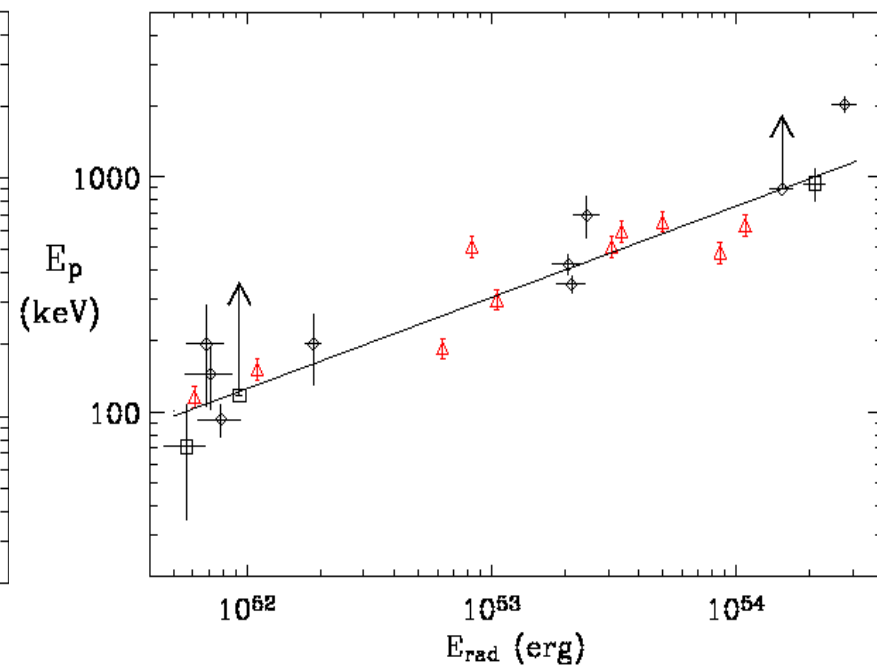
$E_{p,i}$ and E_{iso} distributions for a sample of 41 long GRBs (Amati 2006)

The $E_{p,i}$ – Eiso correlation

- Amati et al. (2002) analyzed a sample of 12 BeppoSAX events with known redshift found evidence of a strong correlation between $E_{p,i}$ and Eiso , highly significant ($\rho = 0.949$, chance prob. 0.005%)
- by adding data from BATSE and HETE-2 of 10 more GRBs the correlation was confirmed and its significance increased

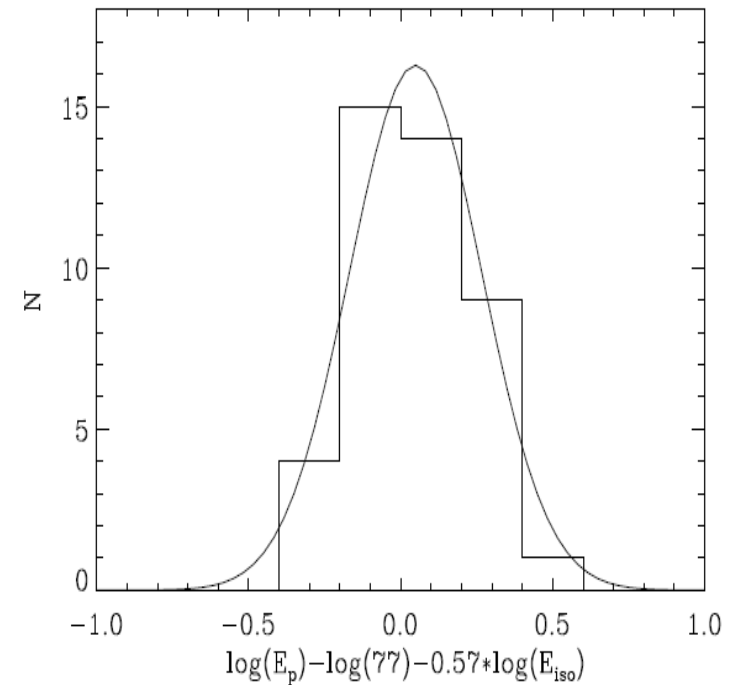
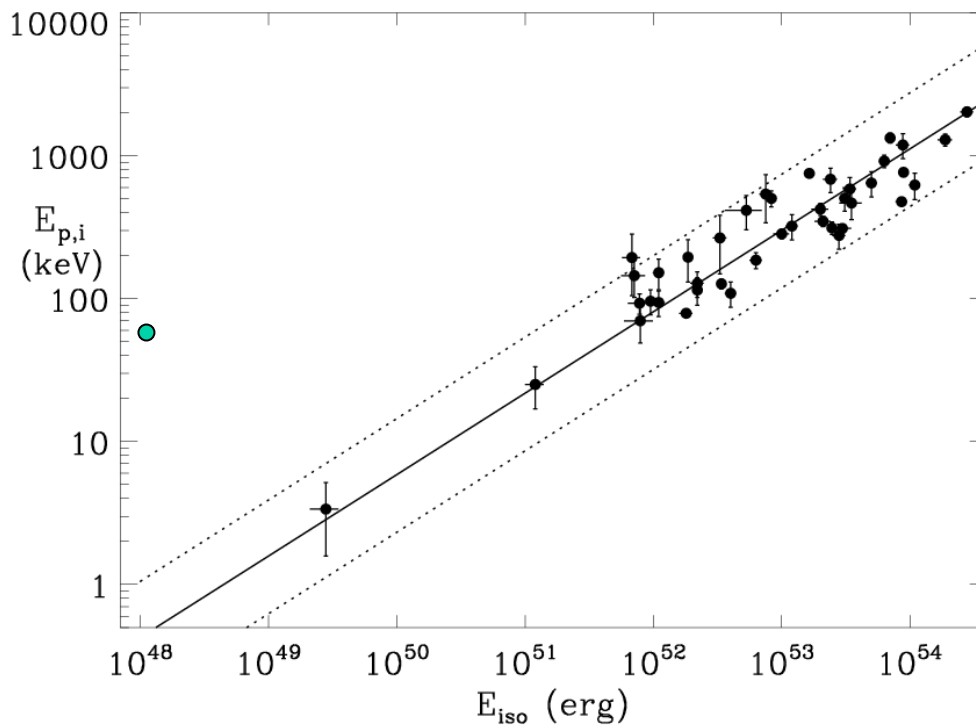


Amati et al. , A&A, 2002



Amati, ChJAA, 2003

- analysis of the most updated sample of *long* GRBs/XRFs with firm estimates of z and $E_{p,i}$ (41 events) gives a chance probability for the $E_{p,i}$ - E_{iso} correlation of $\sim 10^{-15}$ and a slope of 0.57 ± 0.02
- the scatter of the data around the best fit power-law can be fitted with a Gaussian with $\sigma(\log E_{p,i}) \sim 0.2$ (~ 0.15 extra-poissonian)
- only firm outlier the local peculiar GRB 980425



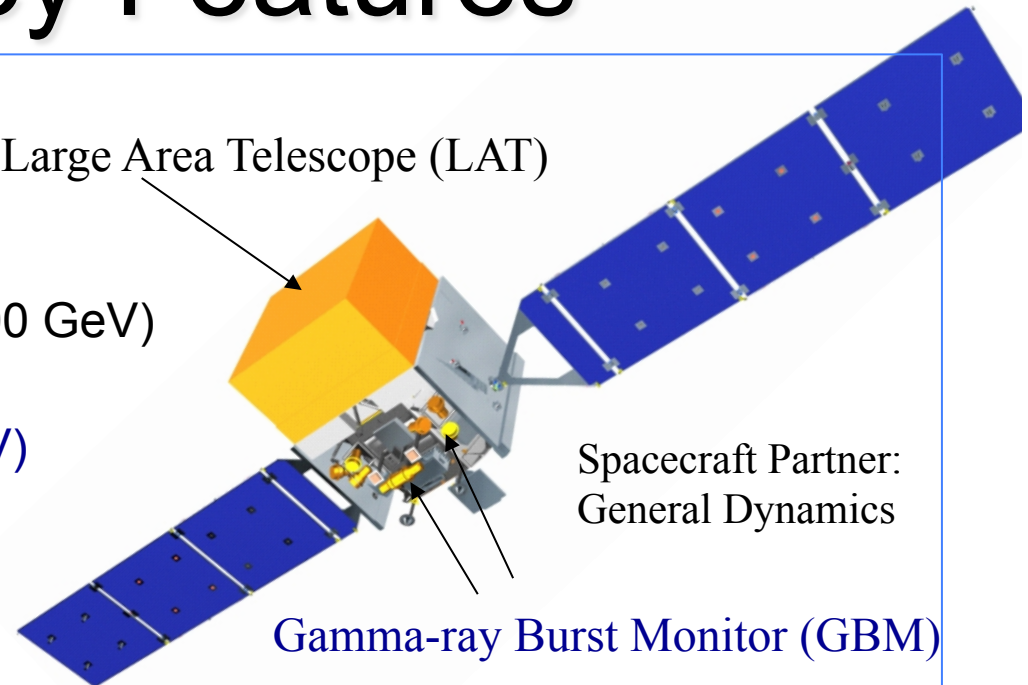
Updated from Amati, MNRAS, 2006

Fermi Key Features

- Two instruments:

- LAT:
 - high energy (20 MeV – >300 GeV)
- GBM:
 - low energy (8 keV – 40 MeV)

Large Area Telescope (LAT)



Spacecraft Partner:
General Dynamics

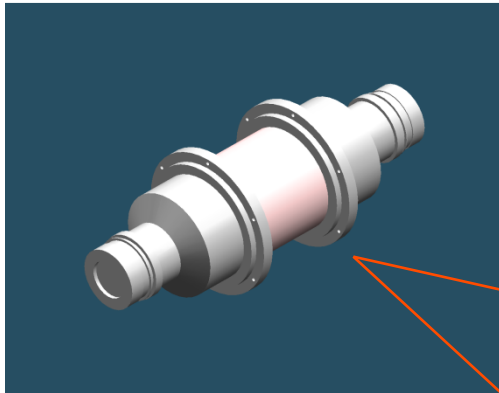
Gamma-ray Burst Monitor (GBM)

- Huge field of view

- LAT: 20% of the sky at any instant; in sky survey mode, expose all parts of sky for ~30 minutes every 3 hours. GBM: whole unocculted sky at any time.

GBM Detectors

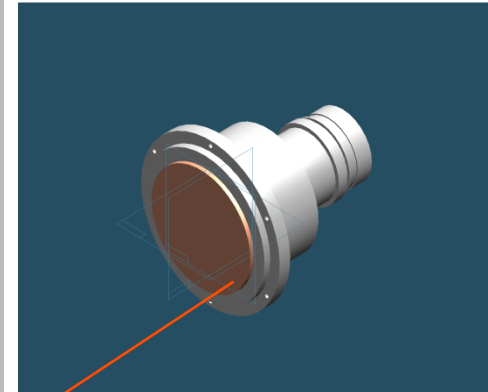
Bismuth Germanate (BGO) Scintillation Detector



Major Purpose

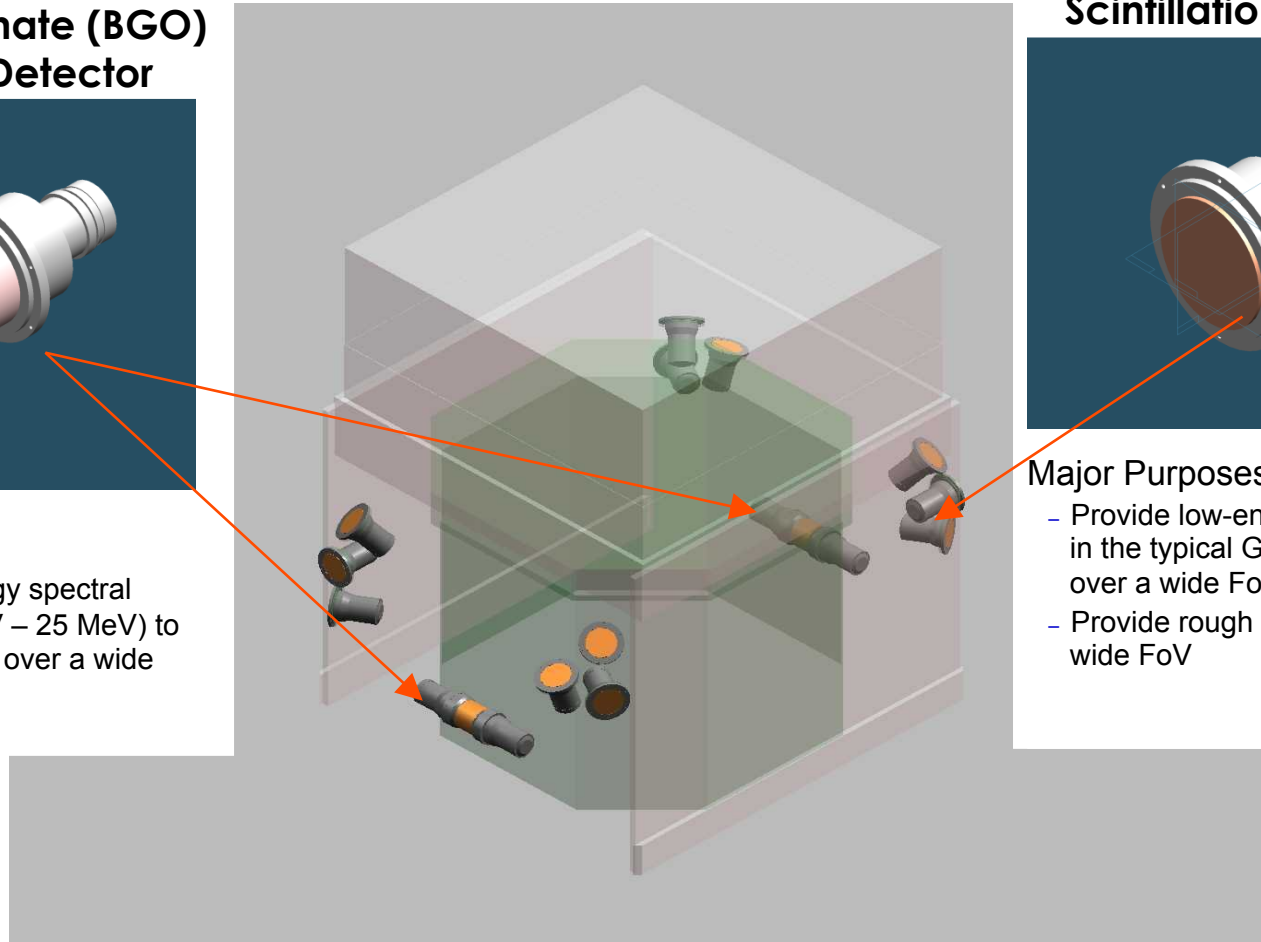
- Provide high-energy spectral coverage (150 keV – 25 MeV) to overlap LAT range over a wide FoV

(12) Sodium Iodide (NaI) Scintillation Detectors



Major Purposes

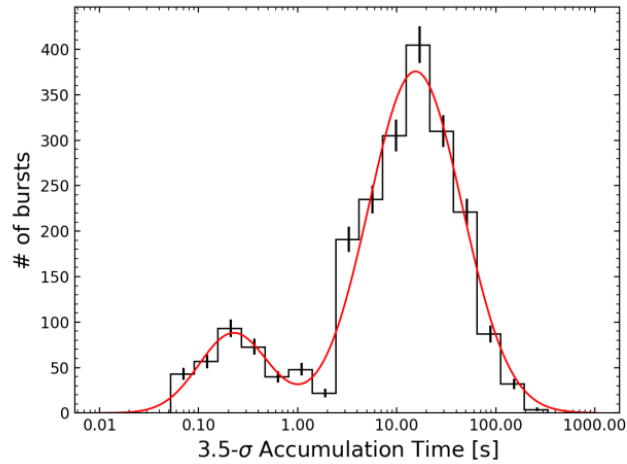
- Provide low-energy spectral coverage in the typical GRB energy regime over a wide FoV (10 keV – 1 MeV)
- Provide rough burst locations over a wide FoV



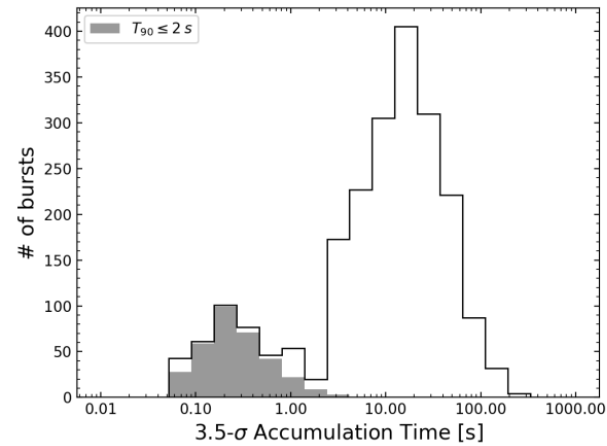
Provides spectra for GRB from 10 keV to 30 MeV.

Provides wide sky coverage (8 sr), enables autonomous repoints to allow for high energy afterglow observations with the LAT.

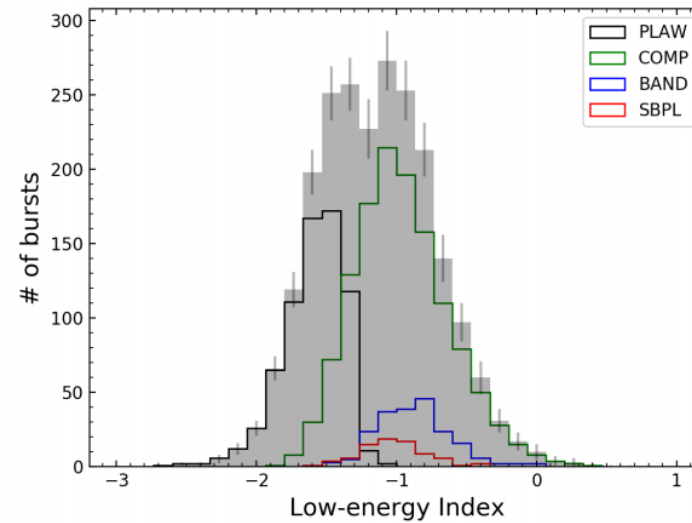
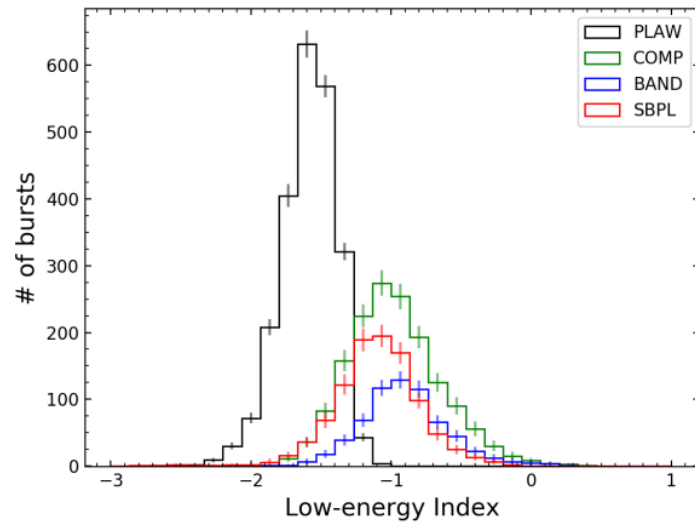
Fermi GBM



(a)



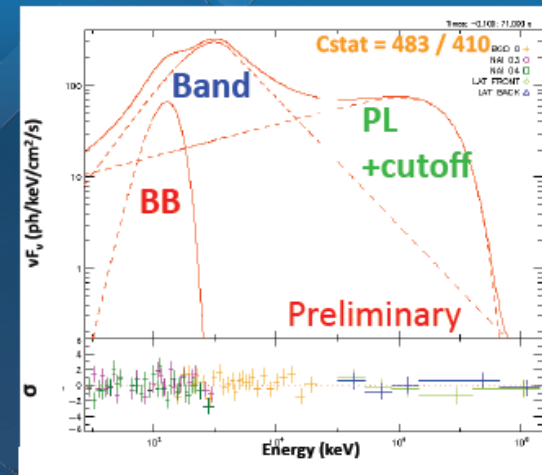
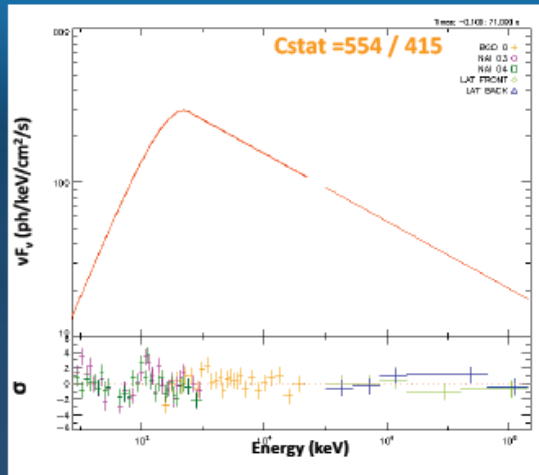
(b)



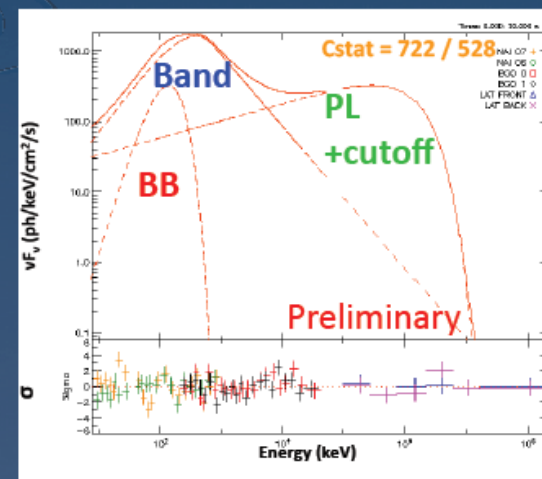
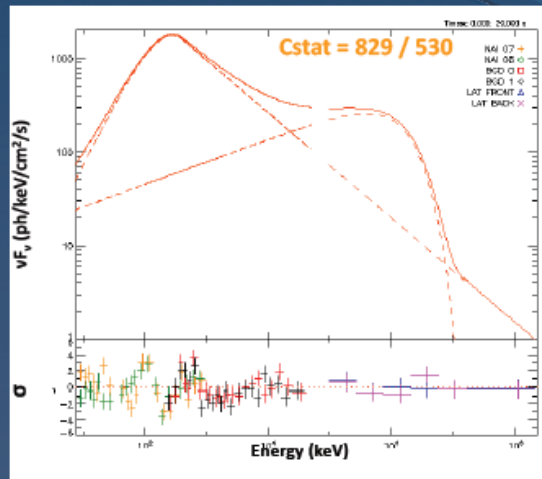
Fermi spectra

Multiple Spectral Components

GRB 080916C

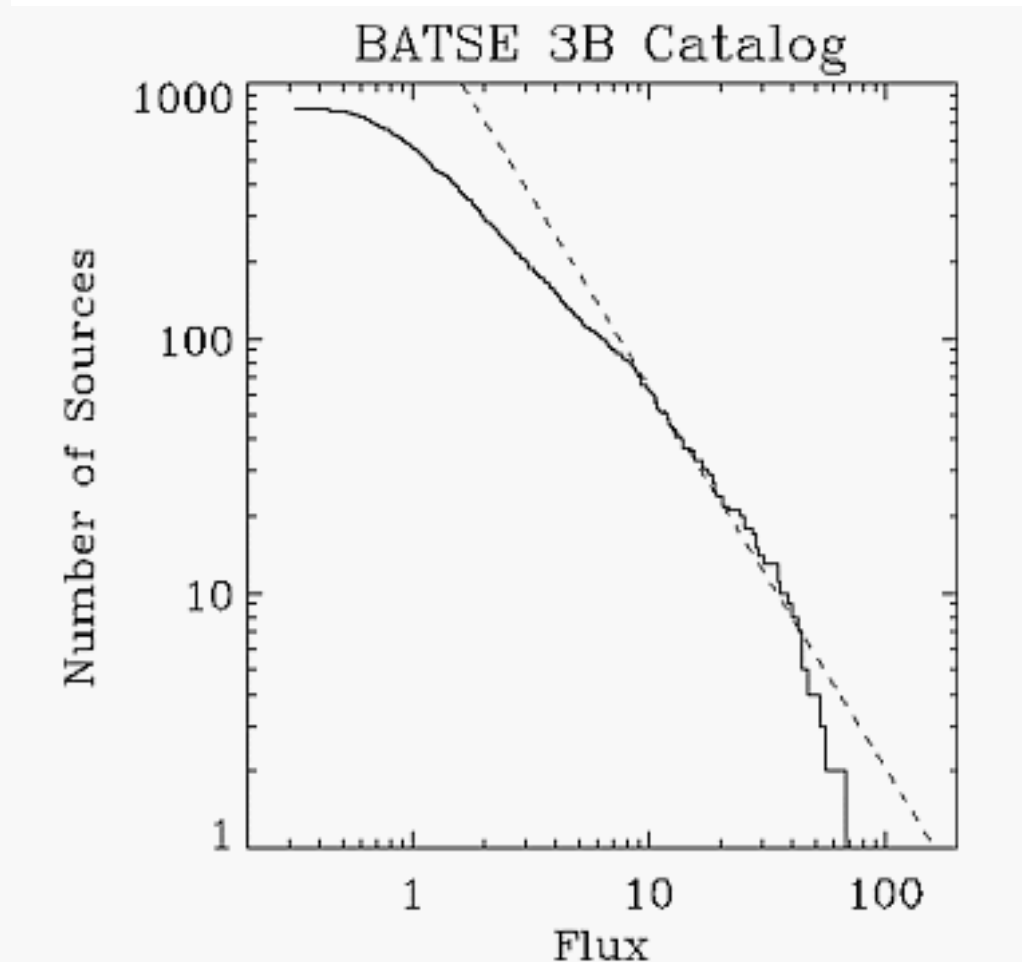
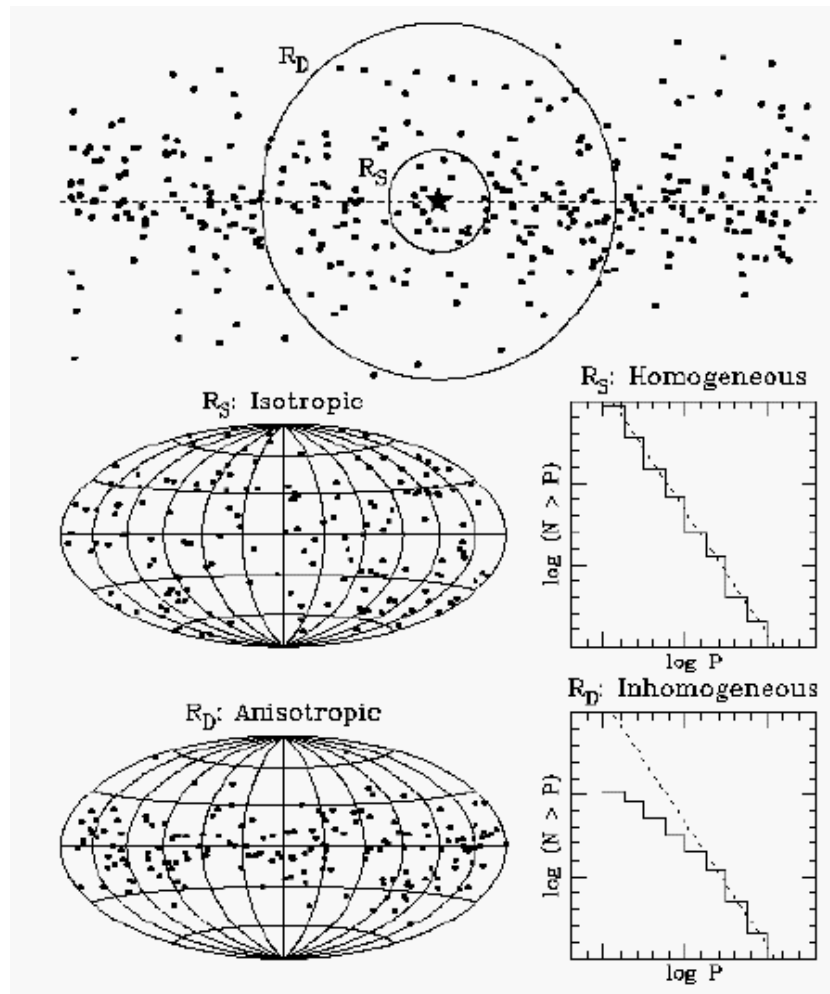


GRB 090926A



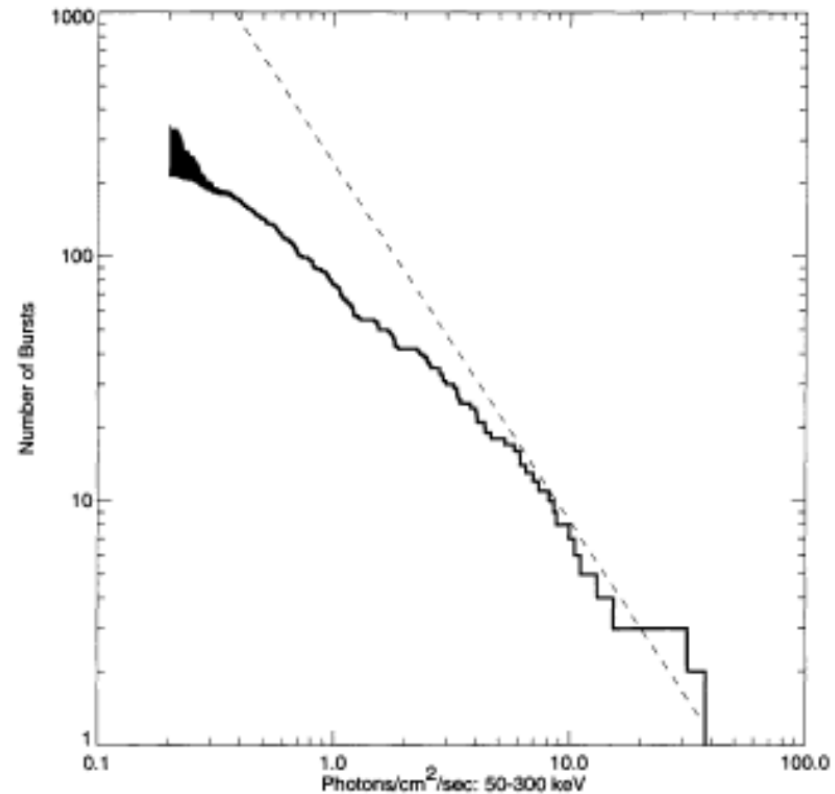
(Guirrec et al. in preparation)

BATSE (1991 - 2000)

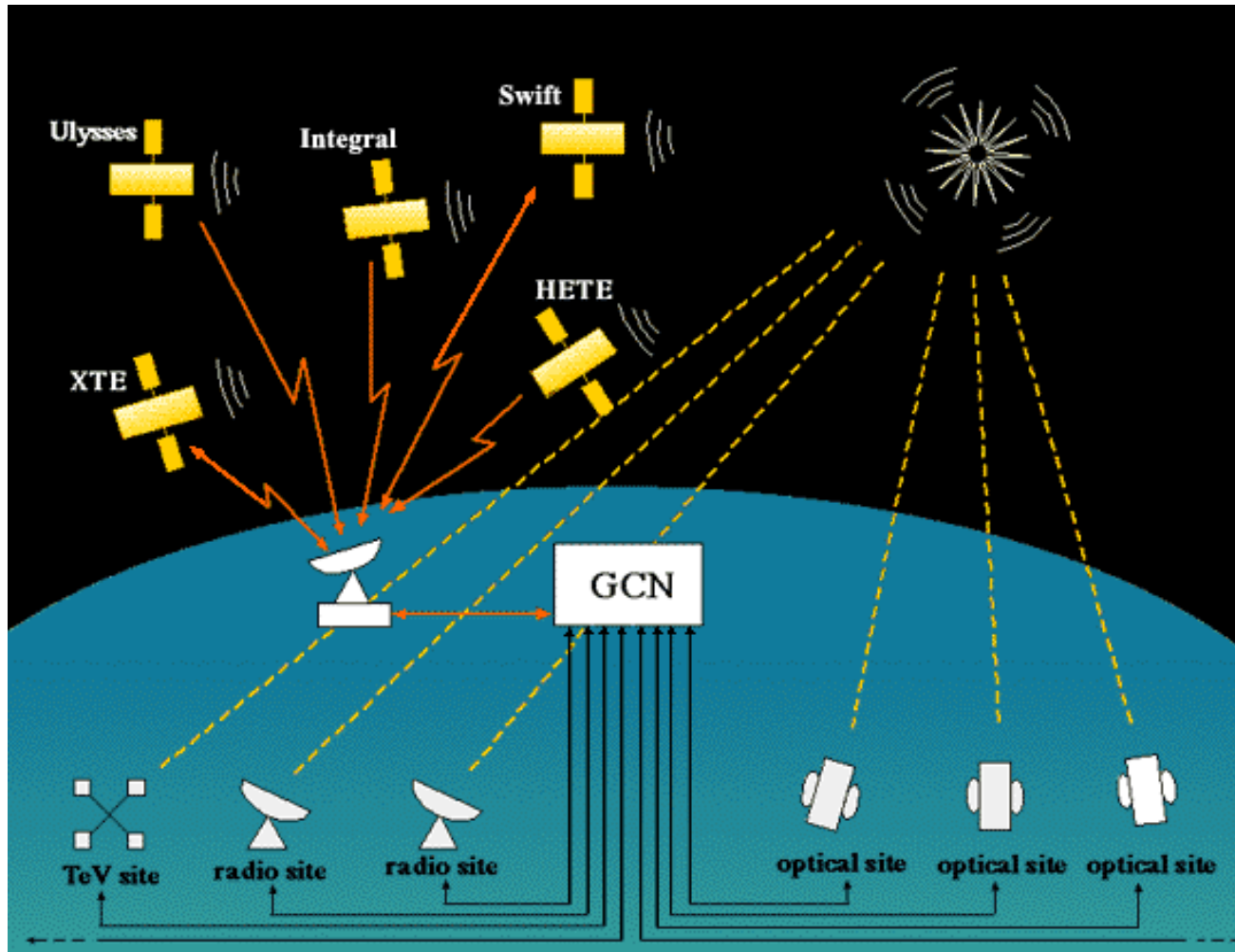


The GRB phenomenon

- Flux $\sim d^{-2}$
- Number $\sim d^3$
- $d \sim N^{1/3}$
- Flux $\sim N^{-2/3}$
- $N \sim \text{Flux}^{-3/2}$



BATSE (1991-2000)



GRB: where are they?

The great debate (1995)



Flux: 10^{-7} erg cm⁻² s⁻¹

Distance: 1 Gpc

Energy: 10^{51} erg

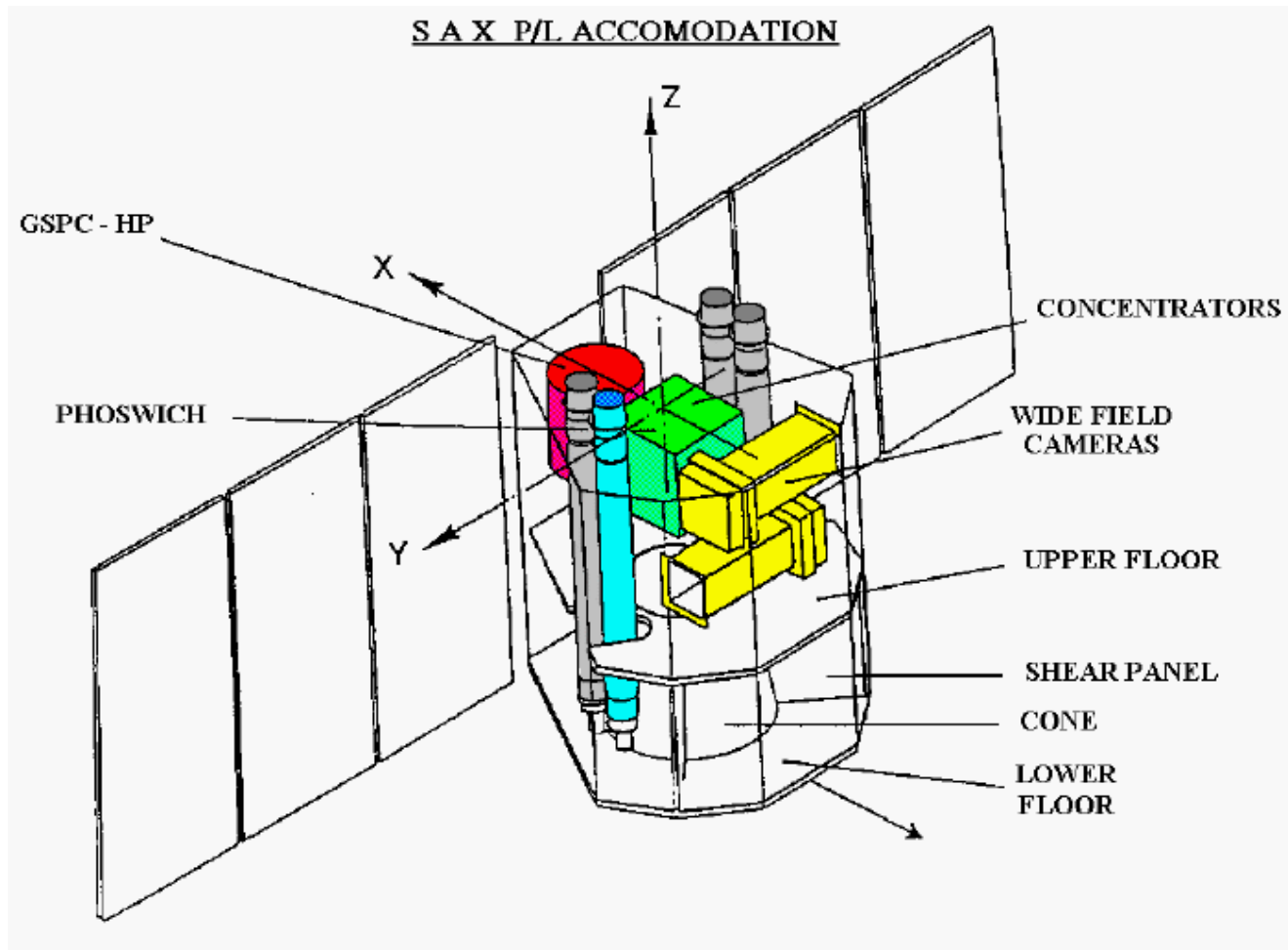
Distance: 100 kpc

Energy: 10^{43} erg

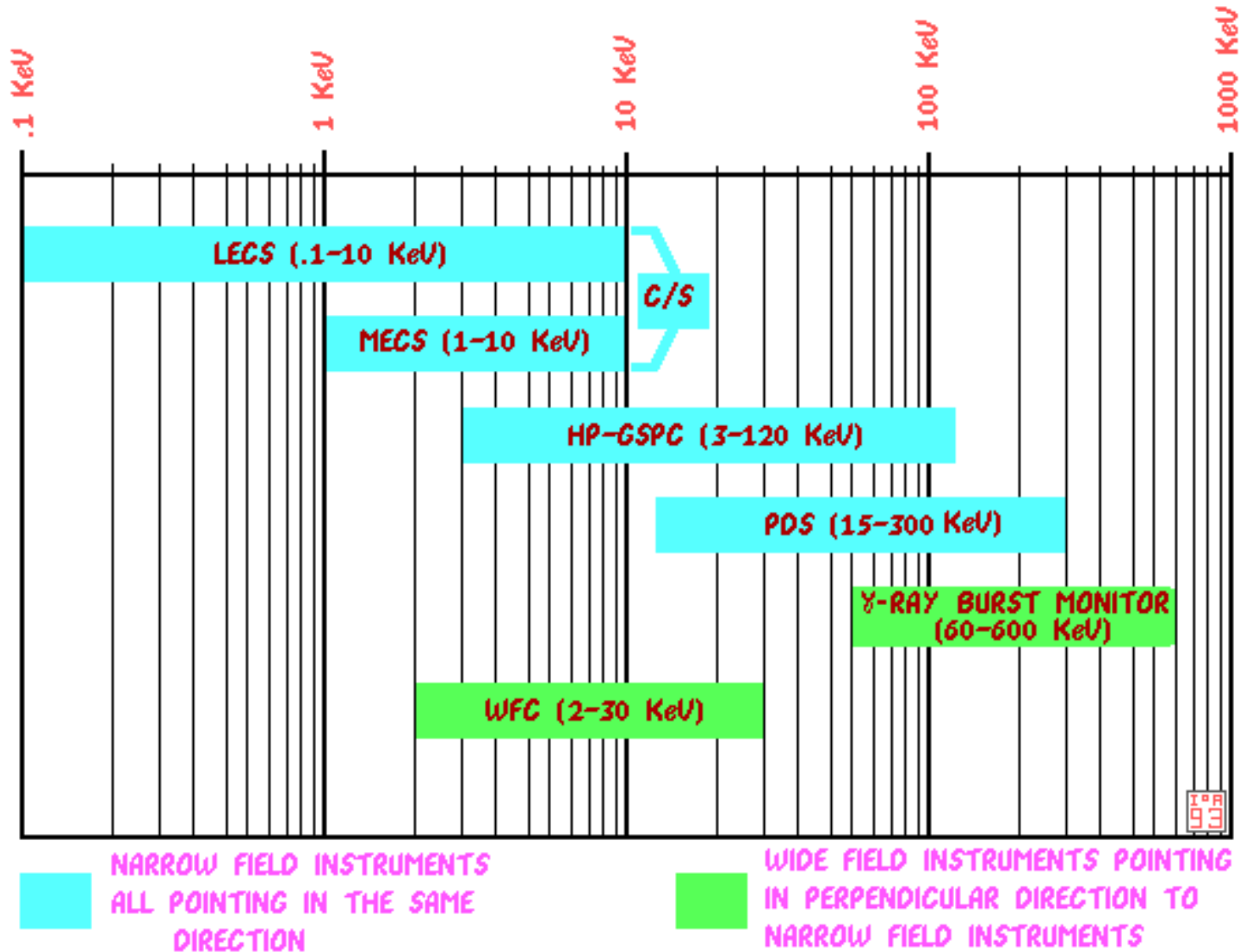
Cosmological - Galactic?

Need a new type of observation!

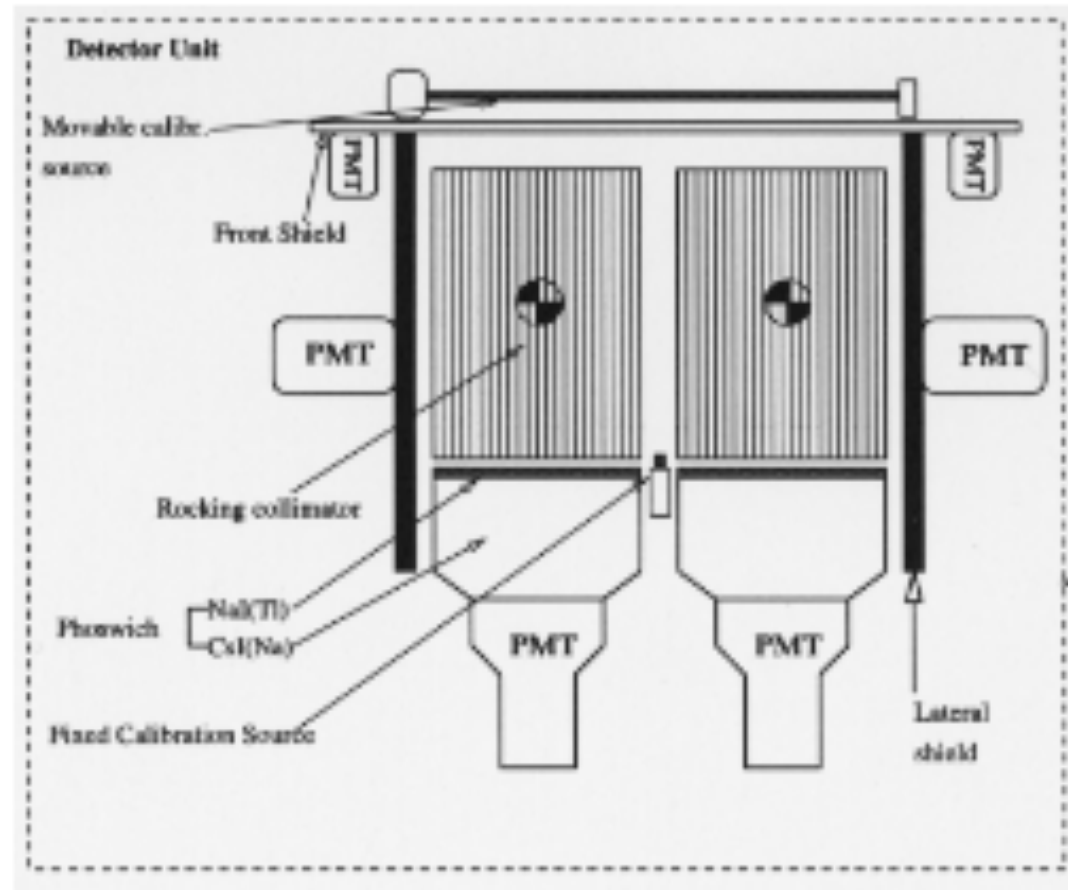
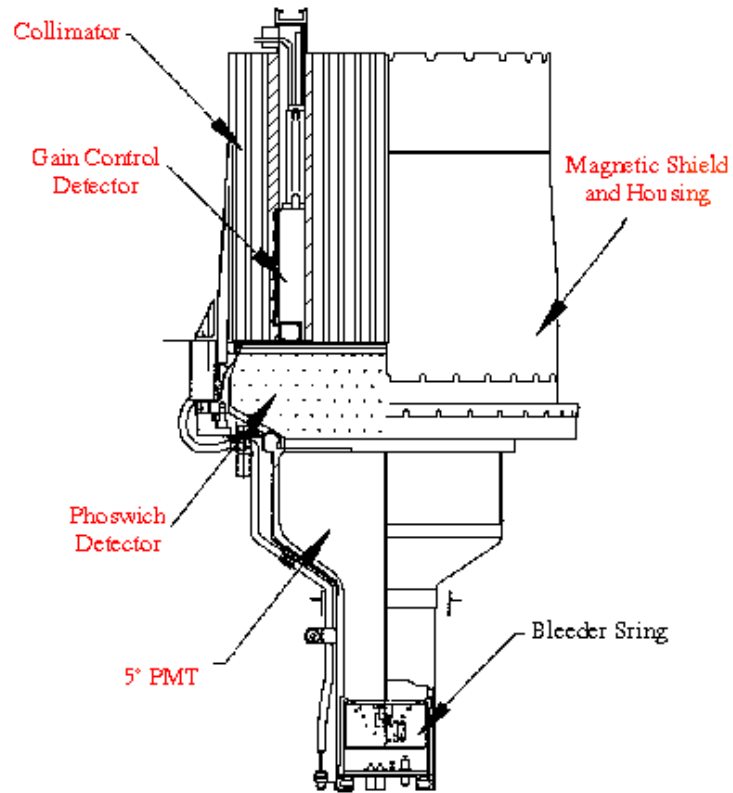
BeppoSAX (1995 - 2002)



BeppoSAX



Phoswich detectors

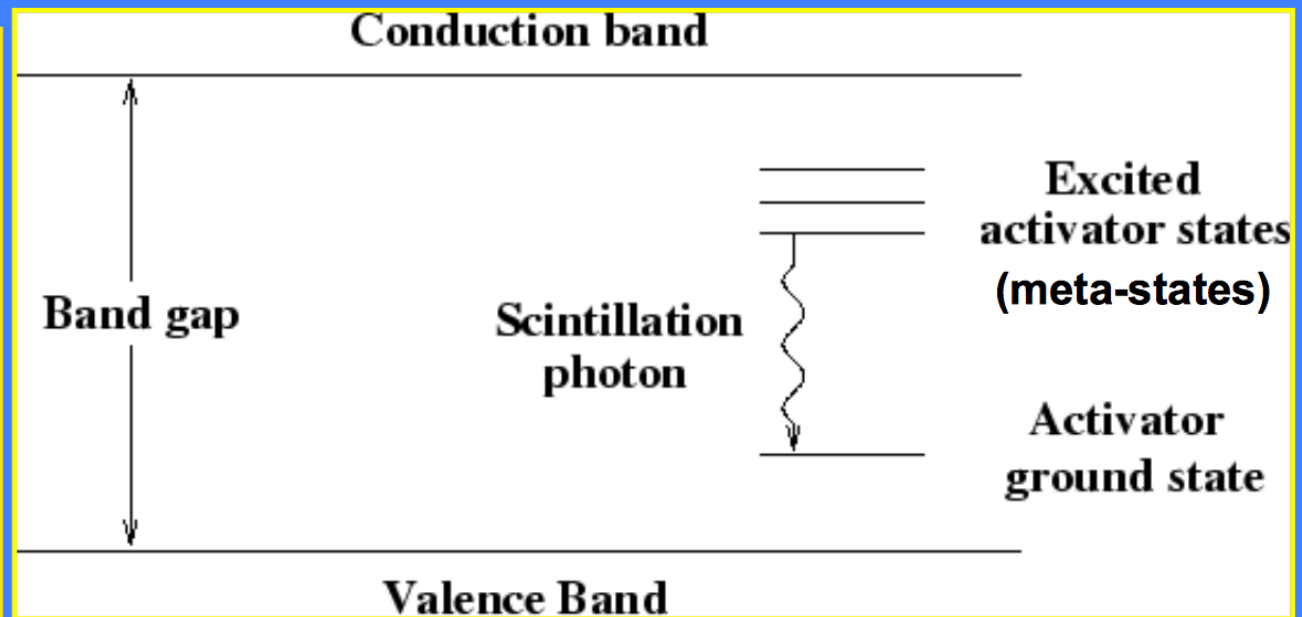


Two scintillators with different decay times. Pulse analysis can distinguish. Back scintillator used as shield at low energy, as detector at high energies.

Rivelatori a scintillazione

- **“Fondamenti” del processo: il γ incidente interagisce nel cristallo creando un elevato numero di fotoni ottici**
- **I livelli energetici sono determinati dalla struttura del reticolo cristallino**
- **La band gap separa la banda di valenza dalla banda di conduzione**
- **Assorbendo energia, un e^- viene promosso dalla banda di valenza a quella di conduzione**
- **Il “drogaggio” del reticolo cristallino con impurità rende più efficiente il processo**

Nel cristallo, gli elettroni possono occupare solo due livelli energetici, la **banda di valenza** e la **banda di conduzione**. Le impurità permettono la creazione di meta-stati che sono particolarmente efficienti per la diseccitazione dalla banda di conduzione



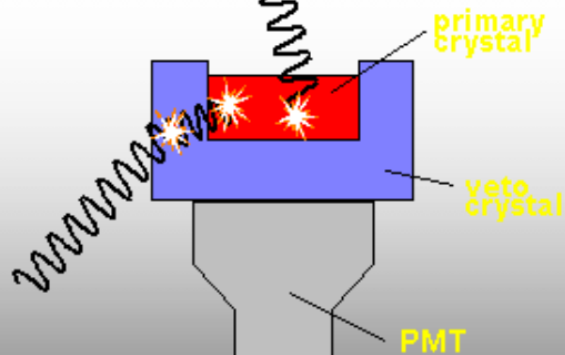
Esempio: phoswich

The Phoswich (e.g. PDS on BeppoSAX)

Phoswich is short for 'phosphor sandwich'

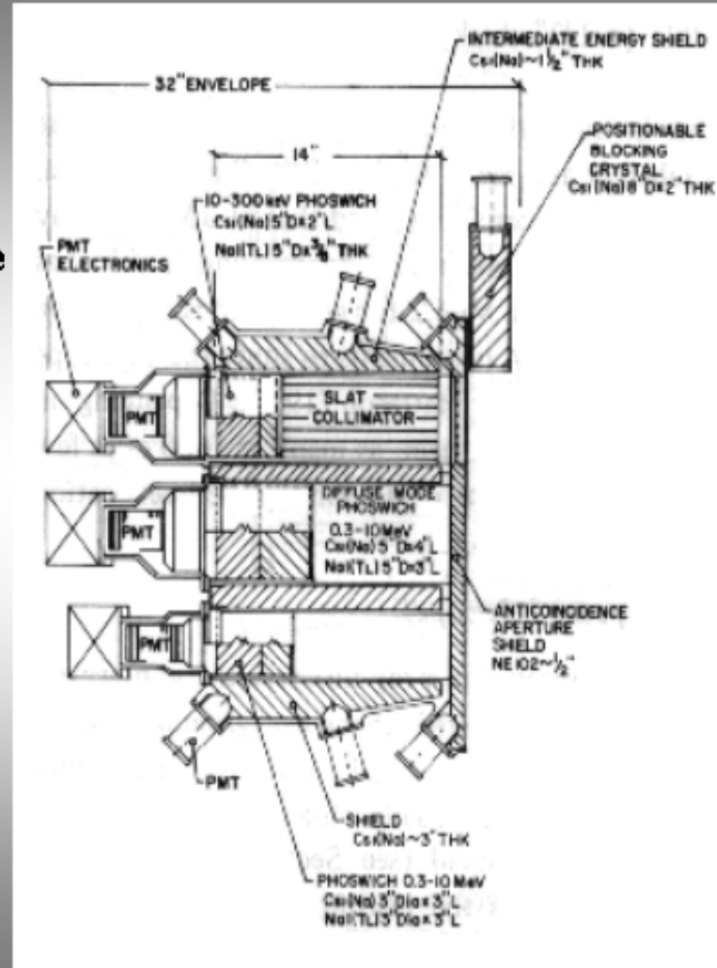
Phosphor is the old name for a scintillator, and more than one are sandwiched together and viewed by the same photomultiplier.

More penetrating particles can produce signal in both scintillators



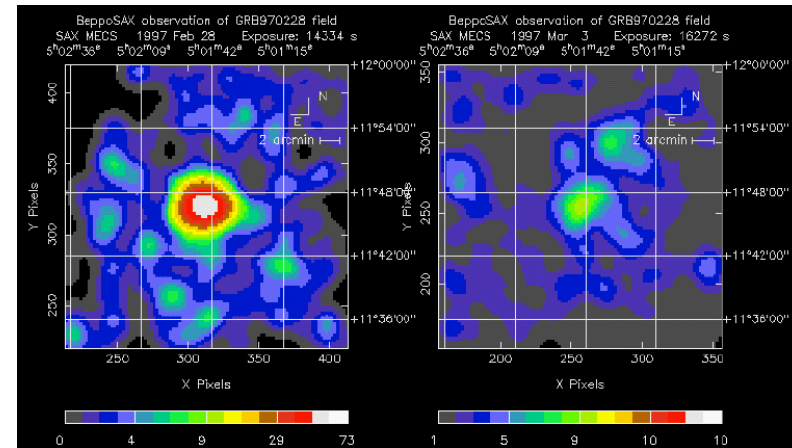
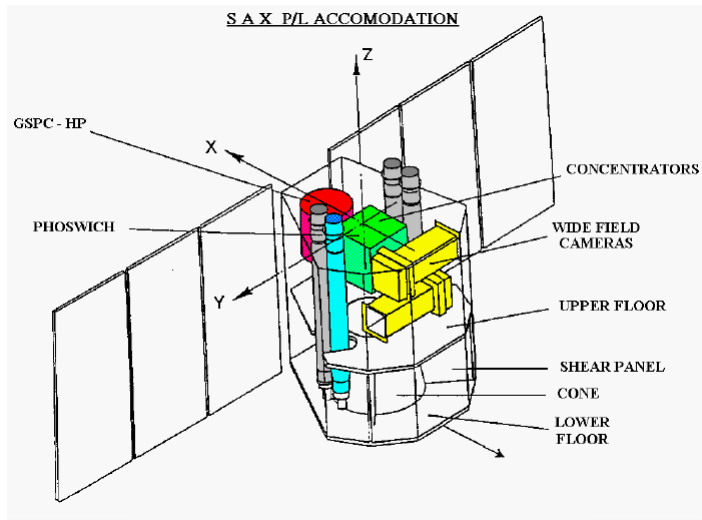
Signals are separated by their pulse shape

Different materials have different pulse shapes and are used to discriminate different events



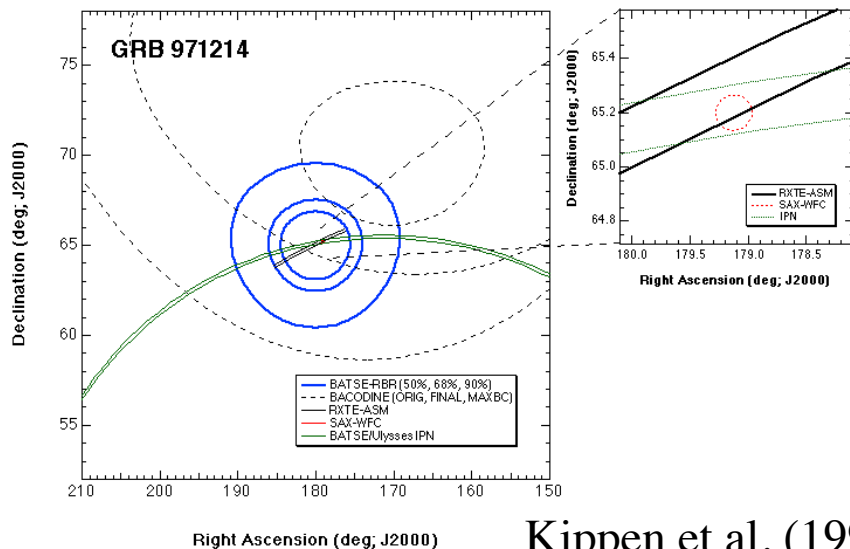
BeppoSAX and the Afterglows

- Good Angular resolution ($< \text{arcmin}$)
- Observation of the X-Afterglow

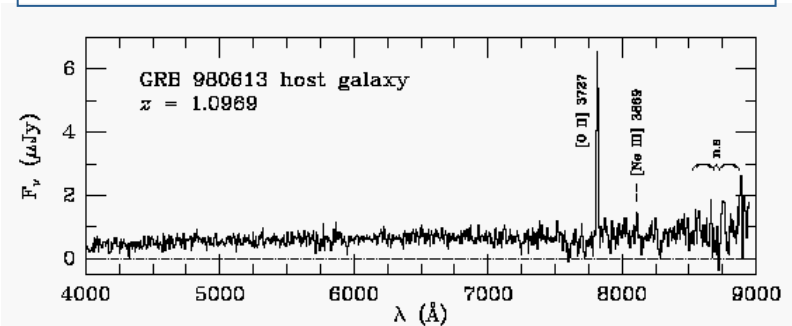


Costa et al. (1997)

- Optical Afterglow (HST, Keck)
- Direct observation of the host galaxies
- Distance determination

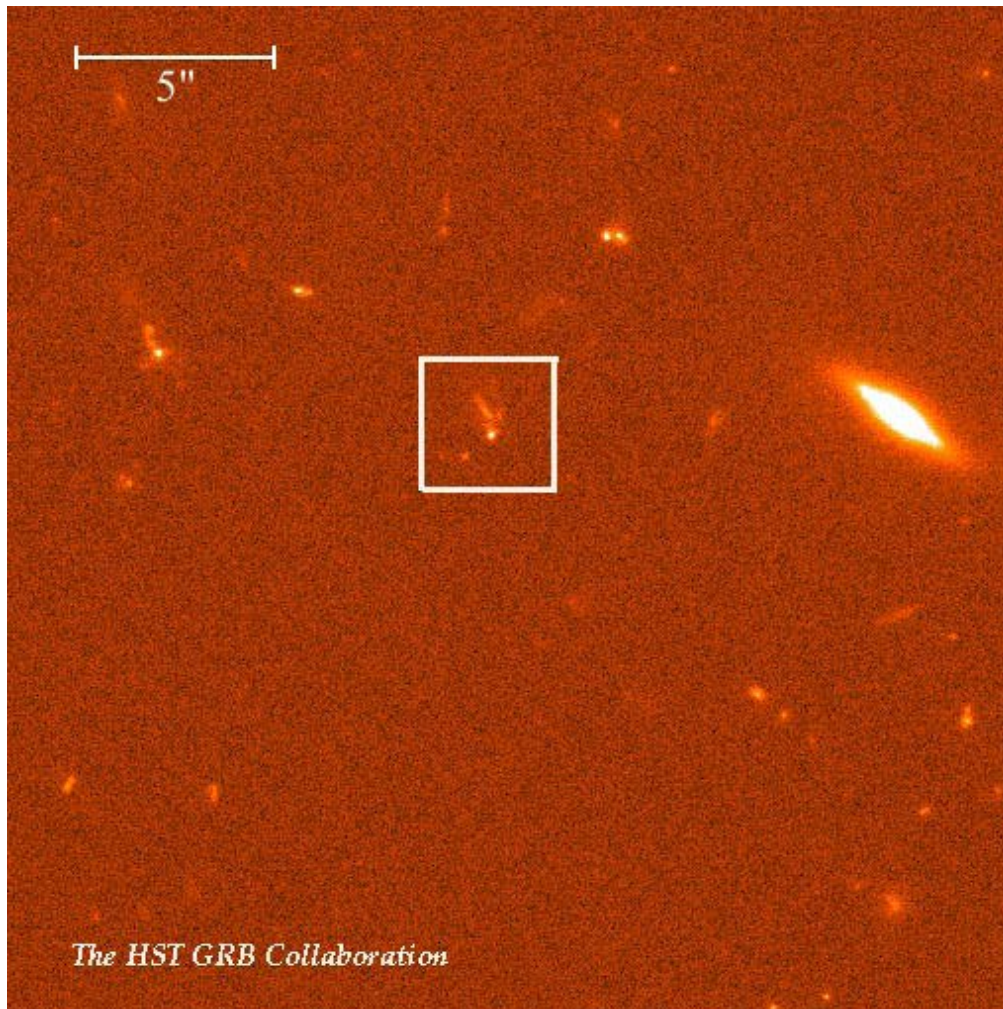


Kippen et al. (1998)



Djorgoski et al. (2000)

Afterglow Observations

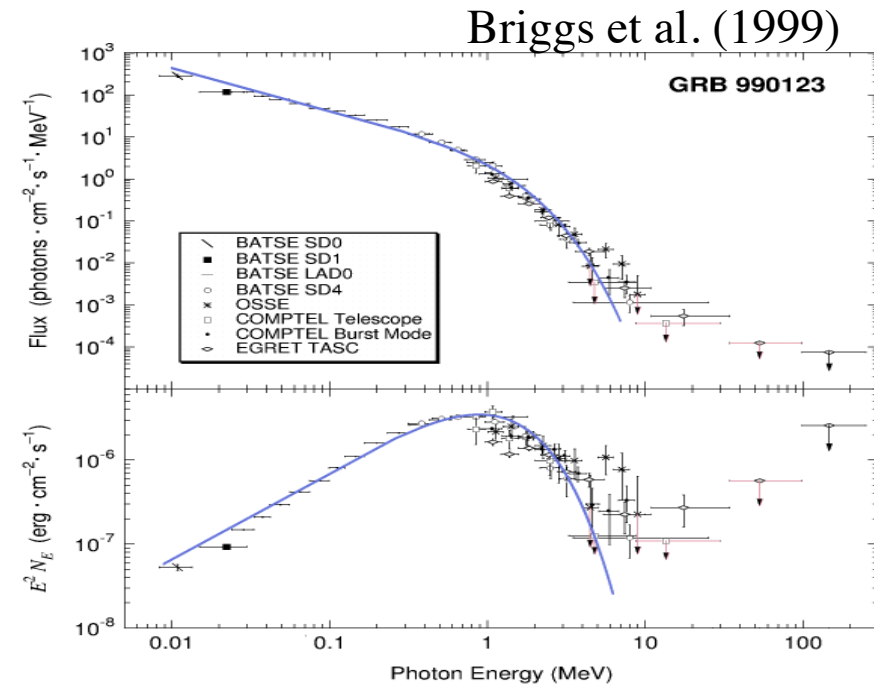
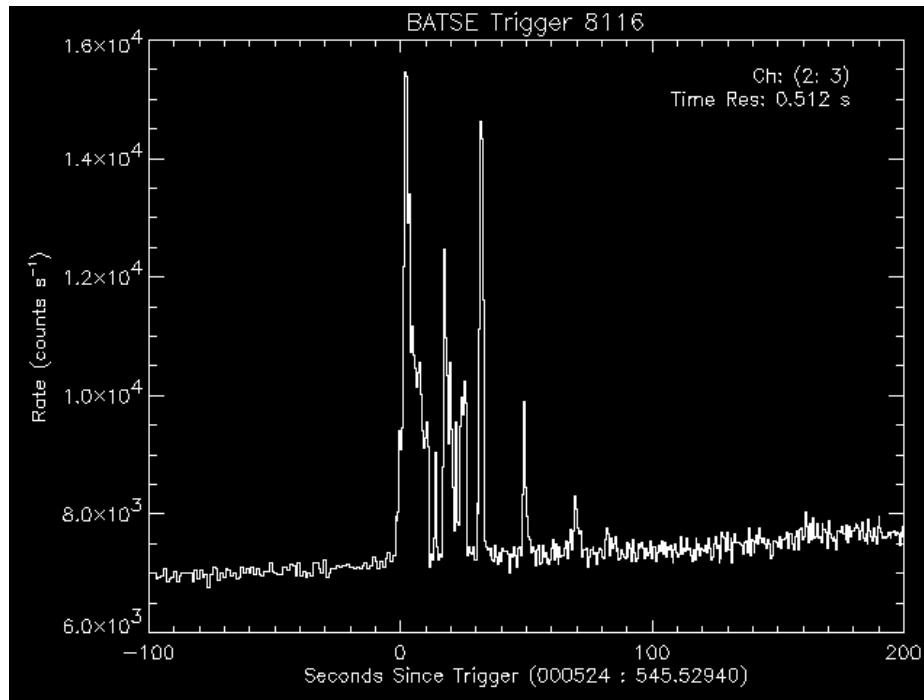


Identificazione delle
Host Galaxies

Fruchter et al (1999)

The compactness problem

Light curve variability ~ 1 ms



Non thermal spectra

- Fluence (γ): $(0.1-10) \times 10^{-6}$ erg/cm 2 ($\Omega/4\pi$)
- Total Energy: $E \sim 10^{51} \div 10^{52}$ erg

The compactness problem

$$R_i < c\delta t \quad \gamma\gamma \rightarrow e^+e^-$$

$$\tau_{\gamma\gamma} = \frac{f_p \sigma_T F D_L^2}{R_i^2 m_e c^2} \approx 10^{17} f_p \left(\frac{F}{10^{-6} \text{ erg/cm}^2} \right) \left(\frac{D_L}{3 \text{ Gpc}} \right)^2 \left(\frac{\delta t}{1 \text{ ms}} \right)$$

$$\tau_{\gamma\gamma} \gg 1$$

Very High Optical Depth to pair production

$$\Gamma = \frac{1}{\sqrt{1 - \beta^2}}$$

$$R_i < \Gamma^2 c\delta t \quad f_p \rightarrow f_p \Gamma^{-2\alpha}$$

Size

Pair fraction

$$\tau_{\gamma\gamma} = \frac{f_p \sigma_T F D_L^2}{R_i^2 m_e c^2} \approx \frac{10^{17}}{\Gamma^{4+2\alpha}} f_p \left(\frac{F}{10^{-6} \text{ erg/cm}^2} \right) \left(\frac{D_L}{3 \text{ Gpc}} \right)^2 \left(\frac{\delta t}{1 \text{ ms}} \right)$$

$$\Gamma \approx 10^2 \div 10^3$$

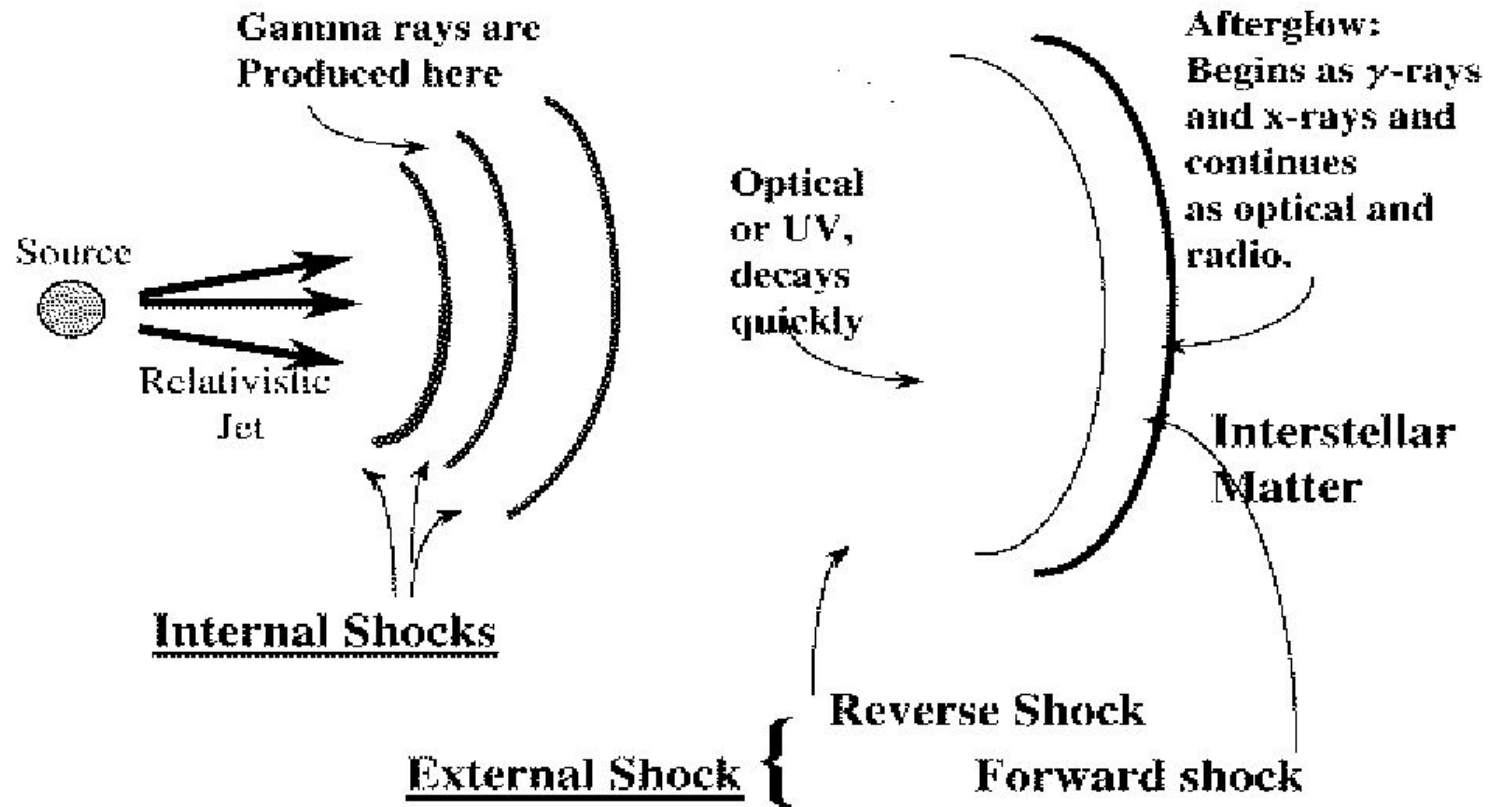
Piran (1999)

Exercise #2

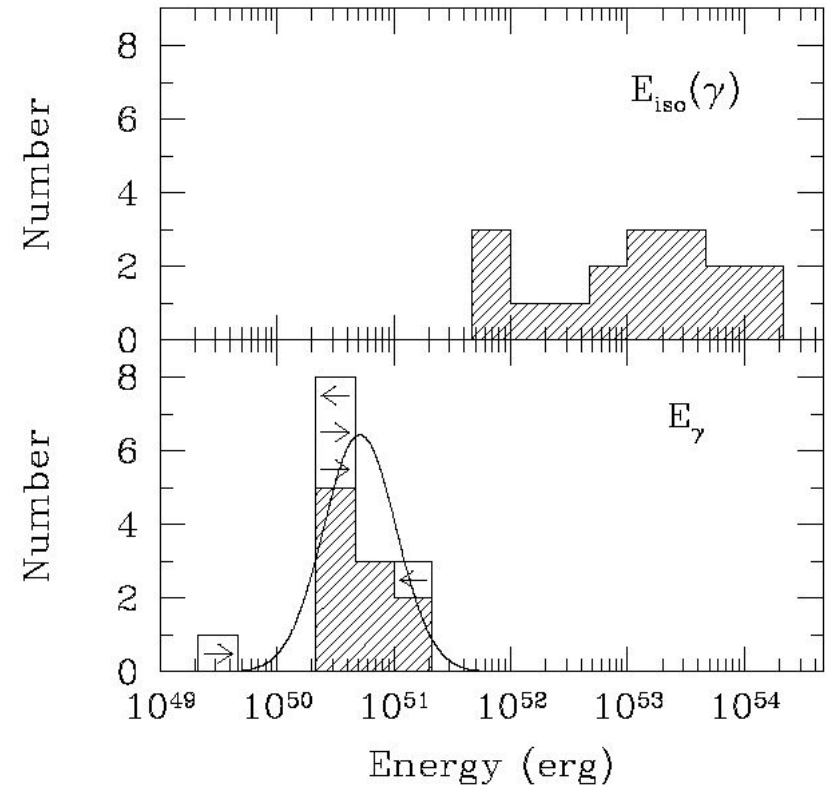
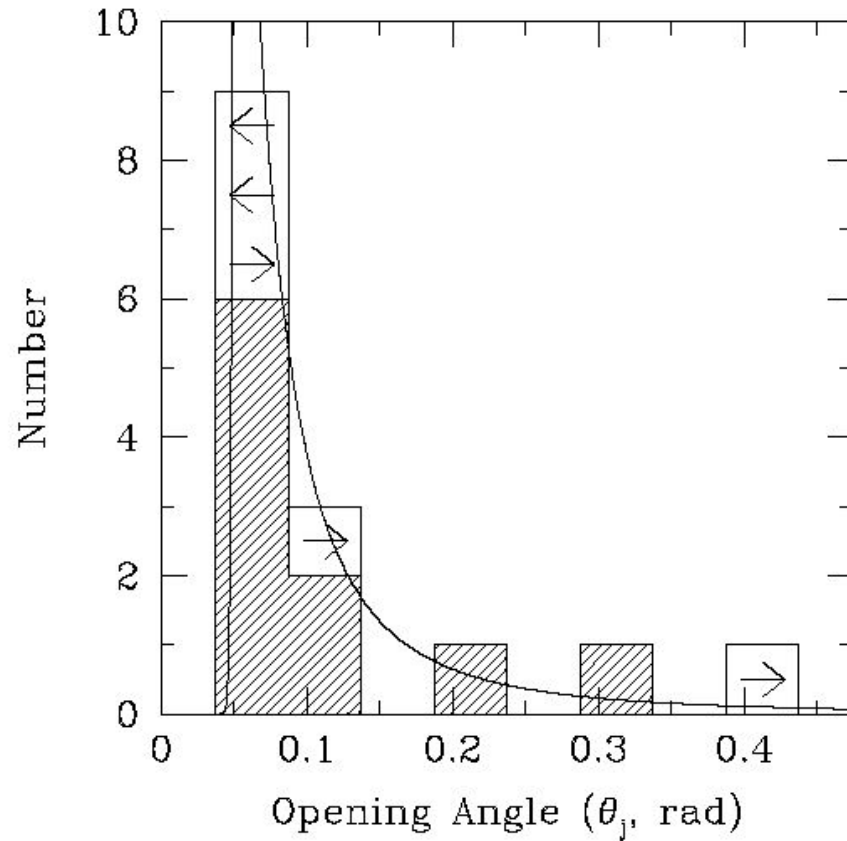
- Find the GRB function by David Band (1993)
- Find the review paper by Piran 1999 on GRB afterglow
- Find the paper by L.Amati on Ep-Eiso correlation (2002)
- Find the papers of the “Great Debate (1995)”

The Fireball Model

The Fireball Model



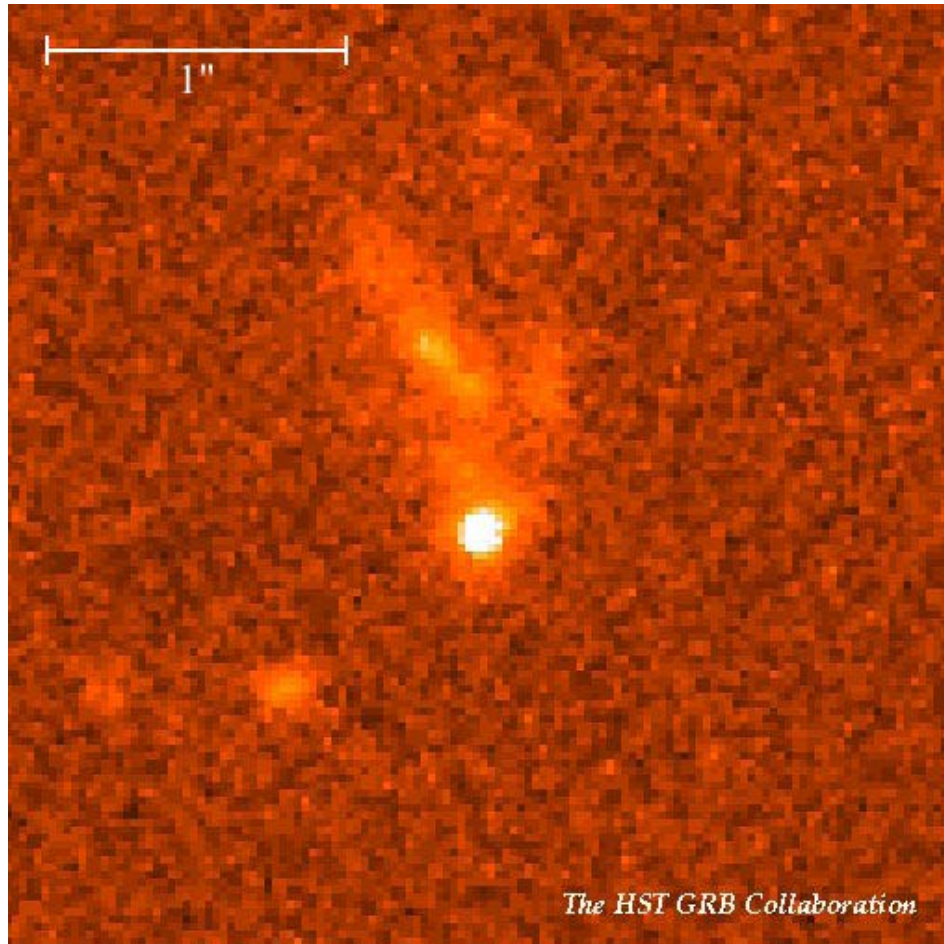
Jet and Energy Requirements



Frail et al. (2001)

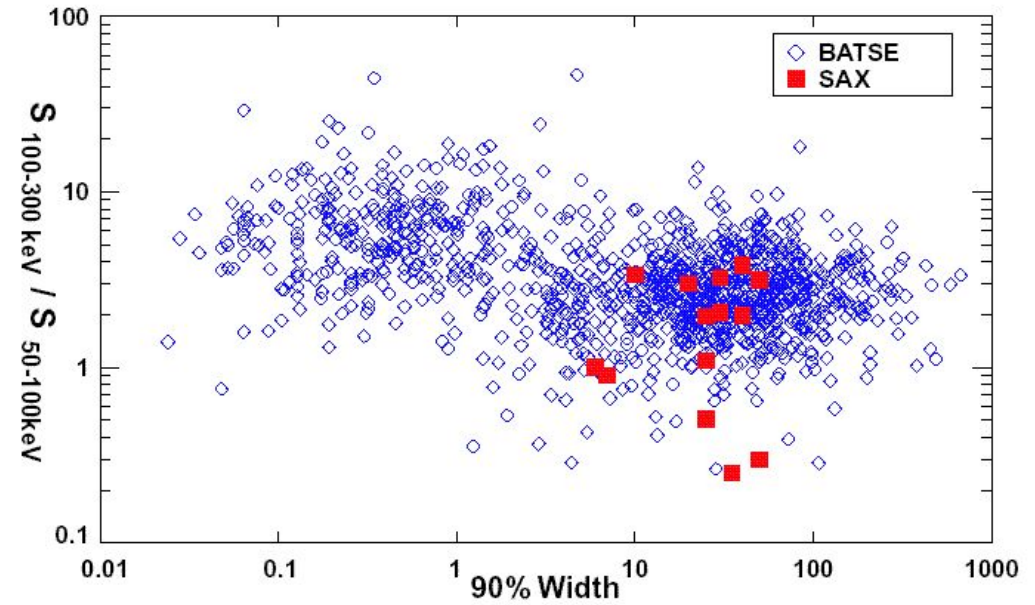
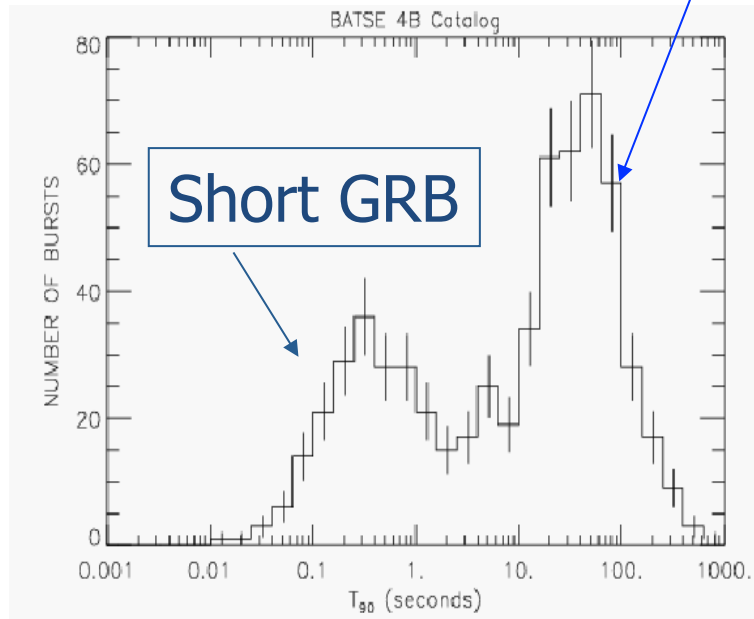
Progenitors

- Two populations of GRB?
- Main models
- Possible solution?

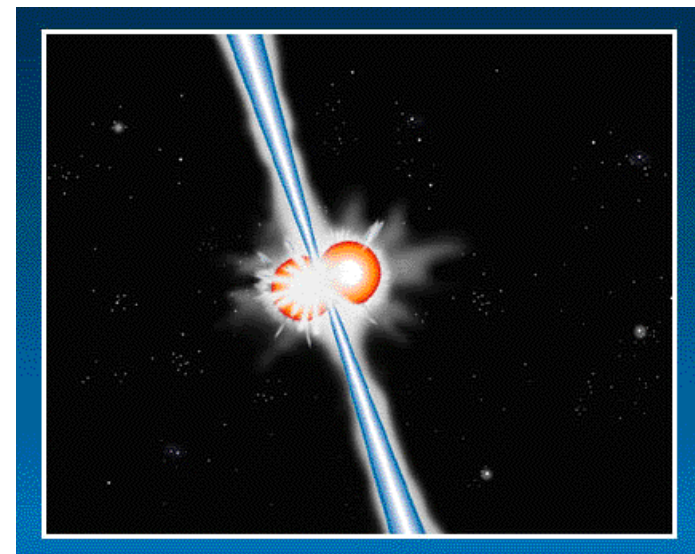
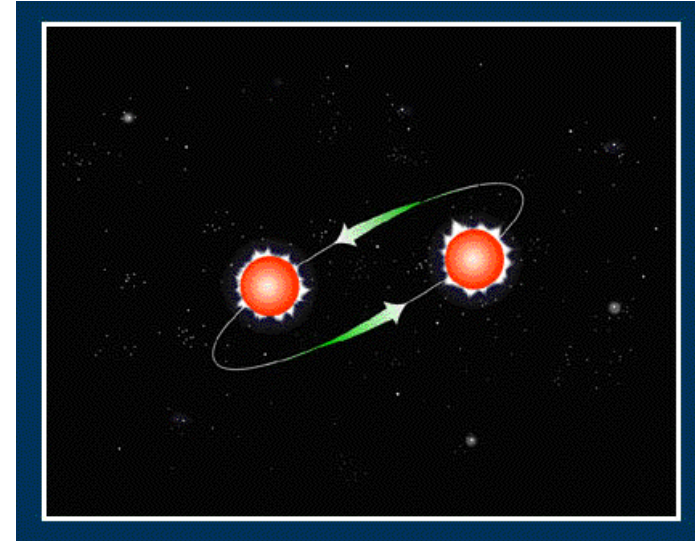
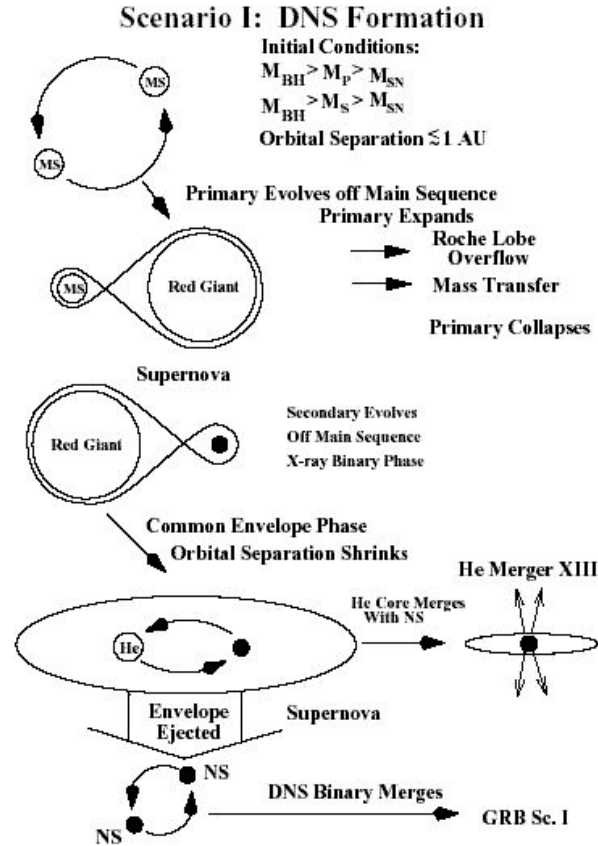


Progenitors

Long GRB

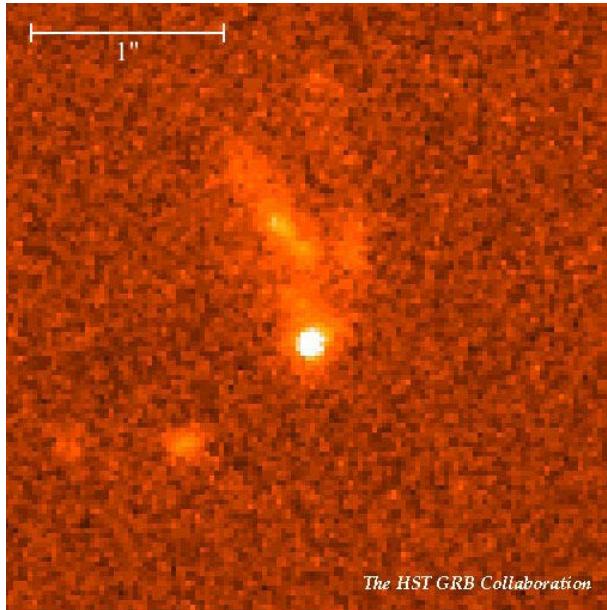


NS/BH Binary Mergers



Merging of compact objects (NS-NS, NS-BH, BH-BH).
 These objects are observed in our Galaxy.
 The merging time is about 10^8 yr, via GW emission.

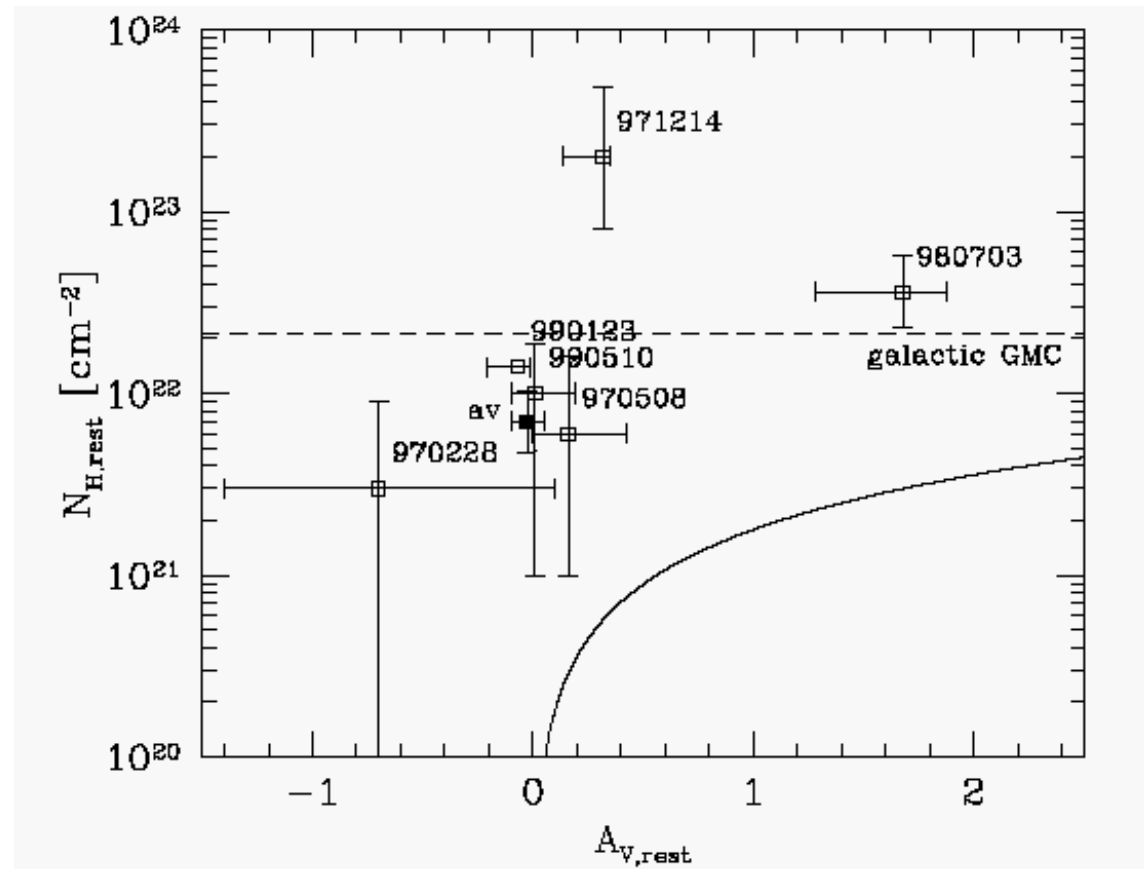
Towards a solution?



Offset from Host Galaxy

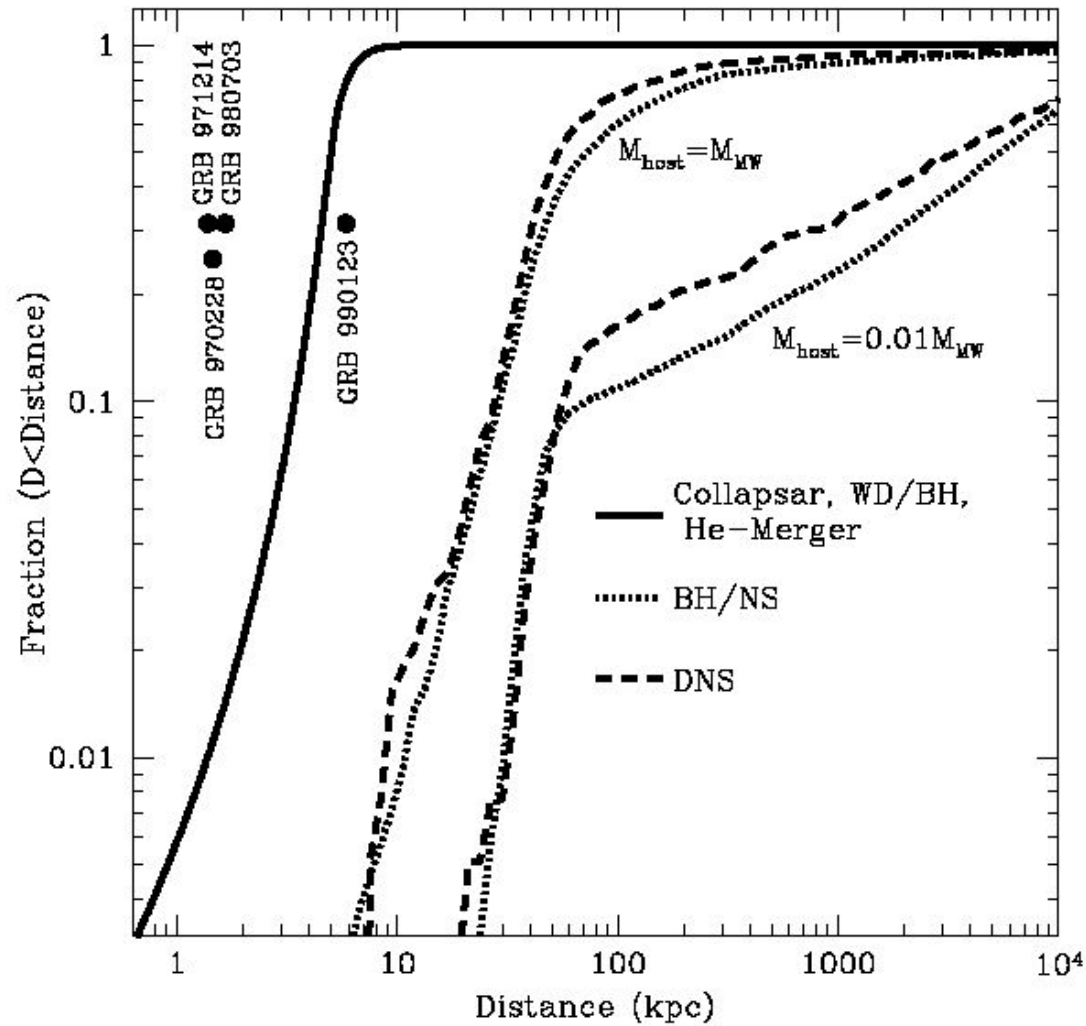
Fruchter et al (1999)

Galama & Wijers (2000)



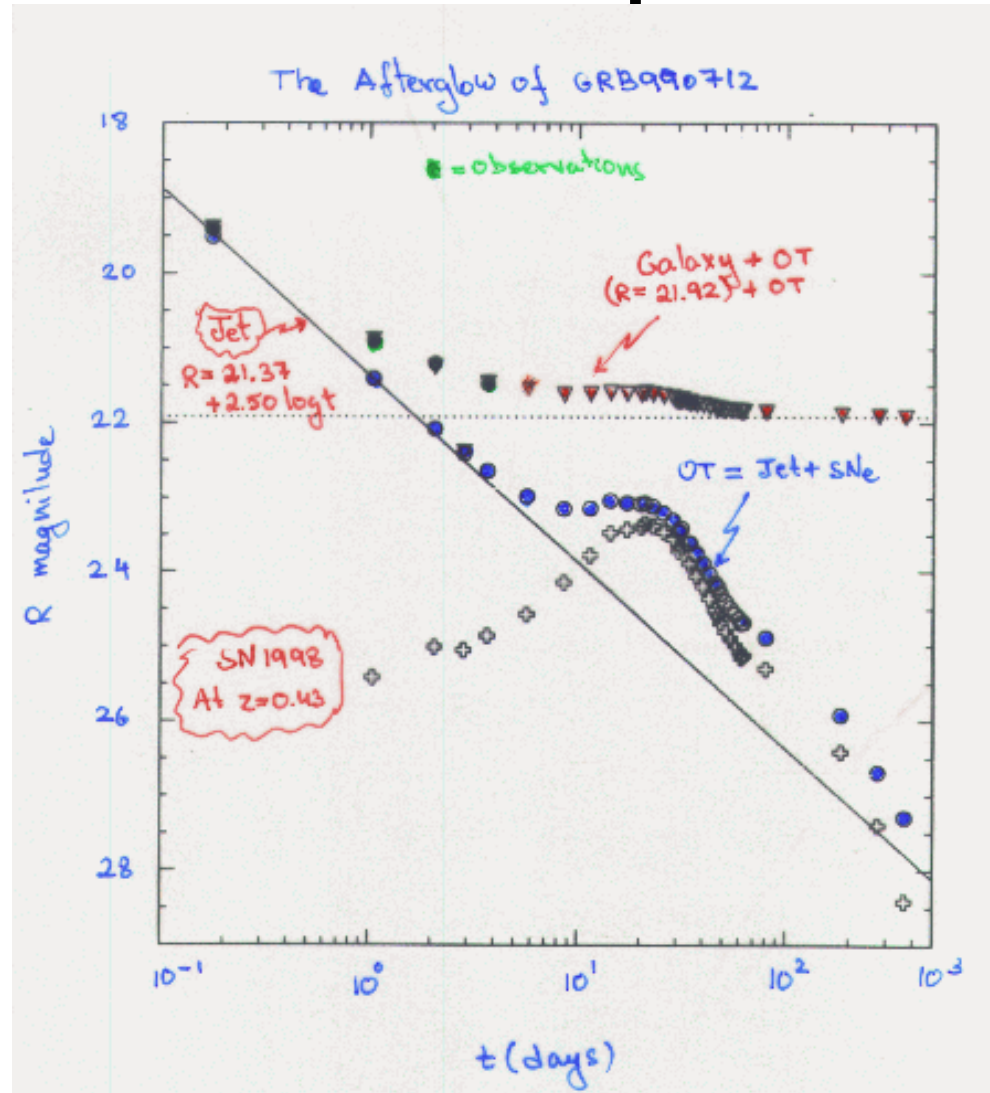
Star forming region density

Towards a solution?



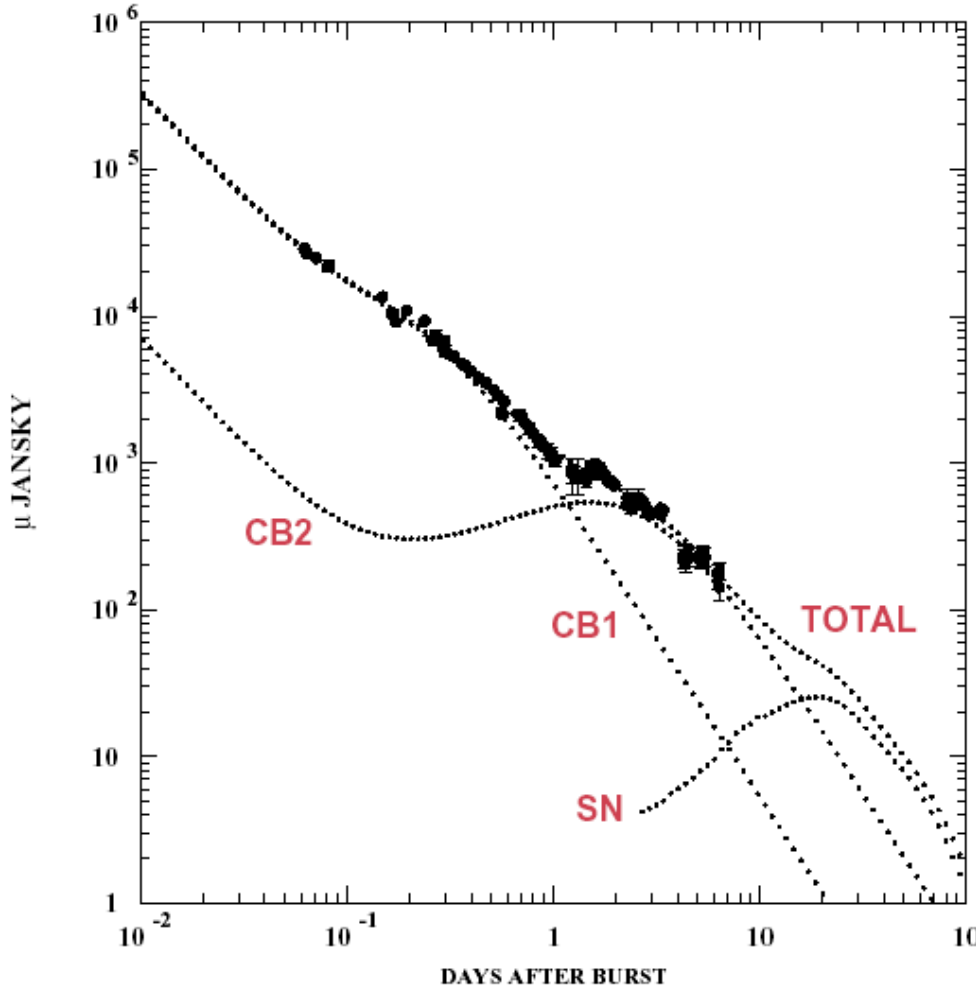
Fryer et al. (1999)

GRB & SN first predictions

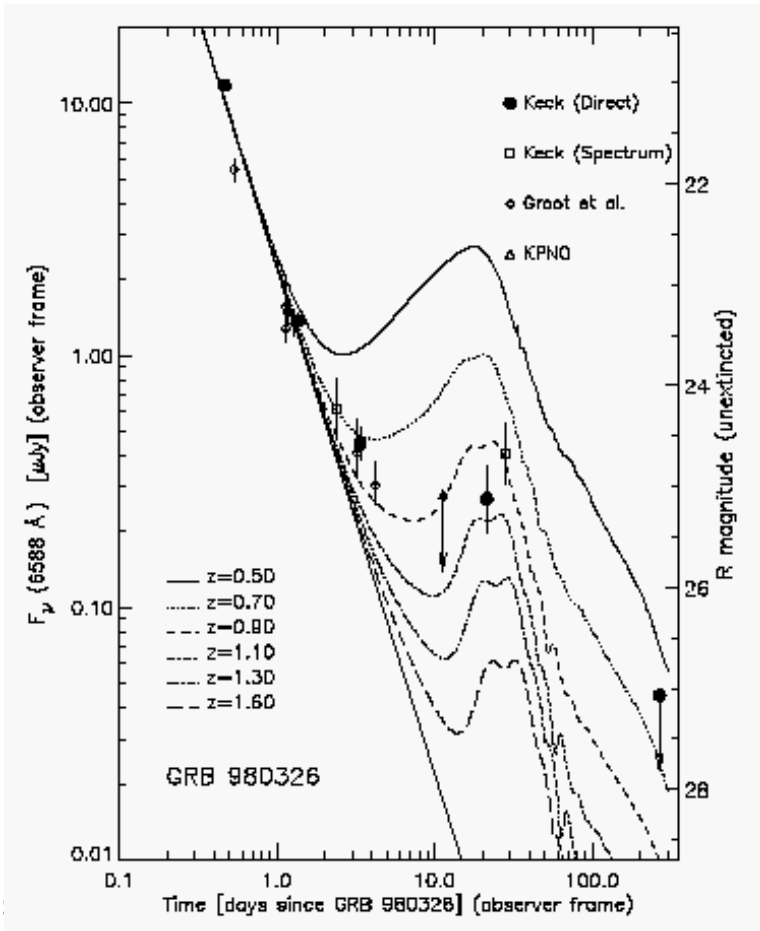


Hjorth, Fynbo, D ar & Courbin (1999)

GRB & SN



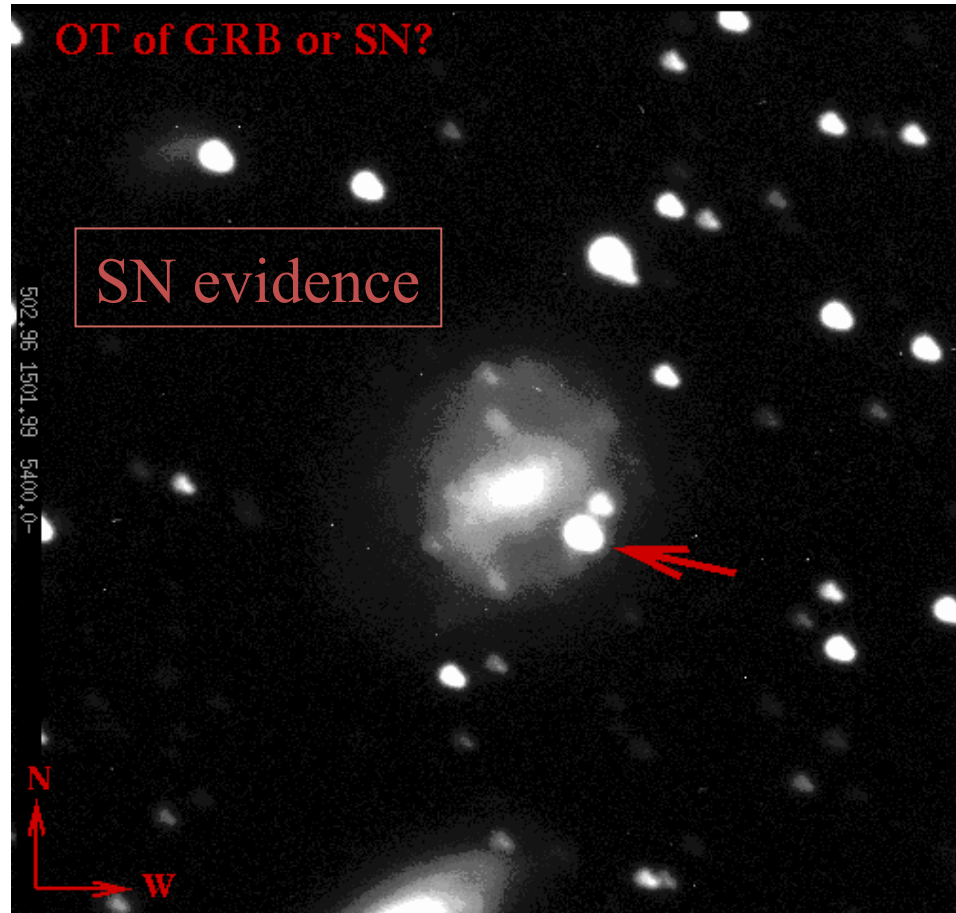
Dado, Dar & De Rujula (2003)



GRB 980326

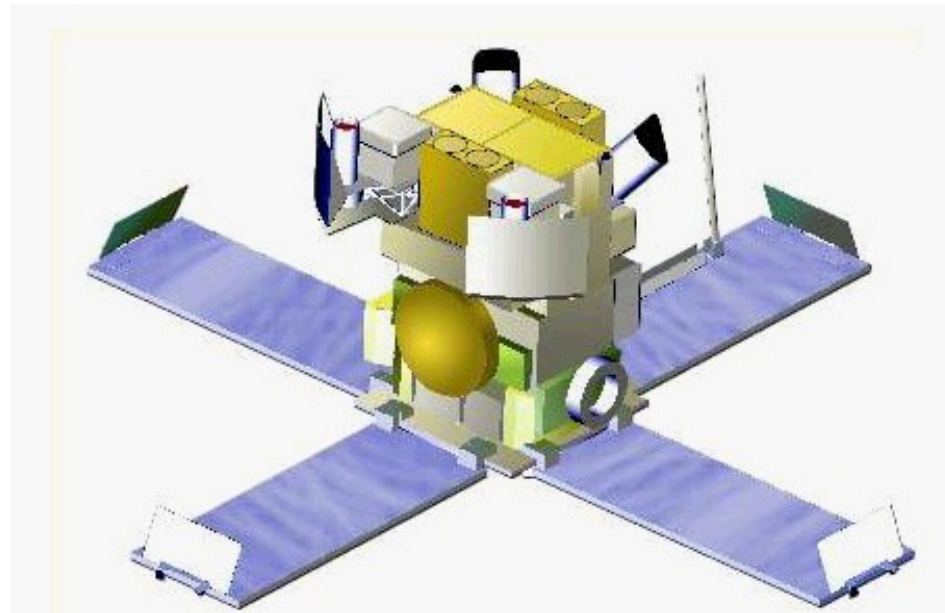
(Bloom et al. 99)

SN- GRB connection

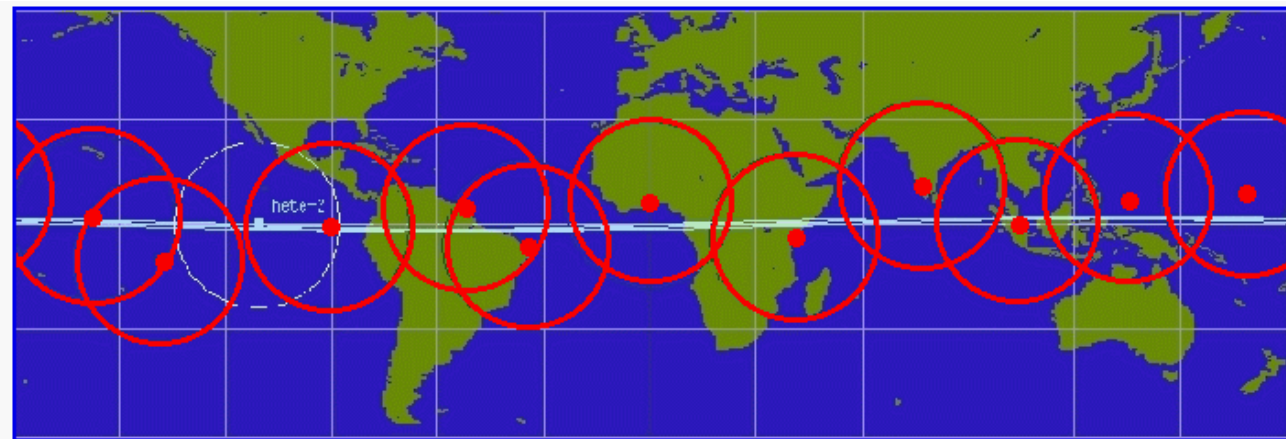


SN 1998bw - GRB 980425
chance coincidence $O(10^{-4})$
(Galama et al. 98) ⁷⁵

Hete2



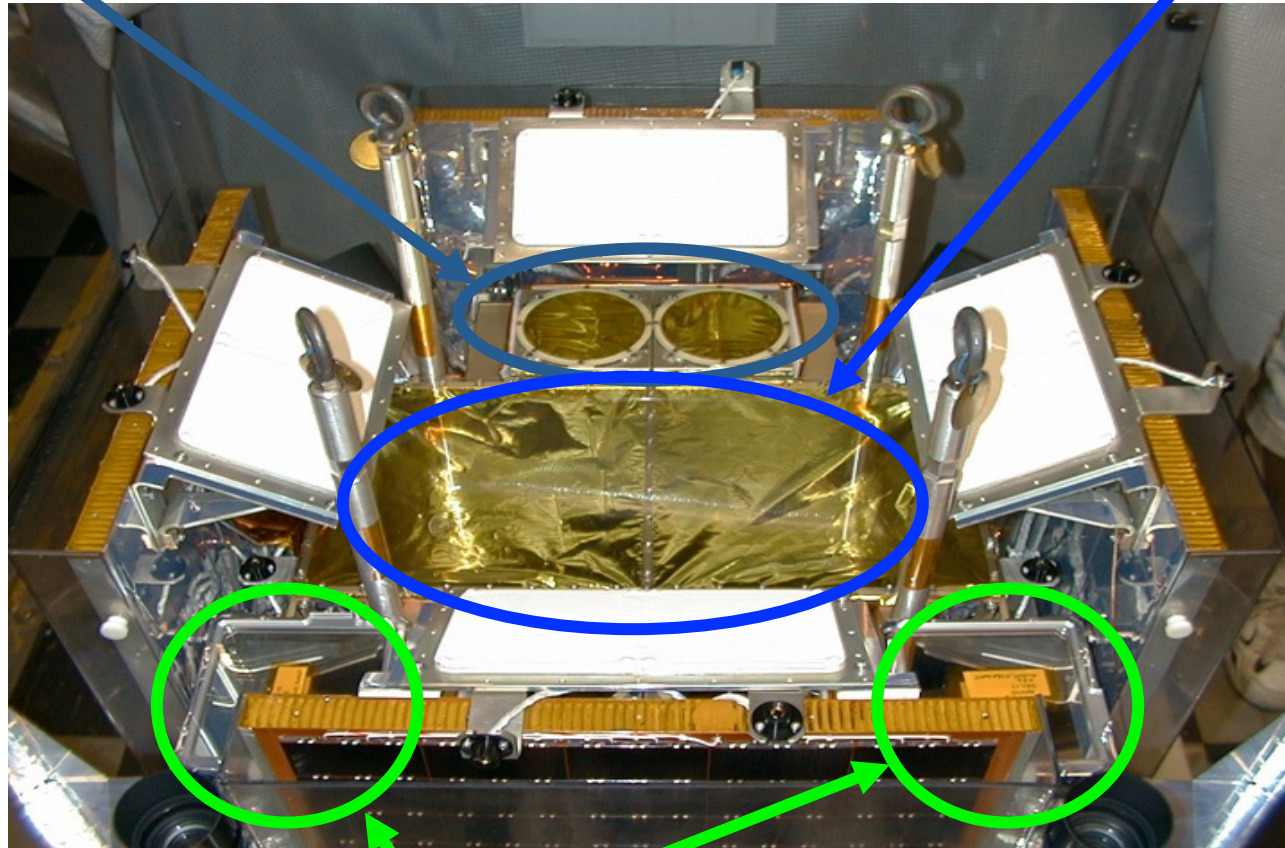
2000 - 2008



HETE-2 Science Instrument Package

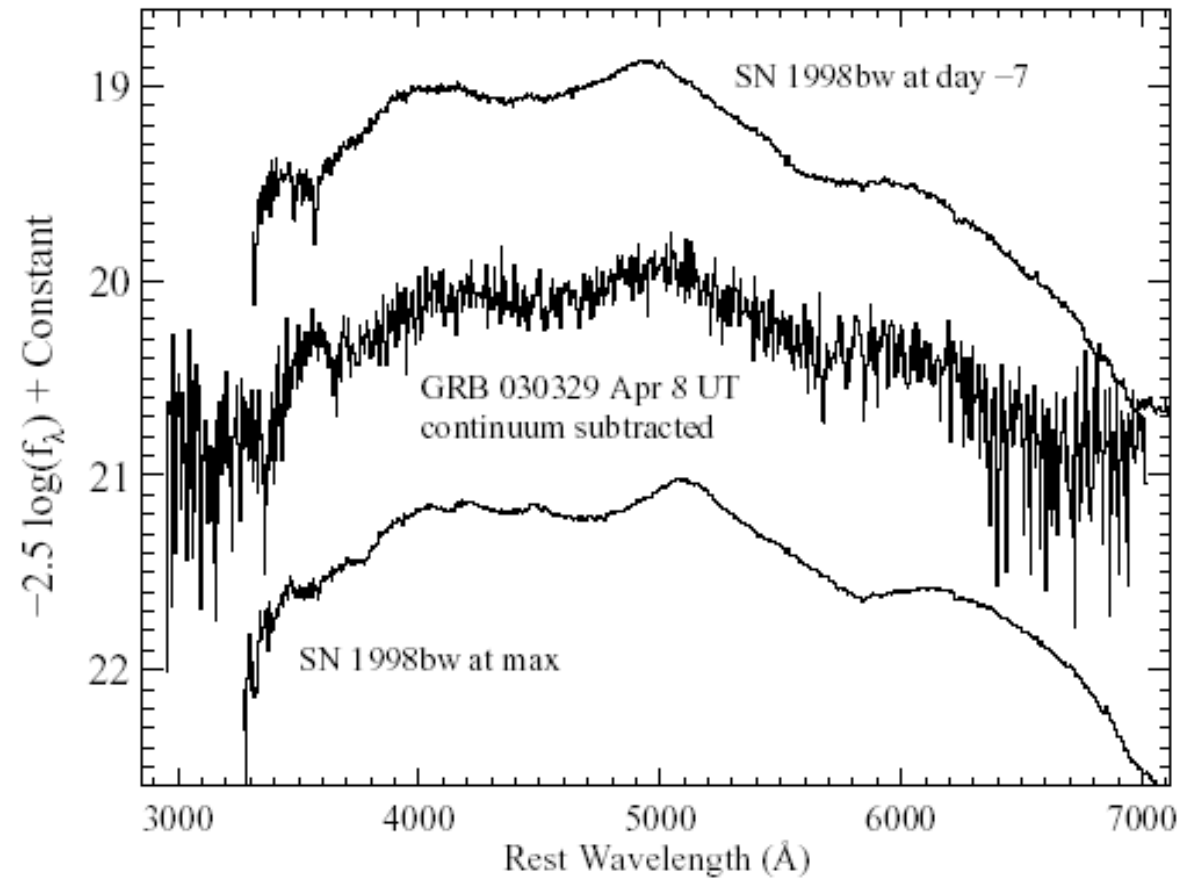
French Gamma-ray Telescope
(FREGATE): 5-500 keV; $\sim\pi$ FOV

Wide-Field X-ray Monitor (**WXM**):
2-25 keV; $\sim 5'$ - $10'$ localizations



Soft X-ray Cameras (**SXC**):
1-10 keV; $\sim 30''$ localizations

GRB 030329: the “smoking gun”?

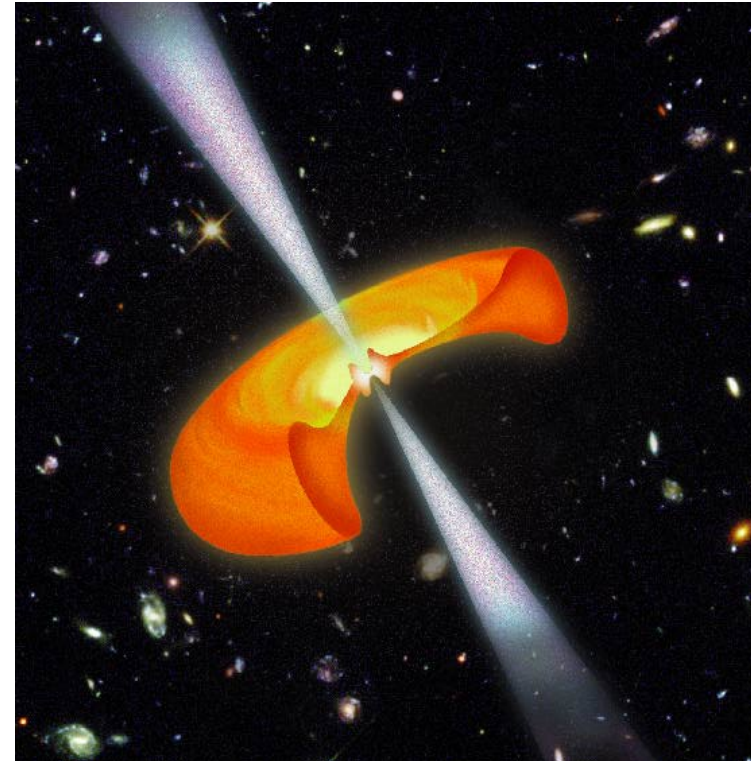
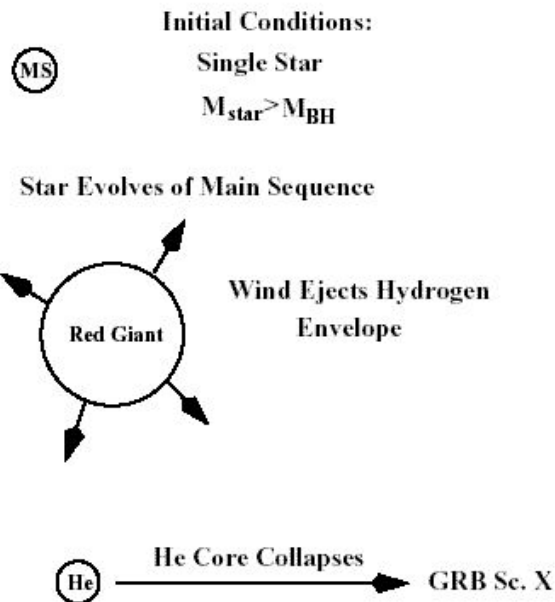


(Matheson et al. 2003)

Collapsar model

Woosley (1993)

Scenario X: Collapsar



- Very massive star that collapses in a rapidly spinning BH.
- Identification with SN explosion.